The Synthesis and Applications of Porphyrin Containing Polyion Complexes

Jawad Kadhim Abaies

PhD Thesis

November 2018

The Synthesis and Applications of Porphyrin Containing Polyion Complexes

Jawad Kadhim Abaies

A thesis submitted for the degree of

Doctor of Philosophy

Department of Chemistry

The University of Sheffield

Sheffield S3 7HF

England

November 2018

Acknowledgment

Foremost, I would like to express my sincere thanks and gratitude to Dr Lance Twyman for sharing his expertise and providing me with guidance and support throughout the project guidance, help, patience, and willingness to listen. I am particularly grateful for the many useful discussions, and most of all for making working for him an enjoyable experience.

I would also like to extend my thanks to the Twyman research group especially, Samira, Greg, Azra, Fatima and Meng for their support; attention and company throughout the course have been encouraging and a delight.

I would like to thank Miss Heather Grievson, Dean R Liversidge, Nick Smith, Rob Hanson, Simon J Thorpe and all of the staff of the Chemistry Department at the University of Sheffield. Numerous members of staff from the chemistry department have helped me in some way and I wish I could thank them all personally. My thanks also goes to Layla Al-Haidari from Spain group.

Finally, I would like to thank, Iraqi ministry of higher education and scientific research, Iraqi cultural attaché in London and Wasit University for the sponsorship.

List of figures

List of Schemes

List of Tables

Table of contents

List of abbreviations

^{13}C NMR	Carbon 13 Nuclear Magnetic Resonance Spectroscopy
^{1}H NMR	Proton Nuclear Magnetic Resonance Spectroscopy
Ala-NCA	L-alanine N-carboxy anhydride
ATRP	Atom Transfer Radical Polymerisation
ABCPs	Amphiphilic block copolymers
BCPs	Block copolymers
DB	Diblockcopolymer
^{o}C	Degree Celsius
CAC	Critical aggregation concentration
$CDCl_3$	Deuterated Chloroform
CMC	Critical Micelle Concentration
CMT	Critical Micelle Temperature
D_2O	Deuterated Water
DCM	Dichloromethane
DMAEMA	2-(dimethyl amino)ethyl methacrylate
DMF	Dimethylformamide
DB_r	Degree of Branching
DDS	Drug Delivery System
DLS	Dynamic Light Scattering
ES	Electrospray
EPR	Enhanced permeability and retention
Fe-TCPP	Iron functionalised tetracarboxyphenyl porphyrin
Fe-PH-HB-COOH	Iron cored hyperbranched polymer bearing t carboxylic acid terminal groups

Fe-PH-HB-COOEt	Iron cored hyperbranched polymer bearing ethyl ester terminal groups
FT-IR	Fourier transform infrared spectrophotometry
GPC	Gel permeation chromatography
HBP	Hyperbranched polymer
HB-COOH	Hyperbranched polymer bearing carboxylic acid terminal groups
HB-COOEt	Hyperbranched polymer bearing ethyl ester terminal groups
PH-HB-COOH	Porphyrin cored hyperbranched polymer bearing carboxylic acid terminal groups
PH-HB-COOEt	Porphyrin cored hyperbranched polymer bearing ethyl ester terminal groups
Mn	Number average molecular weight
Mw	Weight average molecular weight
mPEG	Methoxypoly(ethylene glycol)
mPEG-PDMA	Methoxypoly(ethylene glycol)-block-poly[2-(dimethyl amino)ethyl methacrylate]
mPEG-b-PMAME	Methoxypoly(ethylene glycol)-block-poly N-methacryloyl-l- alanine methyl ester copolymer
mPEG-Br	Methoxypoly(ethylene glycol) bromoisobutyrate
ES-MS	Electrospray Ionisation Mass Spectrometry
MeOH	Methanol
MAME	N-methacryloyl-l-alalanine methyl ester
mPEG-b-Lys	Methoxypoly(ethylene glycol)-block- poly(l-lysine) copolymer
mPEG-Ts	Methoxypoly(ethylene glycol) tosylate

mPEG-NH_2	Methoxypoly(ethylene glycol) amine
mPEG-b-Ala	Methoxypoly(ethylene glycol)-b-poly(l-alanine) copolymer
PDI	Polydispersity index
PB	Phosphate buffer solution
PSs	Photosensitisers
ppm	Part per Million
RAFT	Reversible addition-fragmentation chain-transfer
ROMP	Ring-opening metathesis polymerisation
ROP	Ring-opening polymerisation
ROS	Radical oxygen species
SEC	Size Exclusion Chromatography
TEM	Transmission electron microscopy
THF	Tetrahydrofuran
THPP	Tetrahydroxyphenyl porphyrin
TPP	Tetraphenyporphyrin
TCPP	Tetracarboxyphenyl porphyrin
THBP	Tetrahydroxybenzyl porphyrin
TBBP	Tetrabromobenzyl porphyrin

Abstract

In recent years, there has been a rapid increase in the application of polyion complexes in the field of medicinal chemistry including the drug carrier of prominent biopharmaceuticals. The interaction between counter-charged biopharmaceuticals and the ionic blockcopolymer, generates the polyion complex. PDT depends mainly on three factors: light, oxygen and photosensitiser (PS). PSs are insoluble in water, toxic, and can be distributed to healthy tissues. This project investigated a methodology of preparing polyion complexes which can overcome these problems and focuses on carrying and delivering PSs which are soluble for targeting only tumour cells. Polyion complexes can be formed via the electrostatic interactions between molecule bearing negative charges (polyanion) and compounds bearing positive charges (polycation). The first part of the thesis describes the synthesis of a series of amphiphilic block copolymers bearing amino groups (methoxypoly(ethylene glycol)-poly(2-dimethyl amino ethyl methacrylate) block copolymer). Synthesis of mPEG-PDMA was carried out in two steps. The first step involved the preparation of a macroinitiator suitable for ATRP-methoxypoly(ethylene glycol) bromoisobutyrate macroinitiator (mPEG-Br). Thereafter, mPEG-Br was reacted with the monomer 2-(dimethyl amino) ethyl methacrylate to generate the amphiphilic block copolymer, mPEG-PDMA, via atom transfer radical polymerisation (ATRP). Aggregation and self-assembly of mPEG-PDMA was investigated through CAC studies using tetraphenyl porphyrin (TPP) and pyrene as probes. As such, CAC around 0.1 mg/mL were determined. In addition, tetracarboxyphenyl porphyrin (TCPP) was prepared for use as the photosensitiser.

The second part of the study prepared the polyion complex from mPEG-PDMA (DB) (positively charged segment) and TCPP (negatively charged molecule) using 1:1 ratios of DB:TCPP at 1:1 (w/w). UV, DLS and TEM, which were used to determine the

formation and size of the DB/TCPP polyion complexes. DLS indicated a solvated size of 200-250 nm whilst TEM image showed that the particles had a size of 150-200nmn. The third part of the project studied the release of TCPP from the DB/TCPP polyion complex at pH 7.4 and pH 5. The results showed that 2% of TCPP was released in pH 7.4 and 4% at pH 5, indicating stable complexes, even in acidic conditions.

The fourth step of this project was the synthesis of hyperbranched polymers bearing a large number of negative charges terminal carboxy groups for use as the anionic component of the polyion complexes. Initially, unfunctionalised hyperbranched polymers (HBP-COOH) was prepared for use as a control. This was successful and the porphyrin cored hyperbranched polymer (PH-HBP-COOH) was then prepared as a globular photosensitiser with many negative charges. Capability of HBP-COOH and PH-HBP-COOH forms a polyion complexes with the mPEG-PDMA, which was then the focus of study. UV, DLS and TEM indicated the successful formation of poly ion complex. The PH-HBP-COOH release from the polyion complex showed that 9% of HBP was released at pH 7.4 and 11% at pH 5. This was much higher than a TCPP release and is attributed to weaker interactions between the hyperbranched polymer and mPEG-PDMA.

The final part focused on the preparation of iron-functionalised porphyrin containing polyions for use in catalysis. DB/ Fe-TCPP and DB/Fe-HBP polyion complexes were then tested as a catalyst for cyclohexene oxidation in water using iodosylbenzene as an oxygen source. The results showed that no oxygenation occurred in this heterogeneous medium.

Chapter 1

Introduction

Chapter1

1. Introduction

1. 1. Preface

Macromolecules are an important class of materials with fascinating properties such as programmable design, composition, functioned tolerability and biocompatibility. Therefore, they have been utilized in different fields with many applications [(1)]. Polymers are macromolecules built up of at least ten repeating units or simple molecules called monomers[(2)]. In 1920, Staudinger (Nobel Prize in1953) was the first who introduced the concept that polymers are big covalently bound macromolecules[(3)]. Owing to the significant physical and chemical polymer properties, their applications cover a large area extending from plastics, fabrics and electronics to tissue engineering. Nanomedicine is one of the most interesting fields of polymer applications whereby, they are utilized in drug delivery, gene delivery and imagining agents[(4)].

Polymers are divided generally into three classes based on their architecture, which are linear, branched and cross-linked polymers. This study mainly involves dendritic polymers and amphiphilic diblockcopolymers, so part one in the introduction will focus on dendritic polymers (hyperbranched polymers). The second part will discuss the synthesis and properties of amphiphilic blockcopolymers.

1.2. Dendritic polymers

More than two and half decades ago, a wide area of polymer chemistry focused on traditional linear polymers. Hard efforts have been made during the two past decades to prepare macromolecules with well-defined structure. Great attention has been paid recently to develop symmetrical, globular and branched macromolecules called dendritic polymers, which now one of the regular polymer categories. The term dendritic

refers to many branched structures. Dendritic originate from the Greek 'Dendron', which means tree-like structure. There are a lot of dendritic structures in nature such as nerve cell, spider, web and other. The branching of dendritic systems generates an interior gap that enable the supramolecules to house guest molecule. The external terminal functionalities govern the specific properties of and their application. These functionalities can undergo certain tailoring to suite the required purposes, such as solubility, catalysis, and aggregation. Dendritic molecules include dendrimer and hyperbranched polymers, which are the popular dendritic polymers, and they have many potential applications, including biomedical applications[5].

1.2.1. Hyperbranched Polymers

Hyperbranched polymers (HBPs) have attractive a significant attention due to the fact they have similar three dimensional structures to dendrons, but are easier to make. Hyperbranched polymers usually produced by random polymerisation, resulting in disordered imperfect branched structures with a relatively high dispersity index[6]. However, despite these imperfections, hyperbranched polymers are easier to synthesis, but possess similar properties to dendrimers. Berzelius was the first to develop hyperbranched polymers system through his work on producing resins from tartaric acid and glycerol[7]. The reaction of phthalic anhydride and phthalic acid also generated branched structures and was reported by Watson Smith[8]. Nonetheless, Kim and Webster were the first to coin the term 'hyperbranched polymer' when they succeeded to prepare hyperbranched polyphenylene in 1988[9-11].

1.2.2. Dendritic morphology and structure

The two main classes of dendritic polymer, hyperbranched polymer and dendrimer have similar structures. However, they differ in the nature of the branching. Dendrimer have

a perfect branching structure duo to the full and complete reaction of each monomer. The synthesis is step-wise; as such the molecules grow precisely and regularly. Therefore, the potential for imperfect branching within the produced compound is nil. Subsequently, they are highly uniform, monodisperse in size and structure. Conversely, hyperbranched polymer, which are synthesized using a single polymerization step are less ordered as grow randomly, leading to a nonproductive reaction and unrealized branching opportunities. Subsequently, the product is highly dispersed, as it comprises of series of molecules within a range of molecular weights (**Figure1.1**).

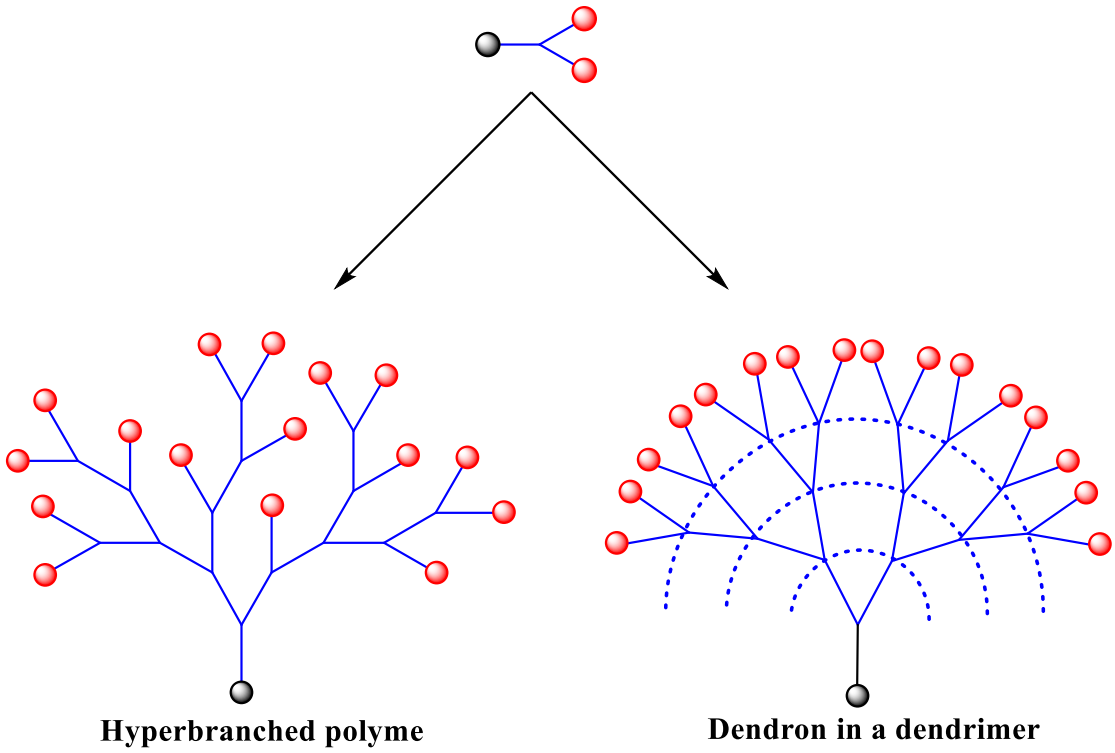

Figure 1.1. The different between perfect branching of a dendrimer and imperfect branching of a hyperbranched polymer.

1.2.3. Architecture of hyperbranched polymers

Hyperbranched polymers have imperfect structure and broad molecular weight distribution. The result is a polymeric system with imperfect branching and is far from the ideal structure of a linear polymer or a dendrimer. This distinctive architecture means that it is difficult to use nomenclature for these macromolecules. To describe this category of these polymers, a particular terminology has been introduced, which uses the structural properties when descriptions these hyperbranched polymer[11]. Three kinds of monomer architectures formed during the synthesis of hyperbranched polymer HBP **(Figure1.2)**.

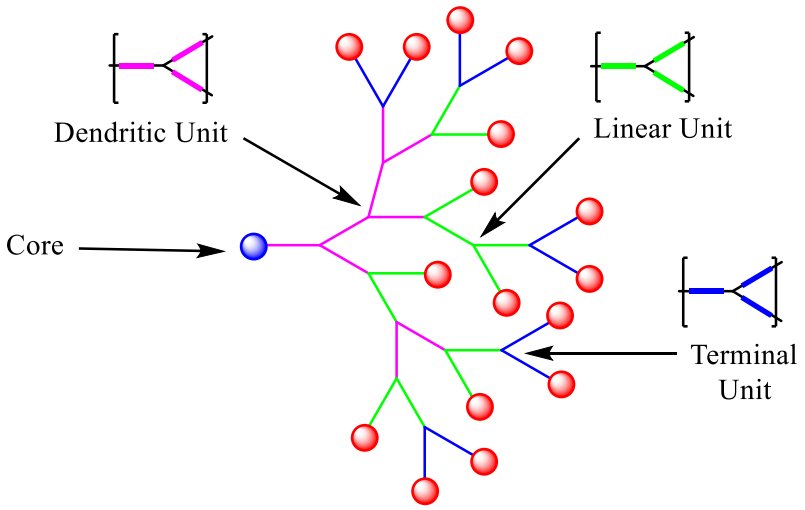

Figure 1.2. Types of possible branching units of a hyperbranched polymer.

The fully reacted monomers that contribute to a perfectly branched monomer is termed a dendritic unit. A linear units refers to a half reacted monomer, while the term terminal units describes the external monomer units (not the external functional groups). In addition, the focal growing point of the polymer chains is called the core unit[11-12]. One of the potential core options of hyperbranched polymer is a functionalised porphyrin, which is important to our project described in chapter 3 and 4.

Hyperbranched polymers differs from the rest of the dendritic polymers by their degree of branching (DB_r). The degree of branching indicates various dendritic properties and can be used to describe and characterise hyperbranched polymer [13]. For hyperbranched polymers, the growth of repeating units at every step occurs randomly and some of them are not fully reacted. Only dendritic and terminal units occur in dendrimers and no incomplete branching (linear units)[12]. Hence, the degree of branching (DB_r) plays crucial role in characterisation of hyperbranched polymer system[9,19,14,15]. Degree of branching (DB_r) can be given in the following equation[16]:

$$DB_r = \frac{D + T}{D + T + L} \qquad \textbf{Equation 1.1}$$

Where D, L, T are dendritic, linear and terminal units, respectively. They can be derived from integration ratio of proton NMR peaks, and usually requires the synthesis of model compound to help identify the three types of units. The equation1.1 indicates that a linear polymer will possess degree of branching equal to 0, as no branching within the polymer. The degree of benching equal to 1 for monodispersed dendrimers as they possess perfectly branching morphology and no linear units. Hyperbranched polymer have a degree of branching between 0 and 1.0. Hyperbranched polymers generated from AB_2 monomers usually possess a degree of branching of 0.5, as it is likely that the A or B groups will react with the growing polymer. As a result of imperfect branching, hyperbranched polymer have many structural isomers. Isomerism is a characteristics of hyperbranched polymer and it is that main element to differentiate between hyper branched and the dendrimer and the rest of polymers. In other words, for any degree of branching, the hyperbranched polymer can have a number of isomers. Therefore,

hyperbranched polymers with the same molecular weight and degree of branching can possesses a number of different structures. The formation of isomers during the synthesis of hyperbranched polymer is due to the random nature of monomer addition during the reaction. Isomerism in polyphenylene hyperbranched polymer is an example (**Figure 1.3**).

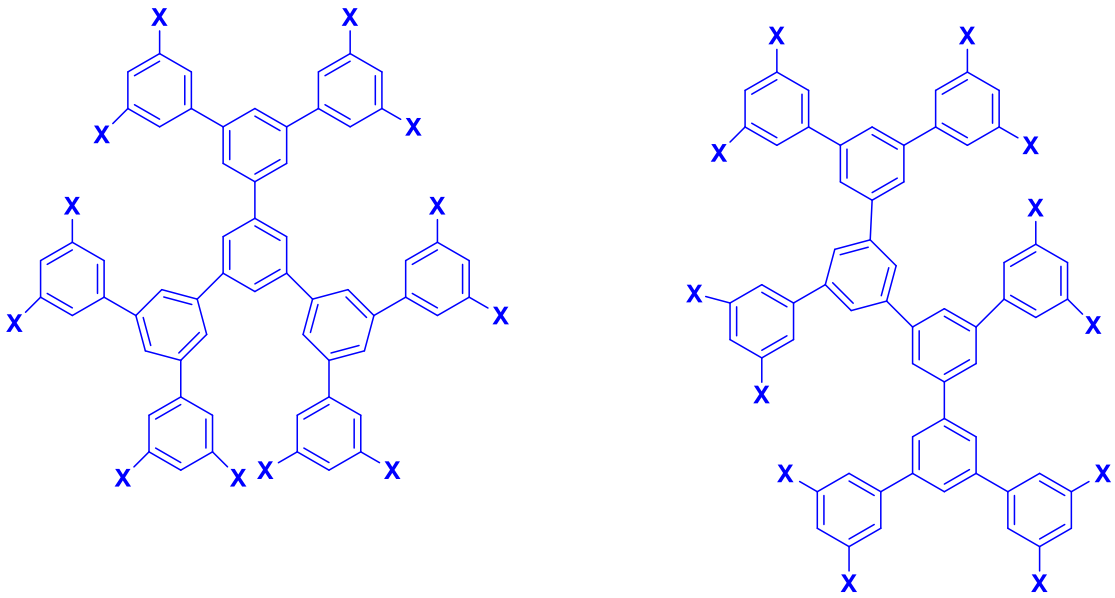

Figure 1.3. Isomers that can be formed during the synthesis of polyphenylene hyperbranched polymer.

1.2.4. Properties of hyperbranched polymers

Dendrimers and hyperbranched polymers possess highly branched and 3-dimentional structures, therefore, they have similar remarkable physical properties that differ from their linear counterparts. These properties include viscosity, hydrodynamic volume and solubility.

1.2.4.1. Viscosity

It is well known that the degree of chain entanglement between linear polymers increase with the molecular weight. As a result, the viscosity will also increases. Initially, dendritic polymers also behave the same at relatively low molecular weight, as the

viscosity reaches a highest value and then start to starts to decrease. The reason is the dendritic polymers adopt a globular morphology in solution, at a certain molecular weight, the molecules can be considered as hard spheres[17]. At this point, it is no longer possible for one dendrimer to form chain entanglements with a second dendrimer. The relationship between the viscosity and molecular weight in dendritic polymers and their peer linear polymers is shown in **Figure 1.3.**

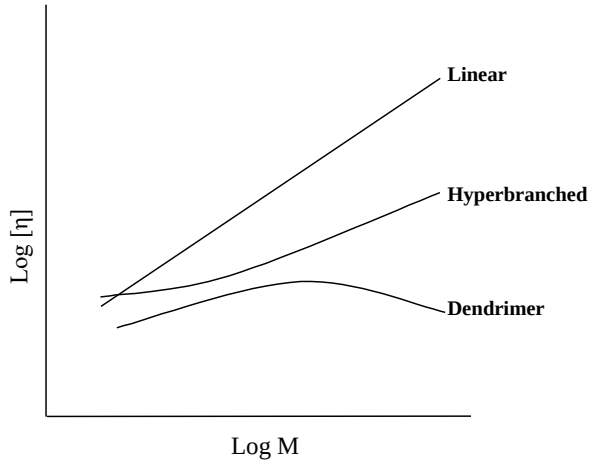

Figure 1.4. The relationship between viscosity represented by log[η] and molecular weight represented by log M of the polymer[18].

The figure shows that the viscosity hyperbranched polymer is located between linear and dendrimer[18], and generally increases with the than linear polymers. The reason for this comes from the globular/tight structure of hyperbranched polymers, which make chain entanglements more difficult between polymers molecular weight. However, the increase is much less. This trend is attributed to the increasing of the viscosity with the increasing the molecular weight despite the relationship between those two factors is not linear.

1.2.4.2. Solubility

The solubility of a conventional linear polymer is may affected by the chin/repeat units. However, the main factor that determines the solubility of a dendritic polymer is the terminal functional groups. The reason behind this comes from the globular structure, which have the repeat units inside, and the terminal groups presented at the surface. As the polymer gets bigger, the terminal groups at the surface, which are exposed to solvent shield the interior. Subsequently, solubility is determined by the properties of the terminal groups and not the monomer[19, 20]. As such, the solubility of dendritic polymers can be tailored to a particular solvent via modification of the surface. However, the modification of linear polymer functionalities has no notable effect on their solubility.

1.2.4.3. Hydrodynamic volume

In addition to and related to viscosity, the hydrodynamic volume of dendritic polymers is smaller than that of traditional linear polymers of equivalent molecular weight. This is attributed to the globular and compact conformation adopted by hyperbranched polymers in solution. Linear polymers have an opened and dynamic that is free to move in all directions and the chain can be easily solubilised, then the open structures are relatively large. As a result, the analysis of hyperbranched polymer by GPC technique is difficult if the system calibrated with linear polymer such as polystyrene, which is usually utilised for the calibration of the GPC machine. Accordingly, the relative molecular weight of dendritic polymers is commonly underestimated[21,22]. When the molecular weight of dendritic polymer increase, this problem becomes more pronounced leading to a wide difference in volume between dendritic system and conventional linear polymer standards.

1.2.5. Synthesis of hyperbranched polymers

In 1952, a paper regarding synthesis of hyperbranched polymer (theoretically) using AB_2 type monomer achieved buy Flory without generating the gelation[23]. Prior to this research paper polymer with high branching and symmetrical structure is accompanied by side reaction products such as cross linked network and intramolecular branching. Flory used one functionality (A) monomer and two or more functionality (B) monomer. Despite the theory of Flory regarded the difficulty in synthesis of hyperbranched polymers, the real first synthetic an example of true synthesising hyperbranched polymer was revealed by Kim and Webster in 1988 using AB_2 monomer. This methodology gave a large advance in the area of hyperbranched polymer research.

Three common methods are used for the synthesis of hyperbranched polymers; step growth polycondensation of ABx monomers or An + Bn monomers; self-vinyl polycondensation of AB^* monomer and ring opening polymerisation of latent ABx monomer. In contrast to dendrimer synthesis, hyperbranched polymers are commonly synthesised via a one pot/one step process[24-25]. Therefore, synthesis of hyperbranched polymers is easier and shorter compared to dendrimer synthesis, but random growth of the produced polymer leads to broad distribution of the molecular weight.

1.2.5.1. Step growth polymerisation (ABx)

Step growth polymerisation is a single step reaction of ABx ($X \geq 2$)[26]. Were A and B are groups that can react with each other's. Because of the high availability and low cost, the monomer molecule AB_2 is usually selected in this methodology. However, monomers of AB_6, which comprise 6 functionalities have been utilised to prepare hyperbranched polymer. Although the difficult control the polymerisation, monomer type A_2B_3 (which consist 2 A functionalities and 3B) have also been employed [27-28]. In

AB_2 method, the B functionality of one monomer reacts with a functional group of another monomer make to the branching (**Scheme 1.1**)

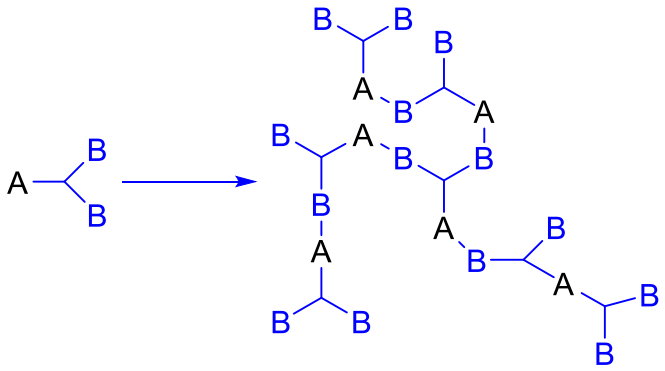

Scheme 2.1. The step growth polymerisation of an AB_2 monomer.

A wide array of hyperbranched polymers have been prepared using this approach, such as polyphenylenes[29], polyesters[16] and polyamides[30]. Although this method have advantages over other methods including speed and cost, drawbacks including cyclisation and cross-linking also occurs, which leads to gelation. This can limit solubility in organic solvent resulting in very difficult purification process. Moreover, side reaction may prevent the successful synthesis of the product or limit molecular weight, due to the exhaustion of the monomer molecules via undesirable intramolecular reaction or generation of cyclic oligomers.

1.2.5.2. Self-condensation vinyl polymerisation (SCVP)

Fréchet and co-workers in 1995 highlighted another approach for the hyperbranched polymer synthesis[30]. This methodology uses a monomer with a vinyl group and a side moiety, which can be converted to an initiator. This initiator can be a (living) free radical, anion or cation. The polymerisation reaction initiated by introducing external stimulus such as light, heat or an additive (**Scheme1.2).**

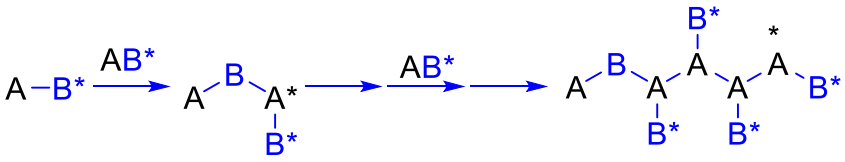

Scheme 1.2. The self-condensing polymerisation of AB* vinyl monomers.

It is worth mentioning that the relative size of the propagation units and the initiator affect the molecular weight, degree of branching and the polydispersity of the product[31]. Compared to the AB_2 approach, where gelation and side reactions occurred, self-condensation vinyl polymerisation can use controlled polymerisation methods. This result in of a high degree of control fore molecular weight of the product, and prevention chain transfer reactions, which causes cross-linking[32].

1.2.5.3. Multi- branching ring opening polymerisation

Multi-branching ring opening polymerisation is the third main methodology of preparing hyperbranched polymer. 1n 1992, Suzuki introduced this approach[33]. He announced the preparation of poly amines via the reaction of cyclic carbamate in presence of a palladium catalyst. Despite no much interest in this methodology compared to rest approach, the hyperbranched polymer prepared using this method possess interesting control over the molecular weight, degree of branching. This polymerisation involves using latent ABx type monomers. No branching points in the monomers, but the branching points are generated through the step of propagation[34]. In this method, is the polymer terminal group turn into the reactive site, which react with another cyclic molecule to generate branched polymer.

1.2.6. Application of hyperbranched polymer

Despite dendrimers and hyperbranched polymers having similar structures, the control over the synthesis of hyperbranched polymers is difficult compared to dendrimers and is due to the random growth of the polymerisation. However, hyperbranched polymers can be used as cost efficient alternate for dendrimers. Due to the distinctive structure and properties of hyperbranched polymers over the rest of polymer categories, this render them to be applied as microelectronics, magnetic, catalysis, optical materials, biomaterials, and nanomedicines[6,35,]. Hyperbranched polymer have unique properties allowing them to be used in various fields. For example, ring opening polymerisations were used by Frey and co-workers to prepare optically active polyether polyols from enantiomerically pure glycidol. They noticed that when this system was subjected to a racemic mixture of glycidol, immediately led to some separation of enantiomers[36]. Moreover, a novel hyperbranched poly(2,5-silole)s system was synthesised by Liu and co-workers. This intriguing system showed disclosure of explosives by hyperbranched polymer[37].There have been many other applications of hyperbranched polymers such as biometics, encapsulation and drug delivery[38-40].

1.2.6.1. Hyperbranched polymer a catalyst

In the literature, there are only a limited an example the use of regarding the use of hyperbranched polymers as a catalyst. This may be attributed to the disordered structure of hyperbranched polymer and imperfect morphology, which could limit properties selectivity. The development of hyperbranched polymer as catalyst, however, it is worth for in investigation.

1.3. Blockcopolymers

Generally, linear polymers are divided into two main classes, homopolymers and copolymers. Homopolymers are constructed from identical monomers, whereas, copolymers are made from more than one kind of monomers. Moreover, block copolymers are subdivided into four main categories **(Figur1.4)**. Alternating copolymers; where monomers are placed along the chain regularly, Graft copolymers; where the main chain of particular monomer is grafted by a block of other monomers, Statistical or random copolymers; in which monomers are distributed along the chain randomly, and block copolymers; where the main chain consists of a block of one monomer covalently connected to one or more of other monomers blocks[41]. Our study will focus on block copolymers and their applications.

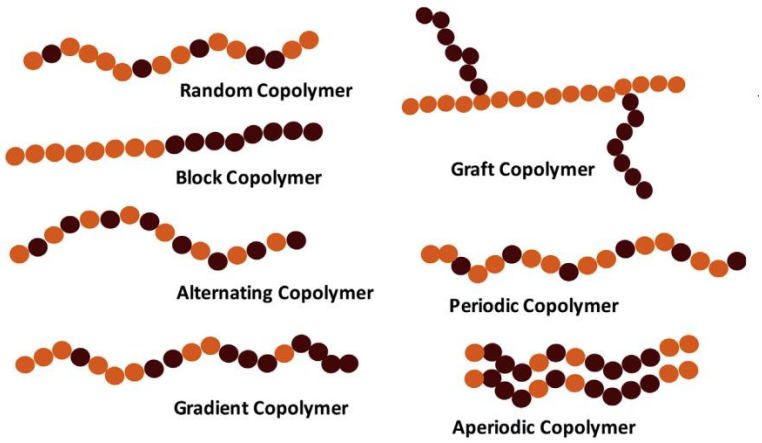

Figure 1.5. Types of copolymers[42] .

1.3.1. Blockcopolymer structures

Block copolymers are macromolecules in a linear or radial arrangement that contain two or more polymer blocks, each with a distinct chemical nature[43]. Besides giving rise to unique properties, the sequential arrangement of the monomer units in block

copolymers determines their appropriate preparation method. Diblockcopolymers are the simplest to synthesis. The terminal units of the first chain or block, A, is connected to another chain or block, B, giving rise to an A-b-B copolymer; where b indicates that the polymer is classified as a block copolymer. If a segment is placed between two blocks, the produced polymer is called a triblock copolymer (**Figure1.5)**. A multi-block copolymer, -(A-B)- is composed of alternating A and B segments arrangement. Block copolymers can be synthesized from a multivalent core. These diblockcopolymers radiate from this central core, forming star-shaped macromolecules[43].

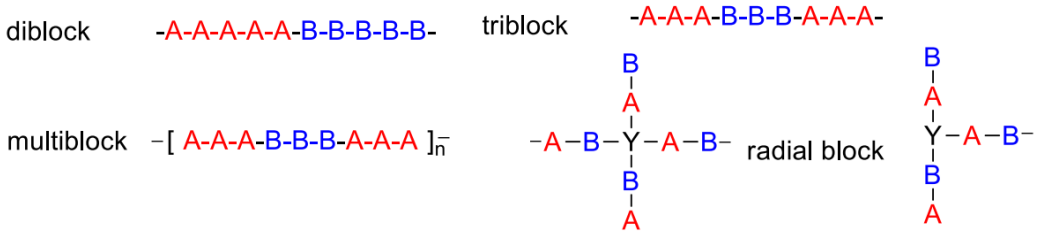

Figure1.6. Architectures of blockcopolymers.

1.3.2. Synthesis of diblockcopolymers

Tedious preparation techniques are sometimes associated with block copolymers, when compared to other, simpler macromolecules (such as random and graft copolymers). Living polymerization methods are commonly utilized where metal-catalyzed, ionic and free radical mechanisms are used[44, 45]. Nevertheless, synthesis of these complex architectures can be achieved via a step growth polymerization[46]. Different preparation techniques can also be combined to synthesise block copolymers consisting of different segments[43].

Any lack of control over molecular weight is an intrinsic problem of step-growth polymerization. The problems arises due to an irreversible transfer reaction and early chain termination. Moreover, this can make it difficult to control the aggregation of

polymers, resulting high polydispersity and a lack of uniformity. In order to overcome these problems, Szwarc et al. introduced a technique termed living polymerization. They noticed that termination and chain-transfer were avoided during the polymerization of styrene when initiated by sodium naphthalene in tetrahydrofuran[47, 48].

True living polymerizations are practically rare in comparison with controlled polymerizations, wherein irreversible chain transfer and chain termination are low because of fast propagation[49]. The mechanism of these polymerizations is chain-growth low concentration of propagating species[50]. The polymerization keeps the active species functional and "alive" within the propagating unit. Hence, no undesired reactions such as chain-transfer and chain termination can occur[45]. The method of sequential addition can be applied to this polymerisation. The method also useful for the preparation of well-defined diblockcopolymers with controlled chain length, and controlled architectures.

Atom transfer radical polymerization (ATRP) is one of the most employed methods of living polymerization. Sawamoto and Matyjaszewski were the first to report ATRP based on Ru and Cu catalysts[51, 52]. ATRP is an efficient controlled/ living radical polymerization due to the efficient control of chain length, distribution, structure and the functional ends of the polymer chains[52]. Several transition metal complexes are employed as catalysts including iron, ruthenium and copper. The dormant carbon-halogen terminals are activated by the catalyst through a one electron redox reaction with the transition metal M(I) to M(II) forming the growing radical species **(Scheme1.3)**. ATRP therefore involves anionic, cationic, transition metal; commonly Cu, and free radical intermediates. Due to radical stabilization and control of the intermediate concentrations, the radical is retained by M(II), and termination is low[53]. The intermolecular or intramolecular reaction between the radical and unsaturated group

of the gives an intermediate radical, which keeps reaction going. The polymer chains grow simultaneously and propagation continues until all of the unsaturated monomer moieties have been consumed. Hence, the length of the propagating chains is almost the same during the polymerization. Usually, it is easy in ATRP to oxidise reactive species by oxygen, so, oxygen must be excluded[54, 55].

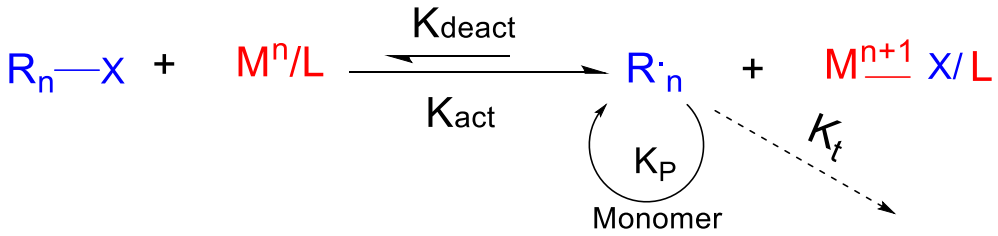

Scheme 1.3. A typical mechanism of ATRP.

A wide range of available vinyl monomers can undergo ATRP. These includes styrene, vinyl esters, acrylamide, acrylate and methacrylate. Polymerization different monomers may require different reaction conditions. At the end of the polymerization, the polymer has a terminal halogen, which can be easily achieved further reacted and used to initiate a new polymer block. Moreover, molecular weight as a function of conversion increases linearly. This means, the reaction leads to 100% monomer conversion with a narrow molecular weight distribution, which result in controlled molecular weights. Consequently, this will allow for preparation of highly controlled copolymers with novel properties.

Ionic living polymerization include cationic or anionic active centre on the end of the growing chain. This active centre enables a monomer to be polymerized at the terminus

chain [43]. It is necessary that these ionic active centres are not replaced by highly active species, such as water, which can terminate the polymerization[45].

The emergence of Ziegler-Natta catalysis facilitated metal-catalyzed synthesis techniques for block copolymers. These includes ring-opening metathesis polymerization (ROMP) and alpha-olefin polymerization. Recently, the ROMP method gave rise to blockcopolymers with different use such as light-emitting devices, with conducting properties and significant water solubility[56, 57].

Reversible addition fragmentation (RAFT) is another living polymerisation method employed when the monomer is not suited for ionic techniques or ATRP (metal-catalysis). This method also has advantages for the production of block copolymers with controlled block length. Recently, adhesive materials for use in photovoltaics have been generated by RAFT[58, 59].

Step-growth polymerization can be utilized to generate some complex block architectures. However, this process is rarely used to prepare diblock or triblock architectures due to problems with control (polydispersity/molecular weight). Nevertheless, step growth still an attractive method for generating high-performance materials (with applications in aviation industry and medicine) because numerous structures can be produced using these methods[60].

1.3.3. Amphiphilic blockcopolymers (ABCPs)

Amphiphilic copolymers are a class of copolymer that have a unique structure. This structure composes of at least two segments with different chemical properties. For example, amphiphilic copolymers have a hydrophilic block, which has affinity for water (water loving), and hydrophobic segment; low/no affinity for water. The interest in preparation and characterization of amphiphilic block copolymers has rapidly increased

due to their ability to create many types of nanoparticles via self-assembly in aqueous solutions[61,62].

The polymers can be made by polymerising two or more of monomers, one of them hydrophilic and the other hydrophobic. The macromolecules produced contain segments with opposite affinities to water. To overcome energetically unfavorable hydrophobe–water interactions in an aqueous solution, amphiphilic block copolymers self-assembled to generate well-ordered architectures at nanometer scale[63, 64].

The reason why self- assembly takes place is due to the hydrophilic-hydrophobic block interactions and between those two blocks and the surrounding medium. When the assembly occurs, an association process takes place between the hydrophobic segments. Simultaneously, the hydrophilic blocks place themselves between the external aqueous medium and the hydrophobic core forming the hydrophilic shell. Therefore, the hydrophilic shell acting as a stabilizer for the hydrophobic part and serves as an interface between the hydrophobic region and the bulk aqueous phase. Hence, polymeric aggregates will act as nanoscopic depots or hosts for other compounds with poor solubility in water[65] (**Figure 1.7**).

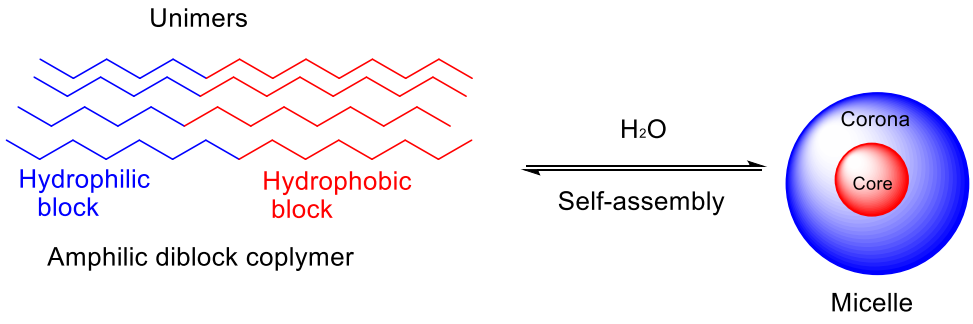

Figure1.7. Amphiphilic blockcopolymer assembly into micelle.

1.3.3.1. Aggregation of amphiphilic blockcopolymers

Amphiphilic copolymers are association colloids and require concentration at or above a threshold critical aggregation concentration (CAC). When the concentration is less than the CAC, the amphiphilic molecules exist in bulk solution as a single unimers. Above the CAC, the expulsion of well-arranged water molecules into the bulk aqueous phase entropically drives the assembly towards the aggregation. For the aggregation process, the change in free energy ΔG is given by the equation[65]:

$$\Delta G_a = \Delta H_a - T\Delta S_a \qquad (1.2)$$

Where ΔG_a is the free energy of aggregation, ΔH_a is aggregation enthalpy, T is the system temperature and ΔS_a is the aggregation entropy

The critical micelle aggregation of low molecular weight species (surfactant)) are about 10^{-3}- 10^{-4} M [66,67] while for those of the amphiphilic copolymers are much lower, around 10^{-6}-10^{-7} M[68,69]. On that basis, aggregation structures generated from low-molecular weight surfactant are thermodynamically less stable than those from amphiphilic copolymers, according to the change in standard free energy ΔG^o that is given by the equation:

$$\Delta G^o = RT \ln (CAC) \qquad (1.3)$$

Where R is the gas constant and T is the absolute temperature of the solvent.

Due to the thermodynamic stability of amphiphilic blockcopolymers aggregation, the tendency to disassemble in dilute concentrations is low compared to standard surfactants. Furthermore, if the system is exposed to high dilution, the dissociation of aggregation to unimers (individual polymer chains) would be a slow process due to the

kinetic stability of amphiphilic block copolymers[70,71]. The stability of the amphiphilic blockcopolymers aggregation system towards dilution is an important property, especially for any association-based carrier system. These systems can be exploited for parenteral administration and amplification for drug release[65]. The most common architecture of self-assembled amphiphilic copolymers in aqueous medium are spherical micelles. The hydrophobic blocks form a hydrophobic core by self-ordering inwards. In turn, hydrophilic segment pervade into the aqueous solution creating the hydrophilic corona. The ratio of hydrophobic volume to the hydrophilic volume governs the formation of spherical micelles dimensions. The total volume of amphiphilic molecules and their two components dictate the ability of amphiphiles to create highly-ordered arrangements[72]. As such, in addition to micelles, a various nanoparticle can be formed by the self-assembly of the amphiphilic copolymers such as nanospheres, polymersomes, and nanocapsules **(Figure 1.8).** The formed structure is controlled by the relative volume of the two blocks in aqueous solution.

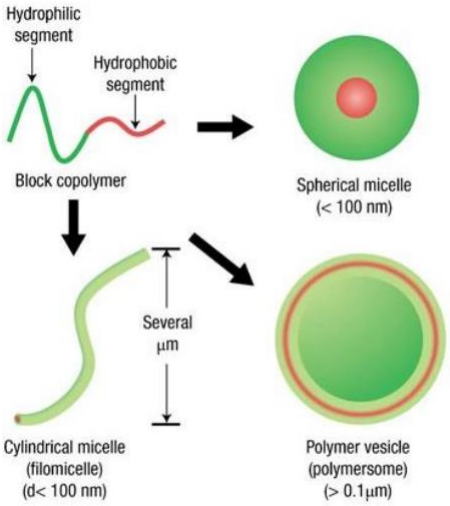

Figure 1.8. A diagram of some aggregated morphologies of amphiphilic diblockcopolymers[73] .

1.3.3.2. Applications of amphiphilic blockcopolymers

Block copolymer self-assembly phenomenon has attracted a significant attention since the ability of blockcopolymers to aggregate in various solvents[70]. Polymeric micelle is one of these aggregates, have been recognized to be used as a drug delivery systems. Since then, considerable interest and attention has been paid to polymeric micelles. Their preparation, biomedical and physiochemical properties have been investigated extensively[74]. Active molecules can be incorporated via physical inclusion or chemical conjugation, which are then stabilised by weak intermolecular interactions. A hydrophobic molecule can be loaded into micelle via hydrophobic interactions, and this is the most common application of aggregated amphiphilic diblockcopolymers.

Amphiphilic diblockcopolymer aggregates can be utilised in a number of application including catalytic experiments. Their composition and functionalities can be controlled and modified. This creates efficient environments to encapsulate reagents with or without catalysts. Micelles can be used to catalyse some reactions, simply by supplying a microenvironment for the reactions to take place. Specific catalysts can also be encapsulated, including sensitive catalysts that may be degraded in bulk solvent, in addition improve the selectivity and kinetics of the reaction[75]. Furthermore, amphiphilic blockcopolymers can encapsulate some metalnanoparticles or metal ions to generate polymeric micelles with interesting applications. For instance, encapsulation of metal micelles generated from poly(acrylic acid)-poly(styrene) blockcopolymers have been utilised for encapsulation of Ag^+ and Ag-carbene complexes. Excellent microbial activity against E. coli and P. aeruginosa bacteria in vitro was showed by these Ag-micelles[76]. Hu Na and co-workers[77] have synthesised poly(styrene)-poly(N-isopropyl acrylamide) block copolymer and immobilised Au in micelles of this copolymer. They found that Au-micelles can be used as a catalyst for p-nitrophenol

reduction. They also found that temperature can modulate the Au-micelles activity besides recovery of these micelles for four times with high catalytic activity.

In addition, amphiphilic blockcopolymers micelles can encapsulate biomacromolecules as well as small molecules. For example, Kataoka and co-workers[78] have prepared poly(ethylene oxide)-ss-poly[aspartamide functionalised with N-(2-aminoethyl)-2-aminoethyl) moieties] PEO-SS-P[Asp(DET)], where SS is link connects the copolymer blocks. They showed that the polymeric micelles are excellent vehicles for genes with marginal cytotoxicity. Moreover, small interfering RNA (siRNA) and proteins can be loaded and transported by polymeric micelles formed by amphiphilic block copolymers[79, 80].

1.4. Targeting strategies for cancer treatment using large molecules.

Encapsulation of anti-cancer drugs is an intriguing field and includes the area of polymeric micelles. Cancer drugs are extremely toxic, water-insoluble and have short half-lives in the circulation of blood[81]. Therefore, significant advantages can be provided by micelles, which encapsulate these molecules; the polymeric micelle core produces an environment to load the drug and therefore improved its solubility; Secondly, the hydrophilic part of the micelle (corona) acts as stabiliser and allows dispersing of macroassembly in water. As is mentioned before, amphiphilic copolymers micelles have low CMC value and stable thermodynamically in solution. What is more, kinetic studies have reported a slow dissolution process of micelles into their unimers upon exposure to higher dilution[82,83]. Due to resisting dilution in blood and remaining sable for longer time in blood circulation, micelles are considered an attractive architecture for biological application[83].

1.4.1. EPR Effect

As it was highlighted before, micelles are self-assembled with nanoscale-sized structure. This characteristic with respect to size renders micelles suitable for targeting tumour cell via the enhanced permeability effect (EPR). In order to acquire oxygen and nutrients for growing cells, tumours generate vascular networks to current vessels of blood. As growing cancer cells are increased, their demand for oxygen is increased as well. As a result, tumours create an extensive vascular system with improved microvascular permeability. Nevertheless, macromolecules are not filtered out and therefore accumulate within tumours due to the lack of a lymphatic drainage system (**Figure 1.9**). This phenomenon, which allows delivery and specific accumulation of anti-cancer drugs in tumours is termed enhanced permeability and retention (EPR) effect[84]. Ttarget specific drug delivery means that smaller drug dosage is required. This

minimizes harm to healthy cells, in addition to diminishing any side effects. Moreover, the EPR effect results in an increase uptake macromolecules and therefore drugs within tumours due to the size-selective nature. These reasons render polymeric aggregated systems as interesting candidates for anti-cancer treatment via encapsulation of chemotherapeutic drugs within their structures.

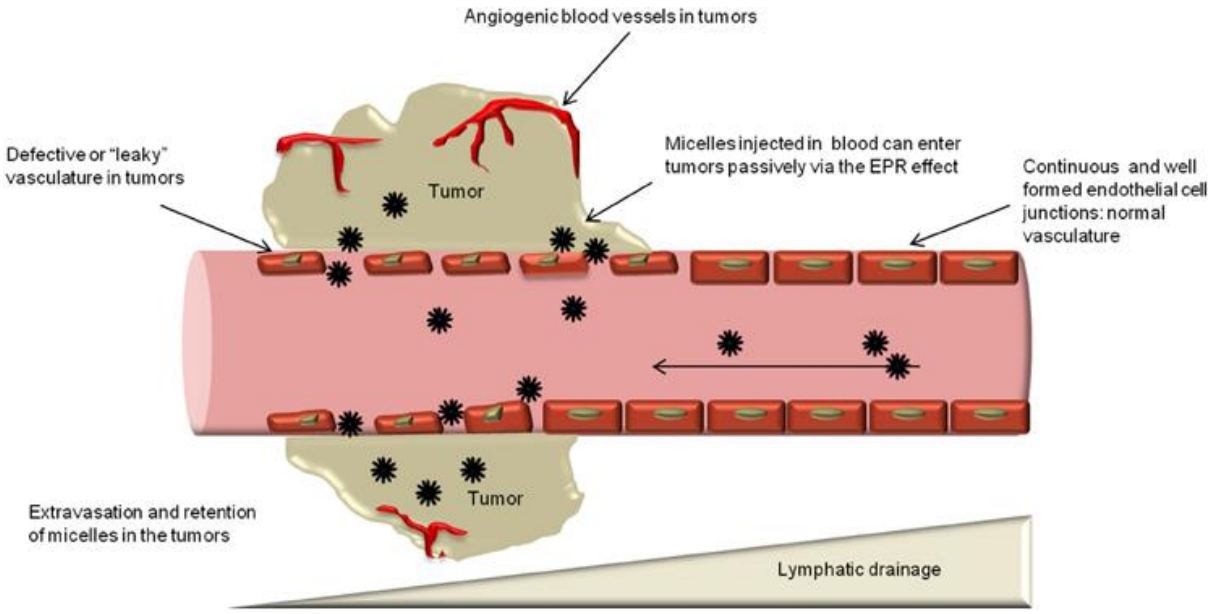

Figure 1.9 . Enhanced permeability and retention (EPR) effect. (Picture taken from Jhaveri, A. M; and Torchilin, V. P. Multifunctional polymeric micelles for delivery of drugs and siRNA, *Frontier in pharmacology*, 2014, 5 77 | 1)).

A wide range of research has employed diblockcopolymer aggregated systems in anti-cancer therapy. Also, the enhanced permeability and retention effect is induce apoptosis cells[85]. Various polymeric micelles have been successfully employed to encapsulate a number of drugs, including doxorubicin, paclitaxel and cisplatin, which are toxic and water-insoluble anti-cancer drugs[86-88]. Additionally, clinical trials are underway for a number of polymeric micelle encapsulated drug system[89-91]. Kataoka and his group have incorporated Doxorubicin (DOX) within a poly(ethylene glycol)-*b*-aspartic acid (PEG-PAsp) micelle. Compared to free DOX molecules, a high

concentration of drug accumulates in tumor cells and high circulating time has been exhibited for the system of PEG-PAsp (DOX)[92]. Moreover, the group have noticed that upon encapsulation of DOX, the stability of micelles was improved. Based on these observations they have deduced a structure-matching property, which has essential considerations when addressing therapeutics **(Figure 1.10**).

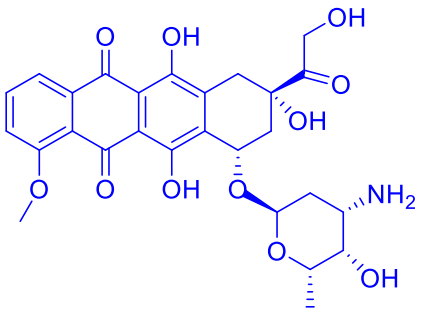

Figure 1.10. Doxorubicin (DOX) structure.

In addition to the wide range of applications of micelles that have been highlighted in literature, other more complex micellar morphologies, such as vesicles and rods, also have interesting application and often show greater properties than micelles for drug delivery. For example, Yang and co-workers have formed a star-shaped vesicle from diblock polycarbonate-PEG micelles for delivery of drugs for anti-cancer treatments. They noticed that the formed vesicles therapeutic properties have been enhanced. The large core of the system can expand the capacity for drug-loading including high loading of DOX. Moreover, the accumulation of DOX in tumor tissues was high via the EPR effect, with no symptoms of cardiotoxicity being observed. This renders the vesicular aggregation system a reasonable candidate for anti-cancer therapy[85].

In addition, Worm-like (filomicelle) morphologies have applications in anti-cancer therapy. This architecture is similar to spherical micelle, but filomicelles are long worm shaped assemblies. Their core size therefore is larger and is a suitable environment for

loading drugs. Furthermore, they show visco-elastic behavior and remarkable hydrodynamics, that enhances blood circulation for up to 7 days[93]. Polylactide-*b*-poly(ethylene glycol) copolymer (PLA-*b*-PEG) filomicelles have been prepared and studied by Jelonek and co-workers[93]. They observed that encapsulation efficiency and loading capacity was higher than those for analogues spherical micelles. They also noticed that rates of drug release were extended. This nanostructure behavior can be attributed to an increased hydrophobic cores stability[93].

1.4.2. Photodynamic therapy

Photodynamic therapy (PDT) is one of the potential applications for amphiphilic copolymers micelles. Due to its negligible toxic and minimally invasiveness, PDT has attracted a significant attention. Treatment of bladder, lung and common skin cancers by PDT has been universally approved. The action of PDT is simply comes from a light–absorbing substance (photosensitiser), which is initially excited upon irritation at a specific wavelength **(Scheme 1.4).** The relaxation process of the photosensitiser occurs by emitting absorbed light energy, which is re-absorbed by dioxygen (within cancer cell). As a result, dioxygen will be converted into oxygen reactive species (ROS), which including superoxide and peroxide anions, which are reactive species and will destroy the tumor[94-95].

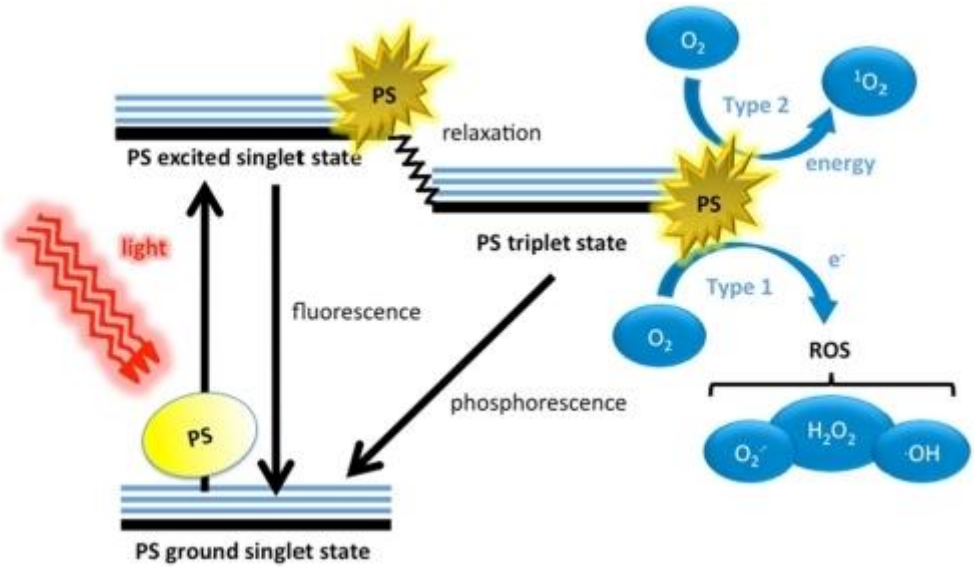

Scheme 1.4. Photodynamic therapy mechanism. (Picture taken from Tegos et al., Concepts and principles of photodynamic therapy as an alternative antifungal discovery platform, *Forentier in pharmacology*, 2012, 3, 120.

The porphyrin structure is the most common photosensitizer used. This structure can be excited at longer wavelengths due to the highly conjugated π electrons system. This property is beneficial as it is allow to avoid using shorter wavelength that do not permeates efficiently through tissues. Photosensitiser accumulation in skin is the major drawback of PDT. In order to avoid side effect similar to severe sunburns, patients must be not exposed to sunlight for 4-6 weeks after undergoing PDT treatment. However, this adverse effect can be minimised by selective targeting via exploiting the EPR effect[(96)]. Consuming oxygen and nutrients is increased sharply during tumour growth, resulting in oxygen shortage to local tissue. To cope with this situation, tumours establish additional vascular connections. In order to obtain more energy, conversion of glucose into lactic acid is also increased. Therefore, the tumour microenvironment will be acidic with a pH at or less than 5[(97)]. This effect can be exploited forwards a pH selective release mechanism

1.4.3. Polyion complex

To investigate polymeric anti-cancer treatment, much effort has been exerted during the last 20 years. Various potential benefits using polymeric nanoparticles as a drug carrier for tumour delivery have been determined. These are include prolonged blood circulation, promote drug stability and selective cancer tissue targeting[98]. When delivery system reaches the targeted tissue, substantial challenges remain regarding drug release and cell uptake. A polyion complex amongst nanocarriers has received a significant attention as an efficient drug delivery system[99,100]. The typical formation of polyion complex is easy and simply involves mixing of an ionic amphiphilic polymer with a counterionic compound. Polyion complexes were originally developed to encapsulate and deliver biomaterials including proteins, DNA and RNA. The pH or ionic strength within cellular compartments is usually different to the bulk and control the release of these ionic biopharmaceuticals from the polyion complex[99]. This occurs via the protonation-deprotonation of the ionic–ionic species holding the polyion complex together. Accordingly, the pKa of the amphiphilic block copolymer is an important parameter of the polyion complex and controls its structural changes.

Polyion complex as a drug carrier

In addition to their purity, the quantum yield of singlet oxygen produced by the ideal photosensitiser should be high and do not cause any toxicity in the dark. For efficient medical process, photosensitises should be highly localisation in tumours and absorb light with long wavelength, and have a good solubility in aqueous medium[98]. However, in aqueous medium, porphyrin photosensitisers simply form aggregates resulting in auto-quenching of the excited state. Aggregation occurs through hydrophobic effects and $\pi - \pi$ interactions. As such, most porphyrin photosensitisers are often water-

insoluble. For over work we propose to avoid the problems of aggregation of the photosensitiser by forming a polyion complex. This will prevent aggregating and provide high solubility in water. A Polyion complex can be formed via the electrostatic interaction between oppositely charged species. Water solubility is provided by the hydrophilic block of amphiphilic diblockcopolymer (commonly polyethylene glycol) attached to at least one ionic polymer[101]. The assembly process is mainly driven by electrostatic interactions. However, hydrophobic interactions also help with completely formation.

The fascinating properties of the polyion complex allow them to be utilised in various fields, but the majority applications are as nanovehicle for therapeutic drugs, enzymes proteins, heparin, and nucleic acid[102-109]. The distinctive design of polyion complexes (which have charges at the core and a neutral surface) allow them to overcome biological obstacles that normally restrict charged therapeutic delivery. In addition, their rate of clearance by liver and spleen (the mononuclear phagocyte system) is reduced, which prolongs the blood circulation time[101].

Several studies have been conducted using polyion complexes as carriers for large photosensitisers including a porphyrin-cored dendrimer. Kataoka and co-workers formed a polyion complex from an mPEG-aspartic acid block copolymer porphyrin cored dendrimer bearing terminal amino groups for PDT[110]. In another paper, kataoka and co-workers used a polyion complex formed from an mPEG-poly(l-lysine) diblockcopolymer and Zn-porphyrin cored dendrimer bearing terminal carboxy groups for PDT[111-112]. The same group also used a polyion complex from thiolated poly(ethylene glycol)-block-poly(L-lysine) [PEG–PLys(IM)] copolymer and a dendrimer cored phthalocyanine. The formed polyion complex showed improved in photodynamic activity, due to the presence of disulphide links, which could be cleaved

to release the photosensitiser [113]. In addition large polyion complexes have been formed from a triblock copolymer of poly(l-aspartic acid)-b-poly(ethylene glycol)-b-poly(l-aspartic acid) and doxorubicin (DOX)[114].

Y. Du et al. prepared a polyion complex from a cationic mPEG-poly(l-lysine) diblockcopolymer and 2,2-dithiodisuccinic acid for the use as effective intracellular drug delivery system. The polyion complex showed distinct pH-responsive degeneration in acidic medium due to the cleavage of its disulphide links[98].

In our study, we are going to investigate the preparation of polyion complexes from amphiphilic diblockcopolymer and small or large counterionic photosensitisers. The amphiphilic diblockcopolymer will comprises of a hydrophobic block that can be easily protonated in aqueous medium (or interaction with an acid). The resulting polyion complex will be studied as a macro photosensitiser for photodynamic therapy. In addition, iron cored polyion complexes will be studied for applications in catalysis.

Chapter 2

Aims and Hypothesis

Chapter 2

2.1. Aims and hypothesis

The aim of this work was to study the ability of polyion complex particles for use as drug delivery systems and, consequently, for photodynamic therapy. Other potential applications include artificial blood and catalysis. Polyion complexes are aggregates formed via self-assembly of oppositely charged polyions (the host and the guest). The reaction between the host and the guest occurs via electrostatic interactions enabling formation of the polyion complex particles (**Figure 2.1**). The formation of polyions requires a specific medium and a specific pH. Usually, formation and stability of a polyion complex depends on the pH. Polyion complexes have interesting properties over the rest of polymeric particles including their large size (EPR effect), stability towards dilution, slow dissociation (prolonged circulation time) and fast accumulation in a tumour.

In drug delivery system (DDS), the drugs, often anti-cancer drugs, are usually hydrophobic compounds. Therefore, the carrier must be an amphiphilic compound with a hydrophobic component, usually an amphiphilic blockcopolymer, which can aggregate and have the ability to dissolve hydrophobic drugs within their cores. The pharmaceutical industry has rejected many drug candidates due to their hydrophobicity. Also, low water solubility and poor delivery to the target tissue was illustrated by 60% of these molecules[115]. Many problems can be caused by lack of solubility, including poor biocompatibility and low bioavailability, which causes to undesired side effects in the body. It is possible to overcome these problems via drug delivery system (DDS)[116] . The solubility of hydrophobic the drug can be improved in several ways and is dependent on the nature and the chemical structure of the drug and the proposed delivery

system. There are a number of drug delivery systems, including linear polymers, dendritic polymers, amphiphilic blockcopolymers and polyion complexes.

The aim of this study is to prepare amphiphilic diblockcopolymers bearing amino groups, which can form ionic interactions with a porphyrin photosensitiser bearing carboxy functional groups (a small negatively charged molecule) to form polyion complexes (**Figure 2.1**). We will study these systems to examine their stability at pH 7.4 and pH 5. At pH 7.4, we expect the system will be stable. However, at pH 5, the amino groups will be fully protonated as well as the carboxylates. As such, there will be no interactions and the polyion complex should fall apart and release any of encapsulated photosensitiser. This is the proposed mechanism for the release of a drug inside tumour cells, which is relatively acidic.

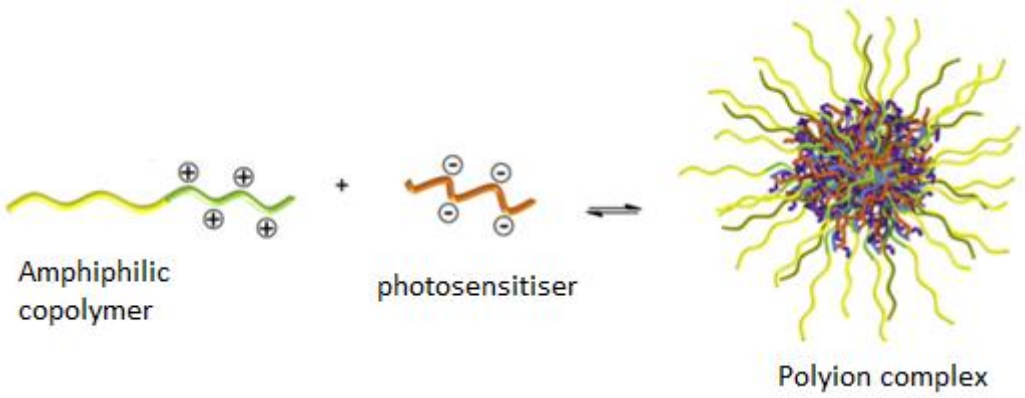

Figure 2.1. Formation of polyion complex from positively charged amphiphilic diblockcopolymer and small negatively charged molecules.

As well as studying a simple porphyrin photosensitiser, we also will investigate a large, well-defined and globular system that have many negative charges. The aim is to examine the effect of the increased negative charges on the formation and stability of

polyion complexes. Towards this aim, porphyrin cored hyperbranched polymers bearing terminal carboxy groups will be prepared (**Figure 2.2**). The results will be compared with those of the first system.

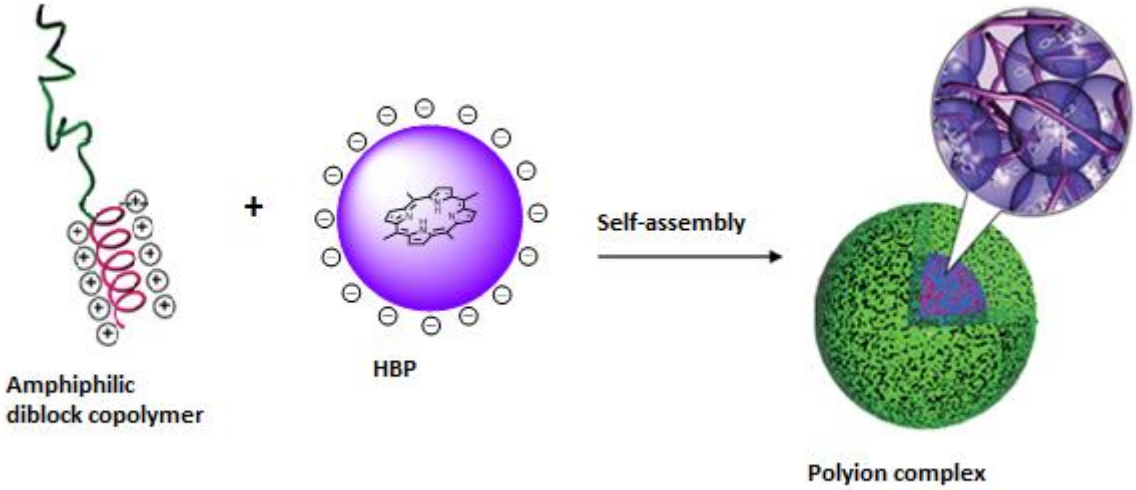

Figure 2.2. Formation of polyion complex from positively charged amphiphilic diblockcopolymer and negatively charged large molecule, which contains contain many charges.

We also propose to study the application of both systems for drug delivery, and possible use in photodynamic therapy. The release of porphyrins will be examined at pH 7.4 and pH 5.and the results will indicate whether or not these polyion complex systems can retain drug at pH 7.4 whiles also release sing drug at pH 5.

The final target of the study will investigate the ability of polyion complexes as catalysts for organic reactants in water. Specifically, the oxidation of alkenes using iron functionalised porphyrin. It is already known that this reaction can proceed often in a homogeneous environment. However, it is impossible to recover the catalyst. In addition, the use of organic solvent is not environmentally good. Therefore, the aim is to

overcome these problems using a polyion complex, which is environmentally friendly (water-soluble) and due to its size, can be recovered and used again.

Chapter 3

Results and Discussion

Chapter 3

3. Polyion complex as drug carrier

In this work, we aim to synthesis an amphiphilic polymer bearing a hydrophobic component that can be protonated at pH 7.4 in an aqueous solution. This polymer should contain a basic group tertiary amino group, as they are more basic than primary or secondary amines. Specifically a repeat unit containing dimethylamine was selected. This group is basic but has less steric hindrance than diethyl or dipropylamine. The formation of a polyion complex also requires a hydrophobic compound with groups that are anionic or can combine with protonated amines, such as carboxy groups, which are negatively charged under basic conditions. In this case, tetracarboxyphenyl porphyrin (TCPP) was selected as it can interact with the polymer and help form the polyion complex, and with respect to the application of the final molecular assembly, TCPP can also be applied as a photosensitiser for photodynamic therapy (PDT).

The first step in this project was the synthesis of the amphiphilic diblockcopolymer. The hydrophobic segments of this amphiphilic copolymer were synthesised from 2-(dimethyl amino) ethyl methacrylate. The amino groups in this component of the polymer can be partially ionised in an aqueous medium at pH7.4, the pH of the physiological environment. Moreover, this segment is biodegradable and is safe for use in biological/medical applications. Polyethylene glycol was selected for the hydrophilic segment, as it is neutral, safe for biomedical applications, commercially available, and water-soluble. In this study, the anion component will be the tetracarboxyphenyl porphyrin (TCPP). Initially, the pKa of the amphiphilic copolymer was determined to estimate the number of amino groups that can be protonated in water at pH 7.0. The pKa of the amphiphilic copolymer was calculated to be 7.4. Since mPEG-PDMA contains

~40 amino groups, it can be assumed that ~20 of these groups will be protonated at pH 7.4.

A controlled living polymerisation method was used to syntheses the amphiphilic diblockcopolymer. Atom transfer radical polymerisation (ATRP) was our favoured approach for the polymerisation reaction, which allow the synthesis of various well-defined copolymers with predetermined number average molecular weight (M_n), narrow polydispersity and controlled structure. In addition, this method has been demonstrated to be highly compatible with a wide range of monomer functionality[117]. Therefore, Methoxypoly(ethylene glycol)-block-poly[2-(dimethylamino) ethyl methacrylate] (mPEG-PDMA) with tertiary amines was chosen as the target amphiphilic polymer. This macromolecule will form a polycation via ionisation of the amino groups upon its dissolution in an aqueous solution buffered 7.4.

3.1. Synthesis of mPEG-PDMA diblockcopolymer (5)

The macroinitiator, methoxypoly(ethylene glycol) bromoisobutyrate (mPEG-Br) (**3**) was used as the starting material in preparation of the amphiphilic diblockcopolymer (mPEG-PDMA). The hydrophobic segment was 2-(dimethylamino) ethyl methacrylate, which contains the desired amino group and is sensitive to changes in the pH. The synthesis of mPEG-Br (**3**) was carried out upon the acylation of mPEG (**1**) using α-bromoisobutyryl bromide (**2**), as the first step in preparation (mPEG-PDMA) copolymer as shown in **Scheme 3.1**.

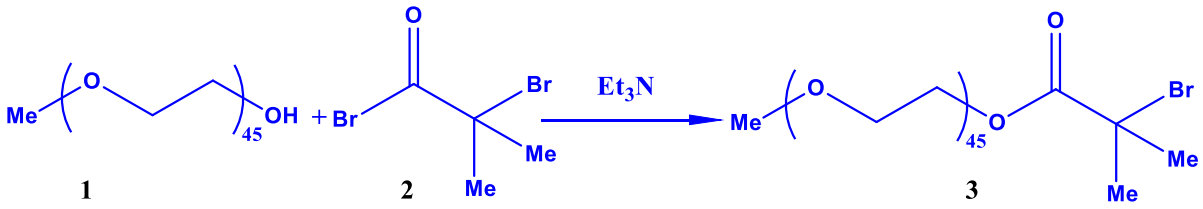

Scheme 3.1. The synthesis of methoxypoly(ethylene glycol) bromoisobutyrate (mPEG-Br).

Methoxypoly(ethylene glycol) bromoisobutyrate (mPEG-Br) (**3**) macroinitiator was prepared (**Scheme 3.1**) by reacting the terminal alcohol of $mPEG_{2000}$ (**1**) with 2-bromoisobutyryl bromide (**2**) in dry toluene. The mPEG (**1**) was first dried by removal of water using dry toluene and azeotropic distillation. To avoid hydrolysis, the reaction was run under a nitrogen atmosphere. Upon cooling the mixture to 0 ^{o}C, (**2**) was added along with triethylamine, which is a catalyst and removes the hydrobromic acid formed during the reaction.

^{1}H NMR was used to confirm the successful synthesis of mPEG-Br (**3**). The α-methylene terminal alcohol of mPEG (**1**) was detected as a triplet peak at δ = 3.52ppm, which was shifted to δ = 4.34ppm in the mPEG-Br (**3**) product. This confirmed the conversion of the hydroxyl group in (**1**) into an ester group. Moreover, the six hydrogens of the two terminal methyl groups were observed a singlet peak at δ = 1.96ppm. The IR spectrum of (**3**) shows the presence of the carbonyl stretching vibration at 1734 cm^{-1} and the absence of the OH stretching vibration at 3480 cm^{-1}. The subsequent synthesis of mPEG-$PDMA_n$ (**5**) was carried out using of mPEG-Br (**3**) as the macroinitiator for the ATRP of 2-(dimethyl amino) ethyl methacrylate (DMA) (**4**) in water as shown in **Scheme 3.2**. The ATRP step requires a catalyst. A 1:2 molar ratio copper(I) bromide and the ligand 2, 2-bipyridine[118] was used[119]. The reaction was performed under strict anaerobic conditions to avoid any radical inhibition by free oxygen. Five freeze-pump-

thaw cycles were applied to the solvents and reagents in order to eliminate any trace of oxygen, and a cannula was used to transfer the solution. The reaction was carried out under a nitrogen atmosphere.

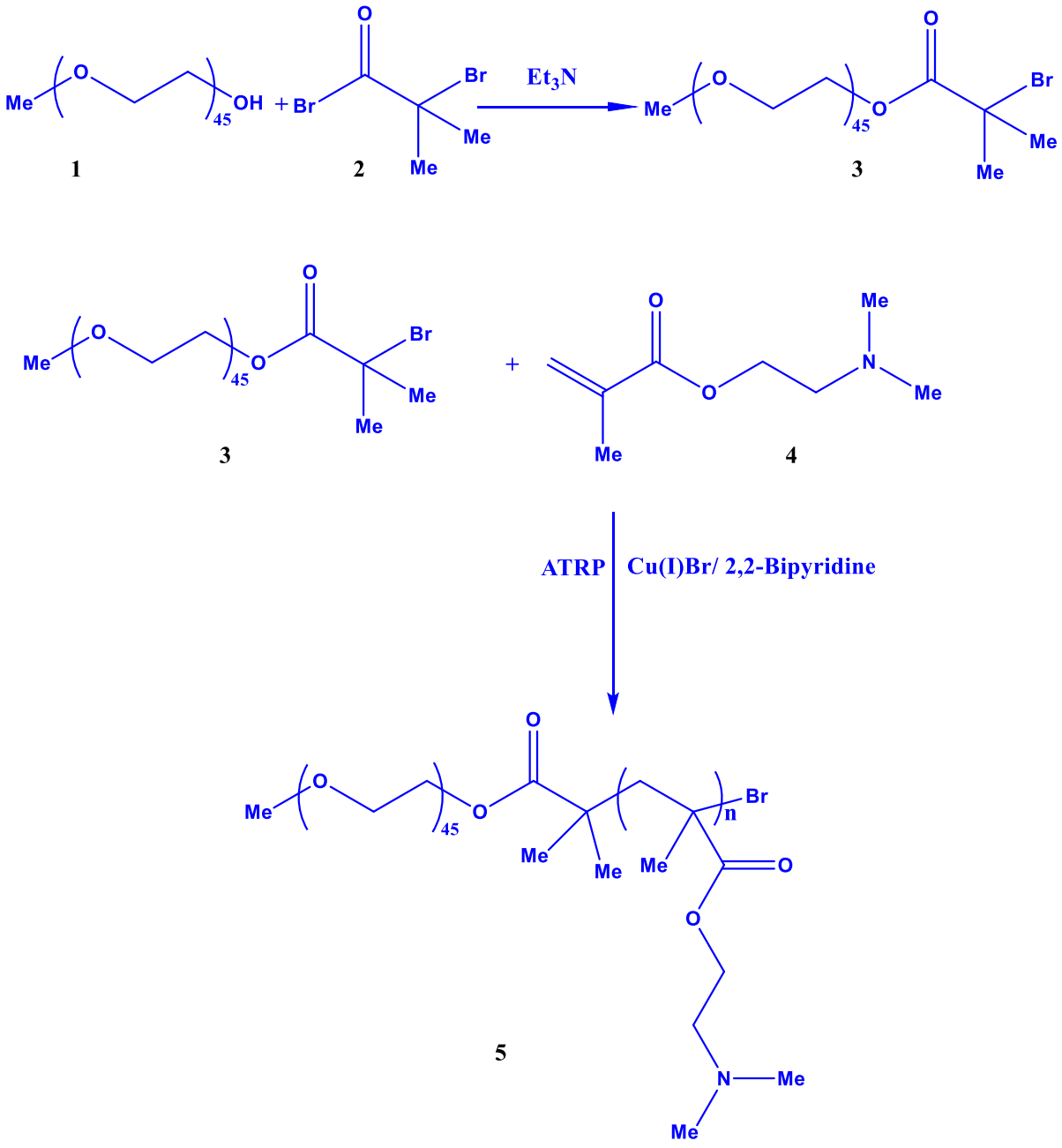

Scheme 3.2. The synthesis of mPEG-PDMA$_n$.

The loss of the alkene protons of monomer (**4**) was confirmed using ^{1}H NMR spectroscopy. New broad peaks at δ = 0.91, 1.05, 1.83 and 1.93ppm were visible and

the loss of the multiplicity for the methylene peaks in the α- and β- positions to the ester moiety confirmed the polymerisation had occurred. Moreover, the targeted degree of polymerisation of mPEG-PDMA was confirmed using ^{1}HNMR spectra recorded in $CDCl_3$ by the comparing the integration values for the peaks observed at δ = 3.65ppm of the mPEG (**1**) with peaks at δ = 4.35 and δ = 2.40ppm corresponding to the methylene and methyl peaks, respectively. A quite different ^{1}H NMR spectrum was recorded in deuterated water at the same concentration. The peaks previously assigned to the mPEG protons in this aqueous solution could be clearly observed, while very weak peaks corresponding to the DMA protons were observed (**Figure 3.1)**. This is attributed to the micelle formation and aggregation of the amphiphilic mPEG-PDMA (**5**) resulting in a compact core, which is a characteristic of mPEG (**1**) in an aqueous medium. As a result, free-motion/rotation of the DMA segment is slow, resulting in coalescence, making it difficult to detect DMA protons using using^{1}H NMR spectrum[120-121].

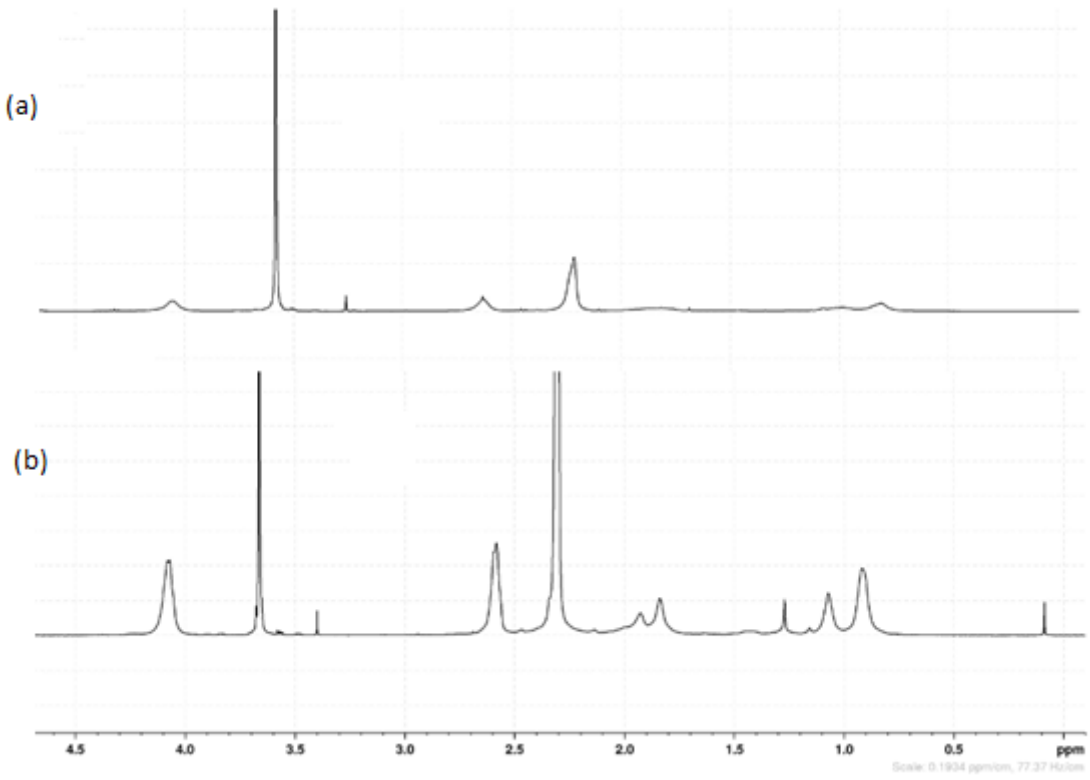

Figure (3.1). ^{1}H NMR spectra of mPEG-PDMA in (a) D_2O (b) $CDCl_3$.

For the purpose of comparison, a series of mPEG-PDMA samples were prepared. They differ in the molar ratio of mPEG/DMA used in their synthesis. An increase in both the M_n from the mPEG-Br (**3**) macroinitiator was emphasized by the ^{1}H NMR spectra and GPC measurements **(Table 3.1)**.

Table 3.1. The molecular weights, polydispersities (PD), and degree of polymerisation (DP) represented by DMA contents (DP) of mPEG-PDMA$_n$ determined by ^{1}H NMR spectroscopy and GPC.

Sample	Degree of polymerisation(n)		Mn			PD
	Targeted[1]	Eperimental[2]	Theoretical[1]	^{1}H NMR[3]	GPC	
5a	20	26	5280	6230	2950	1.07
5b	30	37	6850	7960	2970	1.06
5c	40	47	18420	10100	4500	1.05

1) Calculation based on the DMA/ mPEG ratio; 2) As calculated by integration of the ^{1}H NMR spectra recorded in $CDCl_3$; 3) The DMA units determined from methyl groups of the tertiary amine by ^{1}H NMR spectra at δ = 2.3ppm with the terminal methyl group of the PEG unit set as the reference.

The data in Table 3.1 show that there was a difference in the estimated degree of polymerisation (DP) when compared with those determined experimentally. Nevertheless, it has been reported that the bromo group of a macroinitiator can be easily hydrolysed resulting in the loss of hydrobromic acid. This could be avoided by synthesizing a chlorine functionalised macroinitiator with a chlorine end group and the catalyst copper(I) chloride[(122)]. However, as we had useful polymers, we did not need to use a new synthesis at this point. It can also be seen that the molecular weights calculated using integration were larger than those obtained using GPC measurements. It was also observed that the differences became greater upon increasing the DMA content, which can be attributed to the longer retention time observed as a result of the large differences

in the hydrodynamic radii of the polystyrene standards and DMA segments[119] The polydispersity of the mPEG-PDMA copolymers was narrow, indicating a good level of control via the atom transfer radical polymerization (ATRP).

3.2. Synthesis of tetraphenyl porphyrin (TPP) (8)

Porphyrins are highly hydrophobic compounds, which have high absorption in the visible region of the electromagnetic spectrum. Therefore, tetraphenylporphyrin (TPP) (**8**) was chosen as a probe compound which was expected to load into the micelles via the hydrophobic effect (solvophobic interaction). This phenomenon was employed to help determine the critical micelle concentration of mPEG-PDMA. Moreover. The interaction between TPP and mPEG-PDMA was studied and the results compared with another porphyrin bearing functional group i.e. tetracarboxyphenyl porphyrin (TCPP). In addition, TPP has been utilised as a photosensitiser for photodynamic therapy (PDT) applications.

Tetraphenyl porphyrin (TPP) (**8**) was prepared via the direct coupling of pyrrole (**6**) and benzaldehyde (**7**) in refluxing propionic acid **(Scheme 3.3).** Following vacuum filtration, the resulting product was obtained as a shiny purple solid, which is the appearance of a porphyrin.

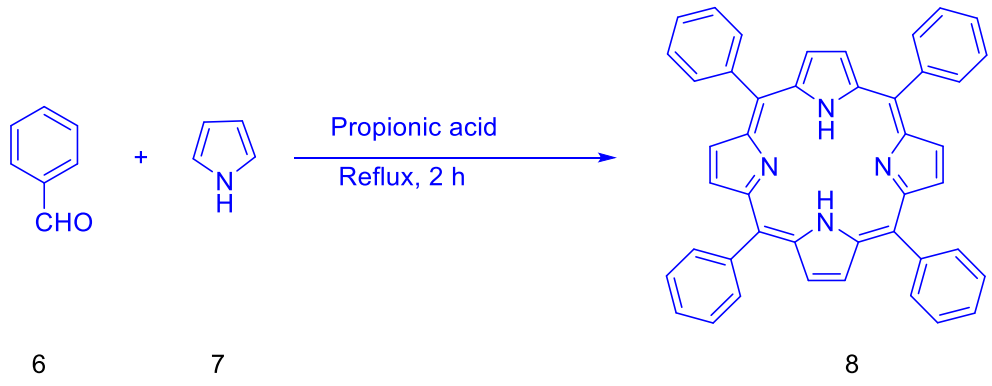

6 7 8

Scheme 3.3. The synthesis of tetraphenyl porphyrin (TPP).

The synthesis of TPP (**8**) was confirmed by the presence of a singlet peak in the ^{1}H NMR spectrum at δ = -2.73ppm, due to the strong ring current of the porphyrin, which shield the central protons. Furthermore, the pyrrole hydrogen peak which was detected at δ = 6.22ppm in the starting material was shifted to δ = 8.91ppm for the pyrrolic protons in TPP (**8**) confirms an increase in the deshelling provided by the large aromatic ring current. The signal m/z = 515 in the electrospray (ES) mass spectrometry corresponded to the molecular weight of TPP. An intense absorption band at 417nm in dichloromethane was observed in the UV-Visible spectrum. This band known as the Soret band and is characteristic of all porphyrins. In addition, the UV measurements showed four absorptions bands in the range of 510-650 nm, which are much weaker and called Q-bands, belonging to the so-called forbidden absorption of the porphyrin. These are also characteristics for all non metallated porphyrins.

3.3. Critical Aggregate Concentration (CAC)

In order to determine the appropriate concentration of mPEG-PDMA (DB) to form micellar aggregates. The onset of micellisation of this amphiphilic polymer was determined using TPP as a hydrophobic probe and utilizing its fluorescence signal (**Figure 3.2)**. Using procedures suitable for this particular diblockcopolymer, a solution with concentration of 10 mg/mL in a pH 7.4 buffered solution was prepared[123]. This high concentration was above the CAC normally associated with mPEG amphiphilic diblockcopolymer[124-126]. From this solution, a number of diluted solutions were prepared. The intensity obtained by fluorescence spectroscopy was used to monitor the amount of porphyrin encapsulating, and therefore the efficiencies of the polymer. If the concentration of diblockcopolymer (mPEG-PDMA) is above CM, the hydrophobic TPP will be encapsulated and can be detected using fluorescence. However, if the

concentration of mPEG-PDMA below the CMC, then the TPP will not be encapsulated and as it is insoluble in water, it will not be detected. An oil-in water emulsion method was used for porphyrin loading. In this technique concentrated dichloromethane porphyrin solution was added dropwise to the diblockcopolymer solution[127]. Upon stirring overnight, the organic solvent evaporated from the open vessel. The resulting solutions were filtered to remove the non-encapsulated TPP prior to recording the fluorescence spectra. The fluorescence data recorded as a function of the concentration of mPEG-PDMA (**Figure 3.2**).

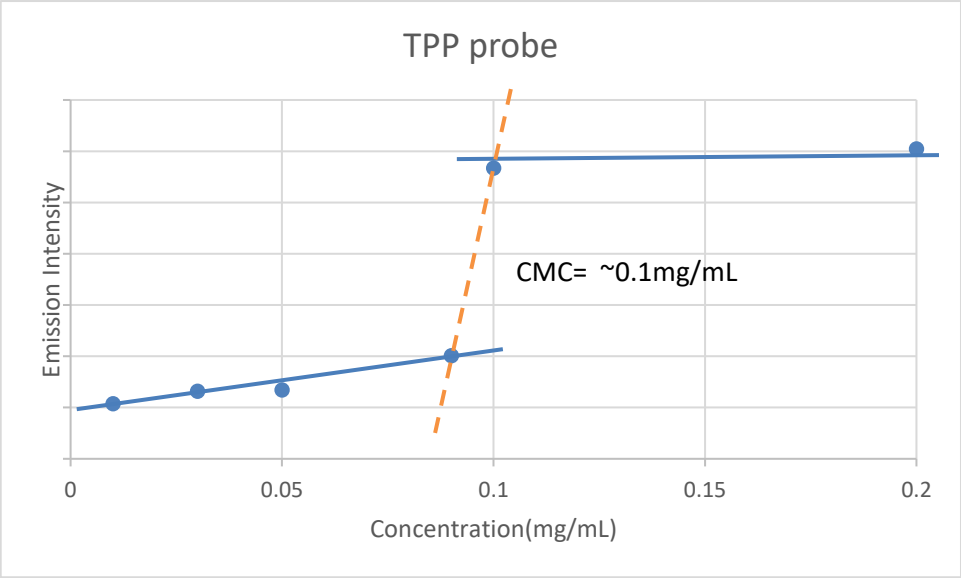

Figure 3.2. Plot of emission intensity of encapsulated TPP in micelles versus mPEG-PDMA Concentration (mg/mL) at excitation wavelength of 420nm.

The fluorescence spectra were recorded at 25 ^{o}C at an excitation wavelength of 420nm, and emission detected at a wavelength of 540-800nm and a slit width of 3nm. The emission peak intensities at 650nm were utilized to monitor the TPP encapsulated into mPEG-DMA (**5C**). The emission data of TPP incorporated into the MPEG-PDMA was

plotted as a function of the concentration of polymer (**5C**) (**Figure 3.2**). The plot shows the CMC value of 0.1 mg/mL.

To confirm the CMC of mPEG-PDMA, it was also measured using pyrene as a fluorescence hydrophobic probe in an aqueous solution at 25 ^{o}C. A stock solution of pyrene in acetone was prepared, and from this stock solution, a 1x 10^{-6} M solution of pyrene was prepared. A 3mL of this solution was transferred into a number of vials. Upon evaporating the acetone solvent, a certain volume of mPEG-PDMA (**5**) solution (ranging from 0.001mg/mL to 1mg/mL) were added into each vial. The mixtures were left to equilibrate over night at room temperature before running the measurements. The emission spectra of pyrene in solution was recorded overt the wavelength range of 350 to 470 nm. The excitation wavelength was 340 nm with a slit width of 3nm for both excitation and emission. The intensities of the peaks seen at 373 and 383nm are characteristic for pyrene and known as I_1 and I_3, respectively. The peak intensity ratios at 373 and 383 nm (I_3/I_1) of pyrene fluorescence spectra were plotted as a function of the mPEG-PDMA concentration (mg/mL). The obtained plots as a function of the logarithm of the mPEG-PDMA concentration (**Figure3.3).**

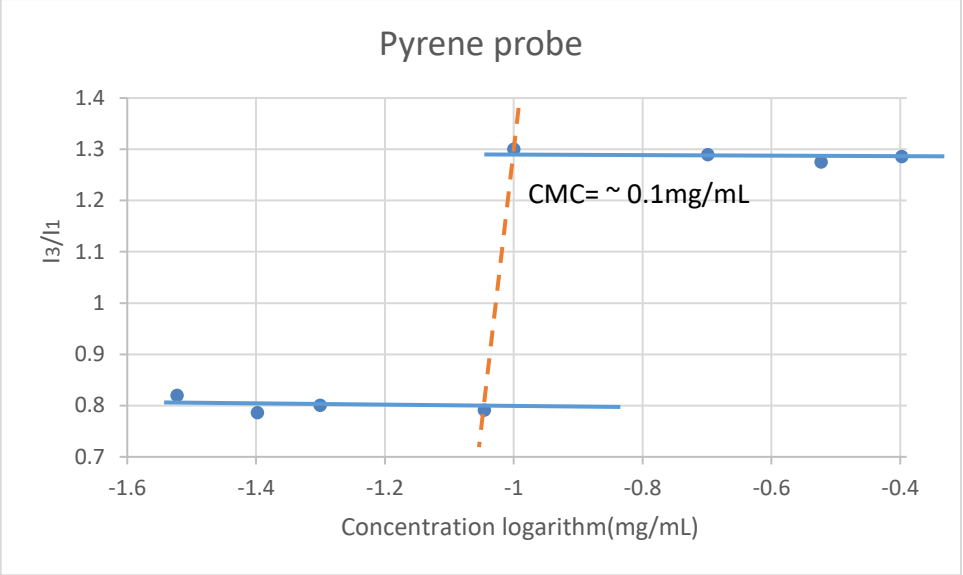

Figure 3.3. Plot of I_3/I_1 emission ratios of encapsulated pyrene in micelles versus mPEG-PDMA) concentration (mg/mL).

The plot shows the CMC of mPEG-PDMA (**5C**) was ~ 0.1 mg/mL which reinforced the results of TPP probe.

3.4. Synthesis of tetracarboxyphenyl porphyrin (TCPP) (10)

The aim of this study was to develop a macrosensitiser using polyion technology. As such, the photosensitiser will be used as the negatively charged compound in the polyion complex. Therefore, tetracarboxyphenyl porphyrin (TCPP) (**10**) was selected.

TCPP has four carboxylic groups, which can be deprotonated by a base such as the basic nitrogen of the mPEG-PDMA (**5**). TCPP was synthesized via the direct reaction of pyrrole (**6**) and 4- carboxybenzaldehyde (**9**) in a refluxing propionic acid **(Scheme 3.3).** Following vacuum filtration, the dark precipitate washed with dichloromethane until the filtrate was colourless. The resulting solid was washed with cold methanol and isolated as a dark purple solid.

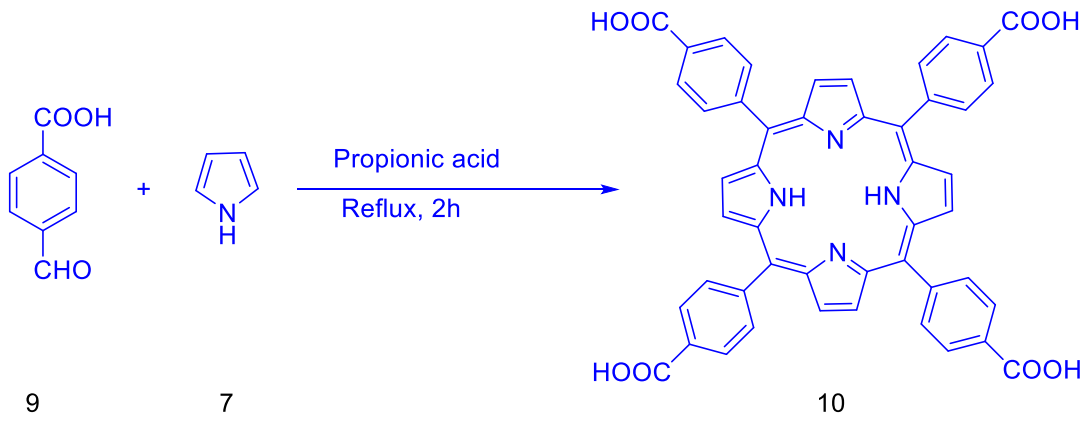

Scheme 3.3. The synthesis of tetracarboxyphenyl porphyrin (TCPP).

The synthesis of TCPP (**10**) was confirmed by the peak observed in the high shielding area (at δ = -2.96ppm) in the ^{1}H NMR spectrum due to the ring current. The ^{1}H NMR showed a singlet at δ = 8.77ppm, which was attributed to the pyrrolic β-protons. Furthermore, a quartet was observed at δ = 8.21ppm, and was assigned to the 16 phenylic protons. A broad singlet at δ = 13.20ppm was attributed to the 4 protons of the carboxylic group. UV/Vis spectroscopy showed the characteristic Soret band and Q-bands at 418, 512, 546, 588 and 645nm in methanol. Furthermore, mass spectrometry showed a molecular ion at MH^{+}/z = 791 which is the molecular weight of protonated TCPP.

3.5. Preparation of TCPP polyion complexes

In order to prove polyion formation, it was necessary to study the solubility of TCPP (**10**) in isolation and compare it to TCPP bound within the polyion. This was done using UV/Vis spectroscopy. For the purpose of this part of the study, the aim was to establish that a polyion had formed and not a simple polymeric micelle. This was accomplished by conducting UV measurements on a number of solutions above and below of the CMC of the homo micelles of mPEG-PDMA (DB) (**5C**) independently at a concentration above 0.1mg/mL (**Figure 3.4**).

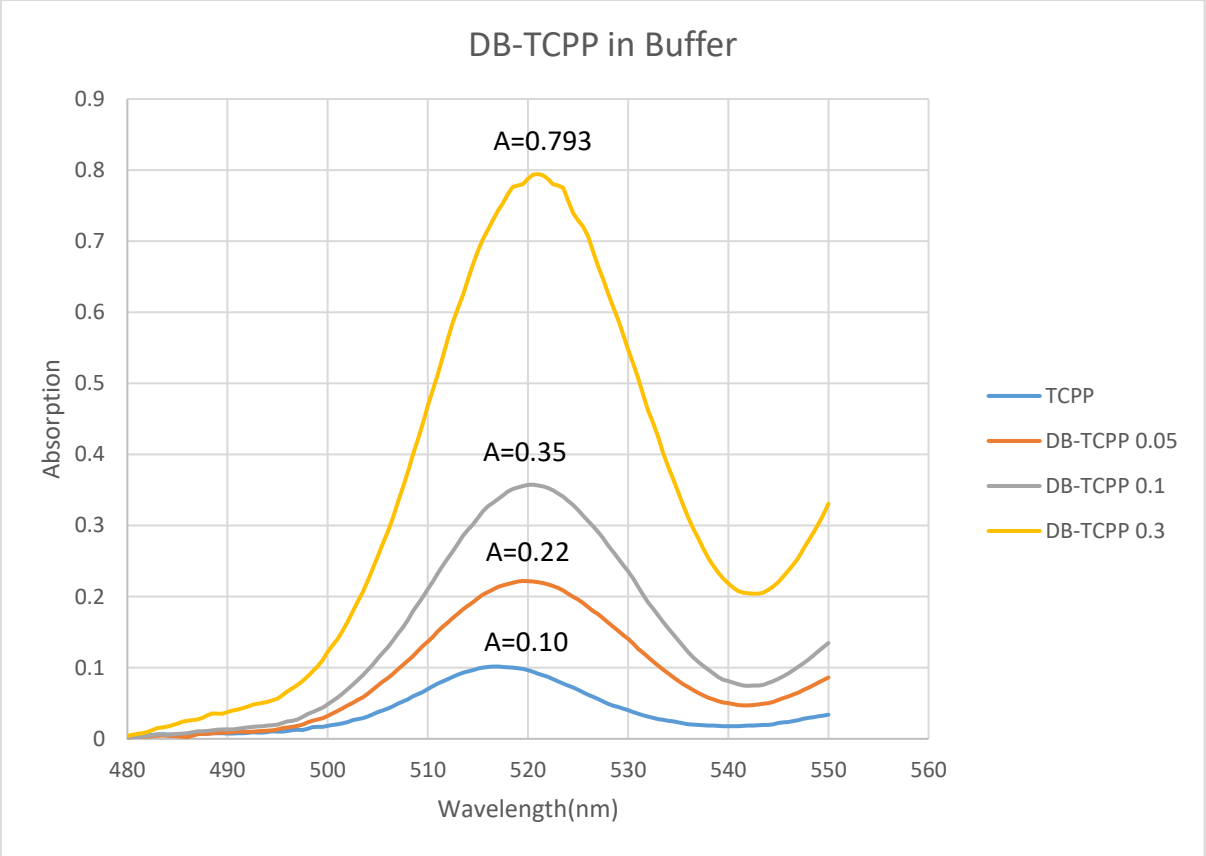

Figure 3.4. UV spectra of TCPP in buffer (pH 7.4) and DB-TCPP in Buffer (pH 7.4) at different concentrations.

The higher absorption tells us that we have more TCPP in solution. This is due to it being encapsulated within a polymeric host. This is supported by a change in λ_{max}, indicating that the porphyrin is in a non-aqueous environment. However, we do not know whether the TCPP is inside a simple polymeric micelle or a polyion. To determine which, we need to dilute below the CMC and see what happens to the absorption and λ_{max}. It can be clearly seen that λ_{max} different for encapsulated. Therefore, all encapsulated occurred even below the CMC. Moreover, the absorption values as a function of the concentration of the mPEG-PDMA (**5**) (**Figure 3.5**).

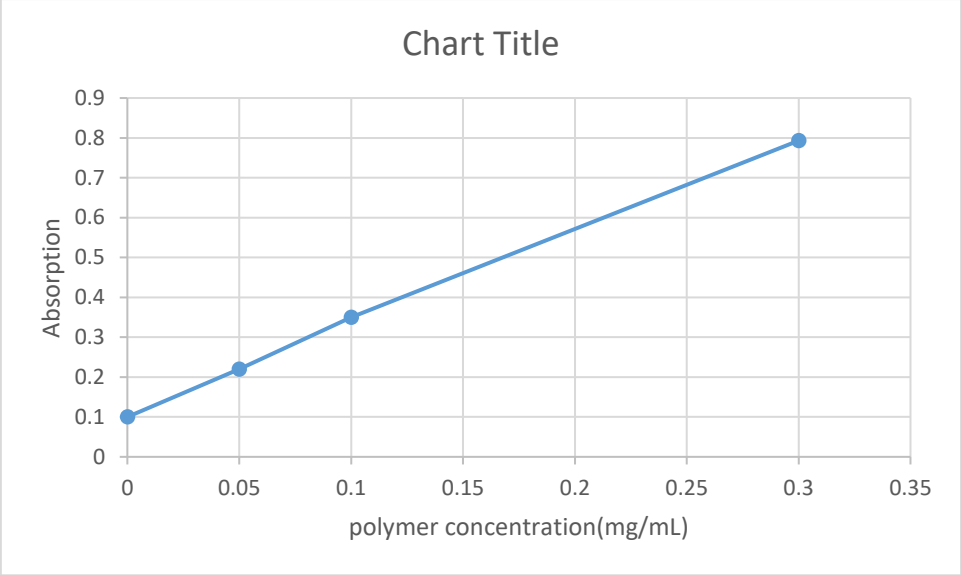

Figure 3.5. The plot of absorption against the concentration of the mPEG-PDMA.

Figure 3.5 apparently shows a linear relationship between the absorption and the concentration of the polymer. This could be attributed to micelle (polyion and/or free porphyrin. If we had a micelle or polyion, then the λ_{max} of the porphyrin would be higher than the free (non-encapsulated) porphyrin. When the polymer concentration below the CMC, then there is no micelle and would predict a change to lower λ_{max} of the porphyrin is not encapsulated. Furthermore, the experiment shows that the λ_{max} is not changed when the concentration drops below the CMC. Therefore, TCPP still encapsulated (and inside a non-aqueous environment), but the host is not a micelle. This host could be a polyion, but need to measure the size

Moreover, an absorption of 0.79 was recorded for a concentration of 0.3mg/mL, while the absorption intensity for free TCPP was 0.1. Therefore, this is subtracted from the polyion complex absorption, so the actual absorption intensity is 0.69. If we do the same for diluted samples, an absorption intensity of 0.25 and 0.12 is achieved for 0.1mg/ml and 0.05 mg/mL solution, respectively. Therefore, when this solution is diluted by 3 times (0.3-0.1 mg/mL) it becomes apparent that the absorption intensity drops by 3 times.

In addition, if it is diluted from 0.1 mg/mL by half to 0.05 mg/mL, it also drops by half. As such, we are confident that that we are dealing with a stable polyion complex and not micelles.

In addition, DLS measurements of these solutions indicated that the presence of large aggregates above and below the CMC. DLS also revealed that no aggregates formed when the mPEG-PDMA (**5C**) was studied at concentration below the CMC (0.1mg/mL) and in the absence of TCPP. In fact, DLS could not detect any large species even when the diblockcopolymer was studied at a concentration above the CMC, even when the neutral TPP (**8**) was present. These results support the conclusion that polyion complexes hade formed.

The polyion complex was prepared as follows: a solution of mPEG-PDMA (**5C**) in MeOH at a concentration of 5 mg/mL (stock solution 1) was prepared. Another solution of TCPP in MeOH (stock solution 2) was prepared at 5mg/mL. From stock solution 1, a diluted solution was prepared in MeOH. Likewise, a dilute solution was prepared from stock solution 2. The solutions were then mixed and the new solution stirred for five minutes. Upon removal of the solvent by rotary evaporation, 5mL of PB (pH 7.4) or water was added and the solution stirred at room temperature for 5 minutes. In order to eliminate any insoluble free porphyrin, the solution was then filtered through a disposable syringe filter (0.45μm). The resulting red solution was then analysed.

To ascertain the appropriate stoichiometry for the polyion complex aggregates, the best ratio of mPEG-PDMA:TCPP needed to be determined through experimentation. This ratio governs the electrostatic interaction between polycation and polyanion, and subsequently, the behaviour and properties of the resulting polyion. mPEG-PDMA:TCPP ratios of 1:1, 1:2 and 2:1 w/w were studied. It was desirable to have a

ratio, which produces polyion complexes that contains the highest amount of TCPP, as the concentration of porphyrin is important for PDT. When the ratio was 1:2, a large amount of free TCPP precipitated and the complex was not overly soluble in an aqueous solution, Furthermore, the process of filtration needed to be repeated in order to eliminate the excess of TCPP. When the ratio was 2 mPEG-PDMA and 1 TCPP the intensity of the colour was very weak, which indicates very little porphyrin had been incorporated into the polyion complex. When the ratio was 1:1, there was very little precipitate, there was TCPP a strong colour, and the product was a highly soluble complex in aqueous solution. These ratios were also assessed by DLS, which showed there was no clear aggregate for the 1:2 or 2:1 system. Conversely, DLS measurements for the 1:1 ratio indicated an average size of 200-250nm (**Figure 3.6**).

The TCPP contains exactly four carboxylic groups, and if we suppose that mPEG-PDMA (**5C**) contains 40 amino groups. As such, the stoichiometry can be estimated. The MW of mPEG-PDMA (**5C**) is around 9000 g/mol. Therefore, the number of moles (in 1g/L) is 1.1E-4. If we multiply this by 40, the number of amine can be estimated as 4.1 E-3. Number of moles of TCPP (in 1g/L) is 1 E-3. Since each TCPP has four COOH groups, the moles of carboxylate equals 4 E-3. These stoichiometric calculations indicated that at a 1:1 w/w ratio, the number of moles of amine and carboxylic acid. This means that the number of positive charges are the same as the negative charges, giving a stoichiometric polyion complex. Therefore, we concluded that the 1:1 ratio is the optimal for mPEG-PDMA (**5C**) and TCPP and therefore it was dependent in this study.

Dynamic light scattering (DLS) measurements had indicated a solvated size of 200-250nm. To confirm size, transmission electron microscopy (TEM) techniques was employed. TEM measurements showed spherical particles of varying size up to 200nm (**Figure3.7**).

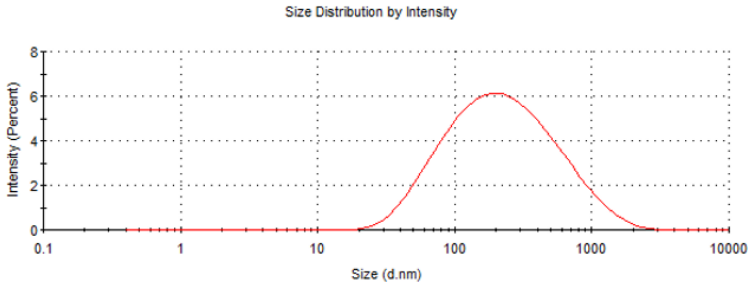

Figure 3.6. DLS measurements of DB-TCPP polyion complexes at 25 ºC.

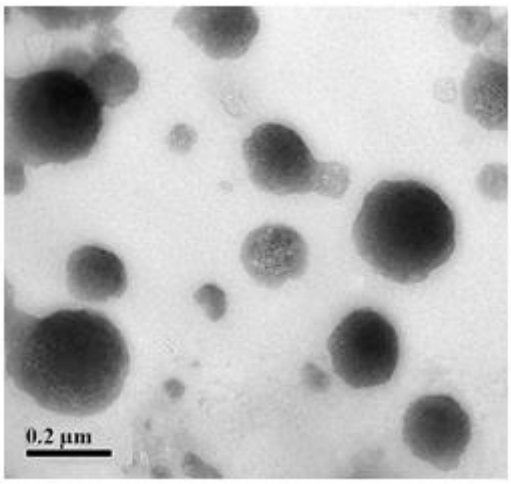

Figure 3.7. TEM image of DB-TCPP polyion complex particles.

3.6. In vitro drug release studies

As the formation of polyion complexes had been succeeded, the next step was to determine the stability of the polyion complexes by studying releases of TCPP from the polyion complex. The amount of TCPP released is an indicator of the stability of polyion aggregates. The stability of the polyion is very important in PDT as the aggregate must reach the target tissues in order to deliver the photosensitiser and this can be facilitated by the EPR effect. Although the pH of the physiological system is 7.4, the pH inside a cancer cell can be as high as 5. Therefore, the stability study will be carried out using polyion aggregates at pH 7.4 and pH 5. It is expected that the polyion complexes will

remain stable at pH 7.4 and retain the TCPP within the polyion as the electrostatic interaction will not be affected at this pH when moving through the circulatory system. Conversely, in a tumour cell, the carboxylate groups bound to positive amino groups will be protonated. If this happens, the majority of the electrostatic links will be broken, resulting in disassociation of the polyion complex. At this point, most of the TCPP photosensitiser will be released. This could lead to an effective delivery system for photodynamic therapy (PDT) process, although release of the PDT photosensitiser may not be necessary.

The release of TCPP from the polyion complexes was studied in the following manner. Polyion complexes in a buffer solution were placed inside a dialysis membrane bag. This bag was transferred into a flask containing phosphate buffer solution and equipped with a magnetic stirrer. The dialysis media was placed in a water bath, which was heated to 37 ^{o}C. 3 aliquots were withdrawn from the bulk solution and replaced by aliquots of fresh buffer solution. Following this, the removed solution was studied by UV to measure the amount released of any TCPP by monitoring the Soret band absorption at 414nm.

All concentrations were calculated using Beer-Lambert analysis. The concentration remaining is the difference between the initial concentration and the concentration outside the dialysis bag. The experiment was conducted over 14 days and the percentage of TCPP remaining in the bag was plotted versus time (**Figure 3.8).** The ratio of mPEG-PDMA diblockcopolymer to the porphyrin (DB:TCPP) was fixed 1:1 (w/w). UV measurements revealed that the release of TCPP from the DB/TCPP polyion at pH 7.4 over14 days was very low (**Figure 3.8).**

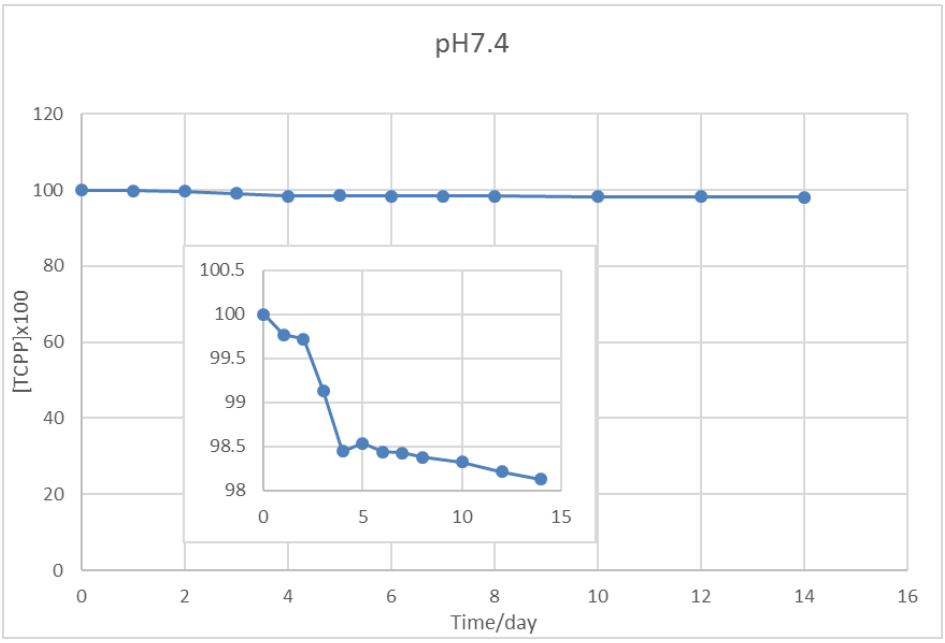

Figure 3.8. In vitro TCPP release from DB-TCPP polyion complex at pH 7.4 PB against time. Insert shows close up of the initial release.

This figure shows that the mount of TCPP released from the DB/TCPP polyion was less than 2% after 6 days. This percentage reflects the stability of the formed particles. For the purpose of comparison, the same dialysis technique was repeated for TCCP on its own. The UV control experiment revealed that 95% of the TCPP moved from the dialysis bag to the external bulk solvent (**Figure 3.9).**

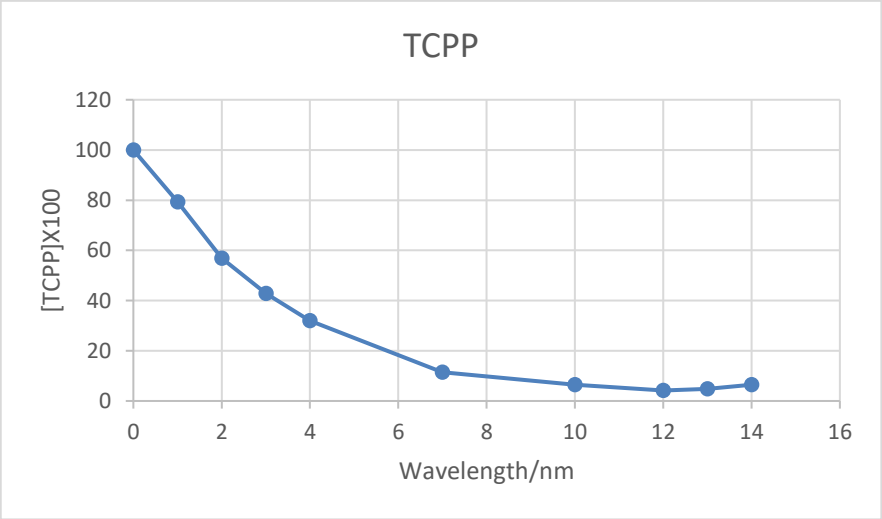

Figure 3.9. In vitro TCPP transferred from dialysis bag to dialysis solvent in pH 7.4 PB versus time shows a close up of the initial release.

The TCPP release from DB/TCPP polyion complex was also investigated at pH 5.0. The UV measurements results revealed that the amount of released TCPP was slightly more than that at pH 7.4, reaches 4% over 6 days (**Figure 3.10**).

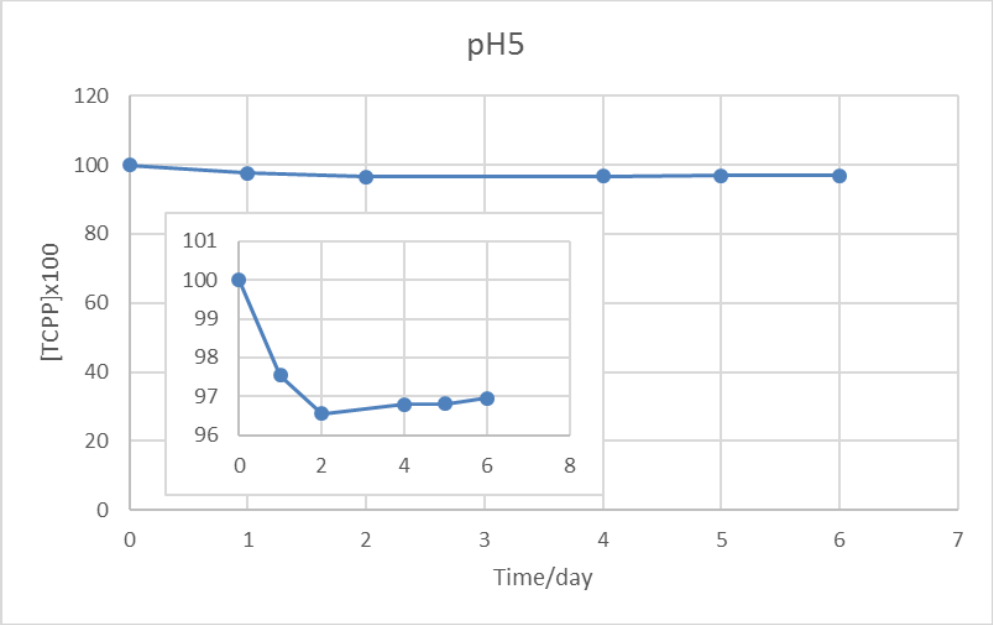

Figure 3.10. In vitro TCPP transferred from dialysis bag to dialysis solvent in pH5 PBS against time shows a close up of the initial release. Insert shows a close up of the initial release.

This further confirms the stability of the DB/TCPP polyion complexes even in an acidic solution. This indicates to strong electrostatic links between the two components of the polyion complex. It is also likely that bulk water (and acid) cannot easily enters the highly hydrophobic portions of the polyion. As such, the carboxylate cannot be protonated. Thus, it is could be concluded that the polyion complex plays very important role in preventing the leakage of the drug. This would minimise any potential side effects and help to ensure that the drug is only delivered to the tumour tissues (EPR effect). Consequently, this may leads to enhanced photodynamic therapy. However, less stability at pH 5 would have been favoured with regards to the general application of polyion complexes for drug delivery.

3.7. Synthesis of tetrahydroxyphenyl porphyrin (THPP) (12)

In order to try and develop a general polyion complex drug delivery system, we needed a weaker interaction. As such, considered the use of phenol for the acidic portion of the polyion. Phenols are much less acidic and would be easier than carboxylate. Therefore, we decided to synthesise tetrahydroxyphenyl porphyrin. Tetrahydroxyphenyl porphyrin (THPP) (**12**) was prepared by the coupling of 4-hydroxybenzaldehyde (**11**) and pyrrole (**7**) in propionic acid. The black slurry obtained was filtered and washed with a mixture of propionic acid/ethanol, and chloroform to give THPP into a shiny purple solid **(scheme 3.7)**.

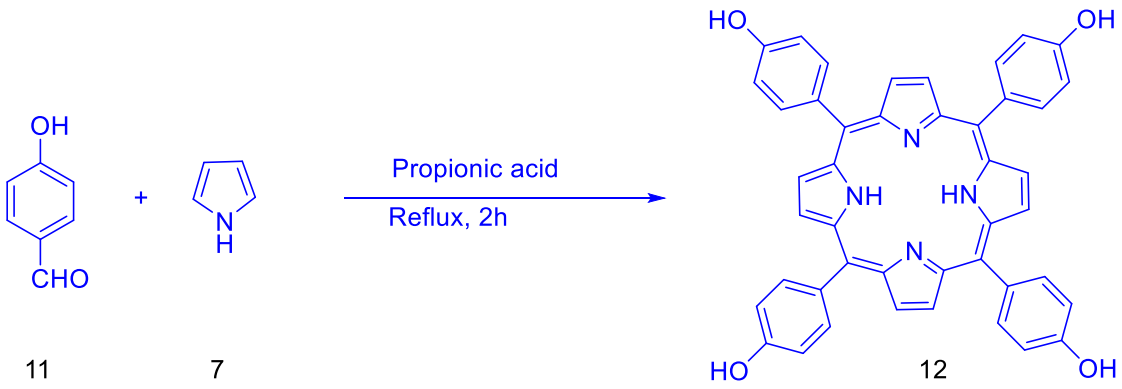

Scheme 3.7. The synthesis of tetrahydroxyphenyl porphyrin (THPP).

THPP (**12**) synthesis was confirmed by ^{1}H NMR. The presence of singlet peak at -2.89ppm in the upfield region attributed to two NH protons. A singlet peak was apparent at δ = 9.99ppm due to the four protons of phenyl groups. Also, a singlet at δ = 8.87ppm was attributed to the eight pyrrolic protons. Two doublet were observed at δ = 7.99, 7.2ppm and attributed to the sixteen *meta* and *ortho* phenylic protons, respectively. The UV/Vis spectrum exhibited a characteristic Soret band at 418nm, and Mass

spectrometry measurement generated a molecular ion at 679 M/z, which is the molecular weight of THPP.

3.9. THPP polyion complex preparation

To prepare the THPP polyion complex, the same procedure used for TCPP was followed. A solution of mPEG-PDMA (**5C**) in MeOH (stock solution 1) was prepared. Another solution of THPP in MeOH (stock solution 2). From stock solution 1, a diluted solution was prepared in MeOH. Likewise, a dilute solution was prepared from stock solution 2. The solutions were mixed and the obtained solution stirred for 5 minutes. Upon removal of the solvent by rotary evaporator, 5mL of PB (pH 7.4) or water was added and the solution stirred at room temperature for 5 minutes. To eliminate any insoluble free porphyrin, the solution was then filtered through disposable syringe filter (0.45μm). The resulting red solution was ready for the analysis.

The polyion complex was prepared at a ratio of 1:1(w/w). Unexpectedly, the residual precipitate (after removing MeOH) was insoluble in buffer or water unless warmed up. In addition, the colour of the solution was very pale. This indicated that a marginal amount of THPP had been incorporated within the polyion. This experiment was repeated at ratios of 1:2 and 2:1, but the result was the same. DLS measurements were carried out for these solutions, which indicated that there were no large particles present. This could be attributed to the fact that no many of the phenol groups had ionised. Consequently, the concentration of the formed polyion complex is marginal. As the intensity of the colour is related to the concentration of porphyrin, which is important for PDT.

One of the aims was to synthesise a simple and large porphyrin containing macromolecules that could be used as a stable macromolecular photosensitiser.

Although we had already demonstrated that TCPP was a good cross-linker for a polyion, we wanted to explore other systems that could form more stable polyion complex.

Having successfully prepared a polyion complex between TCPP (which has only four carboxy groups) and mPEG-PDMA (**5C**), the next target in our research was to study the preparation of a new polyion system formed between mPEG-PDMA and a compound with more charge's and a size that is larger than porphyrins. This compound may be more stable, as it contains many carboxylate groups. In addition, this compound should be formed from well-defined globular macromolecules with many terminal groups. Large, globular and well defined compounds such as dendrimers has been proven to form polyion complexes with potential applications in photodynamic therapy (PDT)[110-114]. Dendrimers however are hard to synthesise and needs prolonged reaction times. Accordingly, a hyperbranched polymer was chosen because their synthesis is much easier than their corresponding dendrimers. As our ultimate target was the synthesis of photosensitiser for PDT, a porphyrin-functionalised hyperbranched polymer bearing carboxy terminal groups was synthesised. This compound can form polyion complex with mPEG-PDMA in a similar manner to a dendrimer. This polymer can form a polyion with mPEG-PDMA (**5C**) with a potential application in PDT. This can be done using a porphyrin with many negative charges such as a porphyrin in the centre of a hyperbranched polymer with terminal carboxylates. This system could be synthesised using TCPP and the AB_2 monomer, 5-actoxyisophthalic acid (AIPA).

3.9. Synthesis of 5-actoxyisophthalic acid (AIPA) (13)

The synthesis of the AB_2 monomer, 5-actoxyisophthalic acid (AIPA) (**13**) was the first step in preparation of hyperbranched polymer bearing globular terminal carboxylic groups. The AIPA (**13**) can undergo melt condensation polymerisation, which directly forms hyperbranched polyesters bearing carboxylic acid terminal groups.

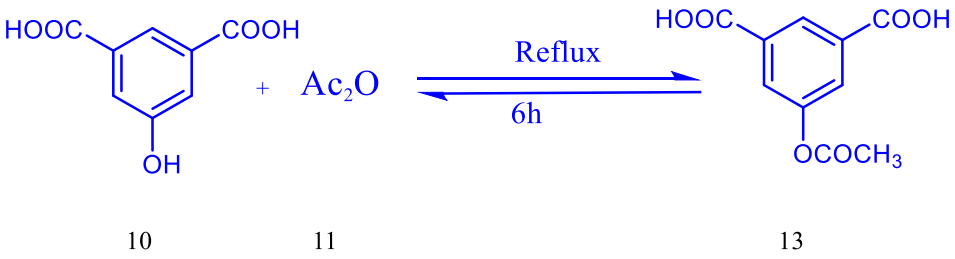

10 11 13

Scheme 3.8. The synthesis of 5-acetoxyisophthalic acid (AIPA).

5-Actoxyisophthalic acid (**13**) was prepared upon heating mixture of 5-hydroxyisophthalic acid (**11**) and acetic anhydride at reflux (**Scheme 3.8**). After 6 hours, the mixture was subjected to a high vacuum to eliminate the excess acetic anhydride. The crude product was then purified via recrystallization from ethyl acetate/ petroleum ether. AIPA (**13**) was isolated in 95% yield and the structure confirmed using ^{1}H NMR spectroscopy. The spectrum showed the presence of a singlet peak at δ = 2.32ppm, which was attributed to three protons in the methyl ester group, as well as a doublet peak and a two proton triplet in the aromatic region. The ^{1}H NMR spectrum also shows a broad peak corresponding to the carboxylic acid groups proton at δ =13.5ppm. Mass spectrometry also confirmed the preparation of AIPA (**13**) and showed the exact molecular ion peak at m^+/z = 224.

3.10. Synthesis of a hyperbranched polymer bearing carboxylic acid terminal groups (HB-COOH) (14)

The synthesis of a porphyrin-functionalised hyperbranched polymer bearing many terminal carboxylic acid groups (PH-HB-COOH) would be carried out to examine whether or not that this polymer could be incorporated within a polyion. The stability results would be compared with the corresponding results obtained for the mPEG-PDMA/TCPP polyion system. However, before synthesising the porphyrin cored hyperbranched polymer bearing terminal carboxy groups, we decided to test the methodology by starting with the unfunctionalised hyperbranched polymer bearing terminal carboxy groups, HB-COOH. This was simpler to construct and could be used to study the stability of any polyion complex. The HB-COOH is not soluble in water. Therefore, polyion complex aggregates would be confirmed using solubility experiments in an aqueous solution and DLS measurements. If the mixture of HB-COOH with mPEG-PDMA (**5C**) (DB) is soluble in aqueous media and DLS confirmed the presence of large particles, then this would be a good evidence for the formation of the polyion complex.

The simple unfunctionalised hyperbranched polymer bearing terminal carboxylic groups (HB-COOH) was synthesised via melt condensation polymerisation as follows[128] : AIPA (**13**) was placed into a two neck round-bottomed flask equipped with a distillation kit in order to collect the residual products. The system was evacuated and flushed with nitrogen. The mixture was then heated to 250 ^{o}C under a nitrogen atmosphere. The system was then subjected to a strong vacuum. The vacuum was necessary to remove the acetic acid formed during the polymerisation, which would result in an unwanted reversible reaction. A foam formed when the vacuum applied, but

collapsed when the vacuum was turned off. The system was cooled to room temperature, and a mixture of THF/water added. Water is very important, as it breaks-down any anhydride linkages formed during the reaction. The mixture was heated at reflux for 5 hours, and the product then precipitated using water. The product was dissolved in THF and precipitated from diethyl ether. The HB-COOH was collected and dried under vacuum to give a white solid (**Scheme 3.9**).

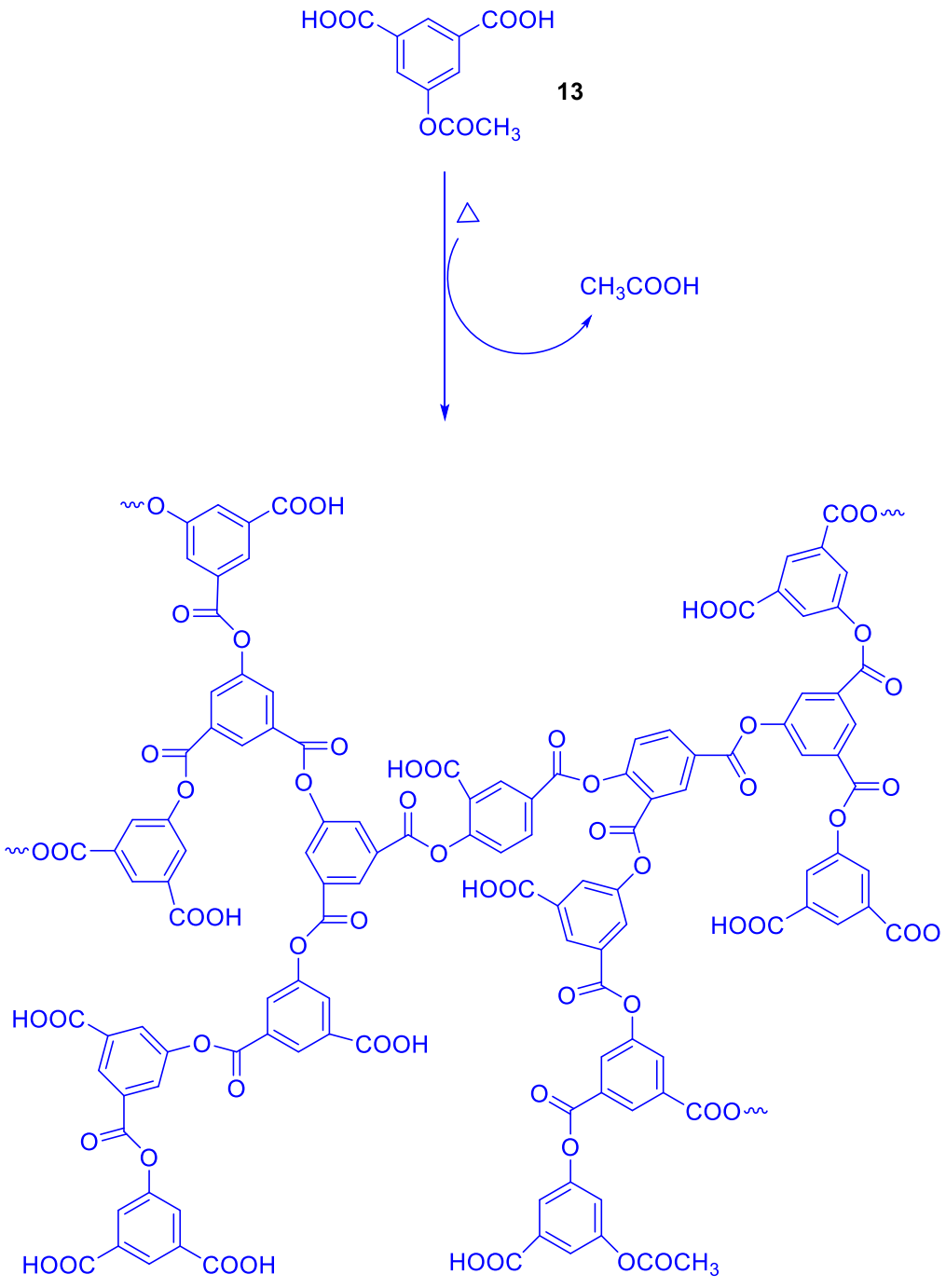

Scheme 3.9. The synthesis of hyperbranched polymer bearing carboxylic acid terminal groups (HB-COOH).

The synthesis of HB-COOH (**14**) was partially confirmed using ^{1}H NMR spectroscopy. The presence of broad peaks between $\delta = 7.5 – 8.84$ppm, corresponding to the aromatic protons, and the broad peak at $\delta = 13.5$ppm assigned to the carboxylic group. Unfortunately, we were unable to determine the molecular weight by GPC measurements as the HB-COOH was absorbed to the column and was not very soluble in THF/DMF. Therefore, it was necessary to make the HB-COOH more soluble and prevent it absorbing to the column via converting the carboxylic groups into terminal ester groups.

Converting the carboxylic groups in the hyperbranched polymer (HB-COOH) (**14**) into ester groups was carried out over two steps (**Scheme 3.10**). Firstly, the carboxylic groups were converted into acid chlorides. This was performed upon the addition of thionyl chloride to a solution of HB-COOH (**14**) in THF and heating the reaction mixture at reflux for 6 hours. THF and excess thionyl chloride were then removed by vacuum. The crude product was then used directly for the next step (assuming a 100% yield). Secondly, the acid chloride groups were converted into ethyl ester groups by stirring in ethanol with triethylamine for 12 hours at room temperature. The triethylamine chloride by-product was removed by filtration and the target product precipitated by adding water. The HB-COOEt (**15**) was isolated as a colourless solid.

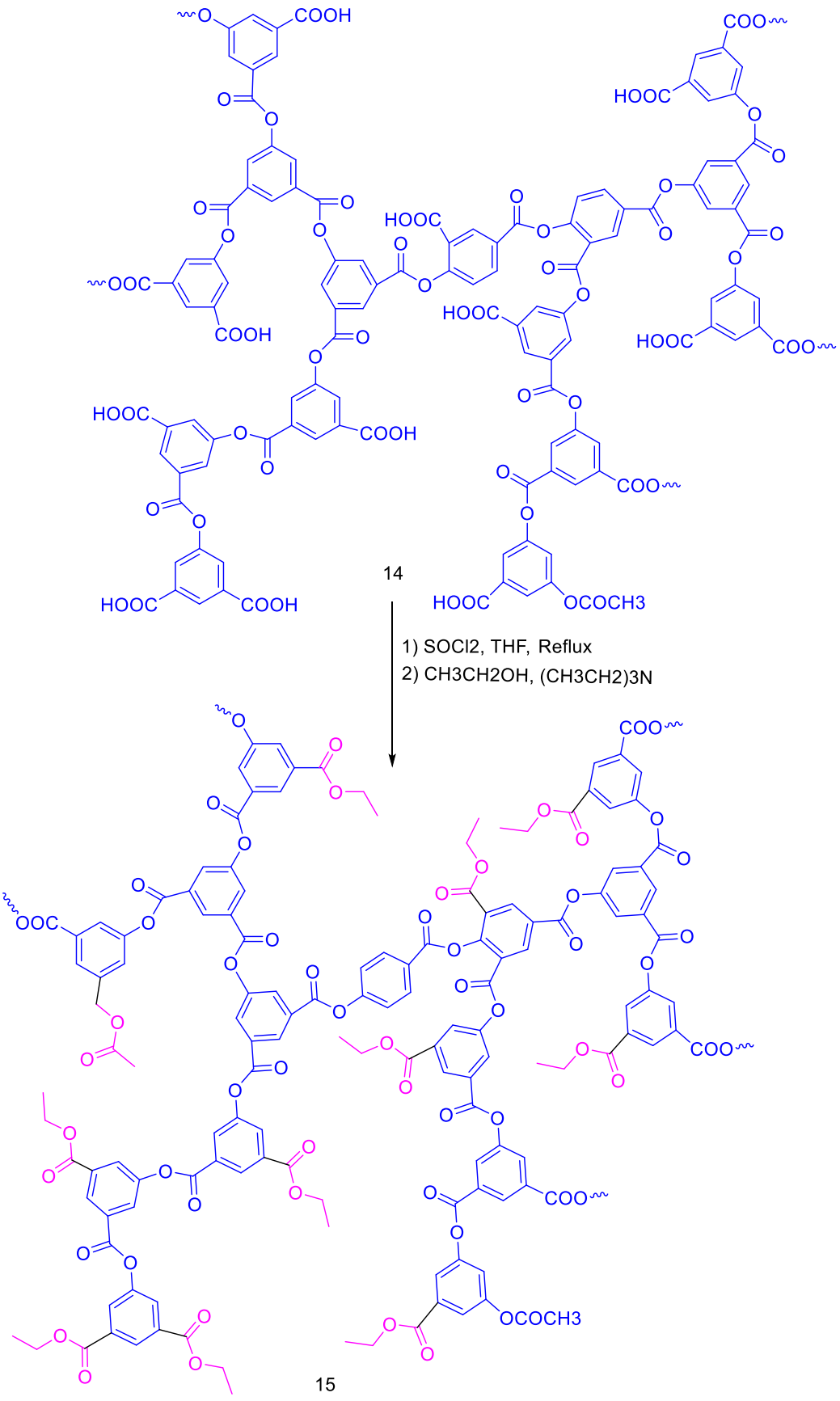

Scheme 3.10. The synthesis of a hyperbranched polymer bearing ethyl ester terminal groups (HB-COOEt).

The ^{1}H NMR spectrum confirmed the conversion of HB-COOH (**14**) to HB-COOEt (**15**) showing loss of the broad peak at δ = 13.5ppm (assigned to the carboxylic groups) and the presence of triplet and quartet at δ = 1.42 and δ = 4.43ppm, which is attributed to methyl and the methylene groups of the ethyl ester. In addition, the broad peaks observed between δ = 7.51 – 8.84ppm for the aromatic protons, shifted slightly to δ = 7.91-9.06ppm. Moreover, the IR spectrum exhibited a stretch at 1719 cm^{-1} which indicated the presence of an ester group. The GPC measurements confirmed the formation of a polymer and gave an estimated M_n of 3000 g/mol. As ester groups would not add much to the hydrodynamic volume of the hyperbranched polymer, we assumed that HB-COOH (**14**) had a similar molecular weight.

3.11. Formation of unfunctionalised hyperbranched polymer polyion complex

As the synthesis of HB-COOH (**14**) was determined, the next step was to investigate whether or not this polymer can form polyion complex with mPEG-PDMA (**5C**). The formation of polyion will be confirmed by solubility in aqueous medium and by DLS. If the mixture of HB-COOH (**14**) and mPEG-PDMA (**5C**) is soluble in water and DLS showed a large aggregates, that is evidence of formation polyion complex. The preparation of polyion complex was conducted using the same procedure that was used for preparation of polyion complex from TCPP and mPEG-PDMA. It was necessary to study appropriate ratio of DB: HB (w/w). A methanolic solution of HB-COOH and mPEG-PDMA (DB) at various ratios (of DB: HB-COOH (w/w) was evaporated. Buffer solution (was then added to the solid mixture and a soluble completely was observed. This experiment was repeated, but instead of buffer water was used. Again the solid residual completely dissolved. Since the HB-COOH is insoluble in water or Buffer (pH

7.4), it is very reasonable to assume that the solubility belongs to the formed polyion. Moreover, DLS measurements for these solutions revealed aggregates had formed with sizes between 100-130 nm (**Figure 3.11**).

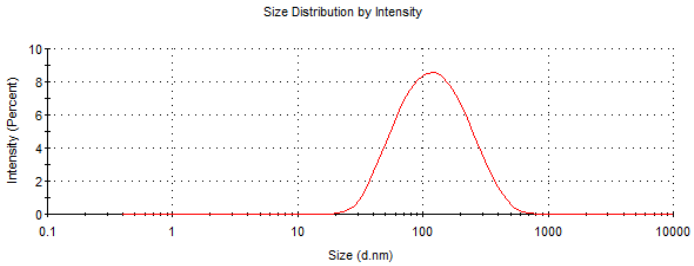

Figure 3.11. DLS measurement for HB-COOH polyion complex in aqueous solution.

The formed solution was left stable for two weeks. No change on the solution was observed. The solution remained transparent which indicated a good stability. As the number of carboxy groups in HB-COOH (**14**) were not determined, It is very hard stoichiometrically estimation the ratio optimal ratio of diblockcopolymer to HB-COOH (like what we done for TCPP polyion complex). Therefore we prepared different ratio of DB:PH-COOH which are 1:1, 1:2 and 2:1 (w:w). As the optimal polyion complex is that with pH around 7.4 (the physiological pH) because that means the number of carboxy and amino groups are almost equal. The pH measurement was carried out for each ratio in water and the obtained results were summarised in Table 3.2.

Table 3.2. pH, precipitate formation and solubility of DB/ HB-COOH polyion in water.

Ratio of DB:HB-COOH (w:w)	pH	Forming precipitate	Solubility at room temperature
1:2	7.4	Yes	Very poor
1:1	7.5	No	high
2:1	8.0	No	high

The data in the table shows that the 1:2 ratio has less pH, but the solubility of the obtained mixture is too low. Despite the solubility of the formed polyion complex at the ratio of 2:1 is high, but the pH was 8, which indicate that the solution is basic. This is attributed to the number of amino groups are highly more than the carboxy groups. The ratio of DB:HB-COOH at 1:1 shows a high solubility with pH close to 7.4. This indicates that 1:1 is the optimal ratio of DB:PH-COOH. From these results, it can be concluded that the polyion has been formed from HB-COOH and mPEG-DMAEMA. These results are encouraging for the synthesis of porphyrin incorporated hyperbranched polymer with terminal carboxylic acid groups (PH-HB-COOH).

3.12. Synthesis of a porphyrin cored hyperbranched polymer bearing carboxylic acid terminal groups (PH-HB-COOH) (16)

As the incorporation of unfunctionalised hyperbranched polymer within the polyion complex was determined, the next step in this study was the synthesis of porphyrin-functionalised hyperbranched polymer bearing terminal carboxy groups, PH-HB towards the preparation of a globular system for PDT that could be more stable with a better defined polyion complex when compared to the mPEG-PDMA/TCPP polyion system.

PH-HB-COOH (**16**) was prepared using the same procedure for the synthesis of HB-COOH (**14**), but included the addition 10% TCPP (as a core unit). AIPA (**13**) was placed into a two neck round-bottomed flask. The flask was equipped with a distillation kit in order to the collect by-products. The system was evacuated and flushed with nitrogen. The mixture was then heated under nitrogen atmosphere to 250 ^{o}C and an isotropic melt was observed. The system was then subjected to a strong vacuum at the same temperature for one hour. As before, a foam formed which, collapsed when the vacuum was removed. The system was then cooled to room temperature, and a mixture of THF/water was added to treat any anhydride linkages. The mixture was refluxed for 5 hours, and the product was precipitated using water. The product was re-dissolved in THF and then precipitated from diethyl ether. The PH-HB-COOH was collected and dried under vacuum to give a dark brown solid (**Scheme 3.11).**

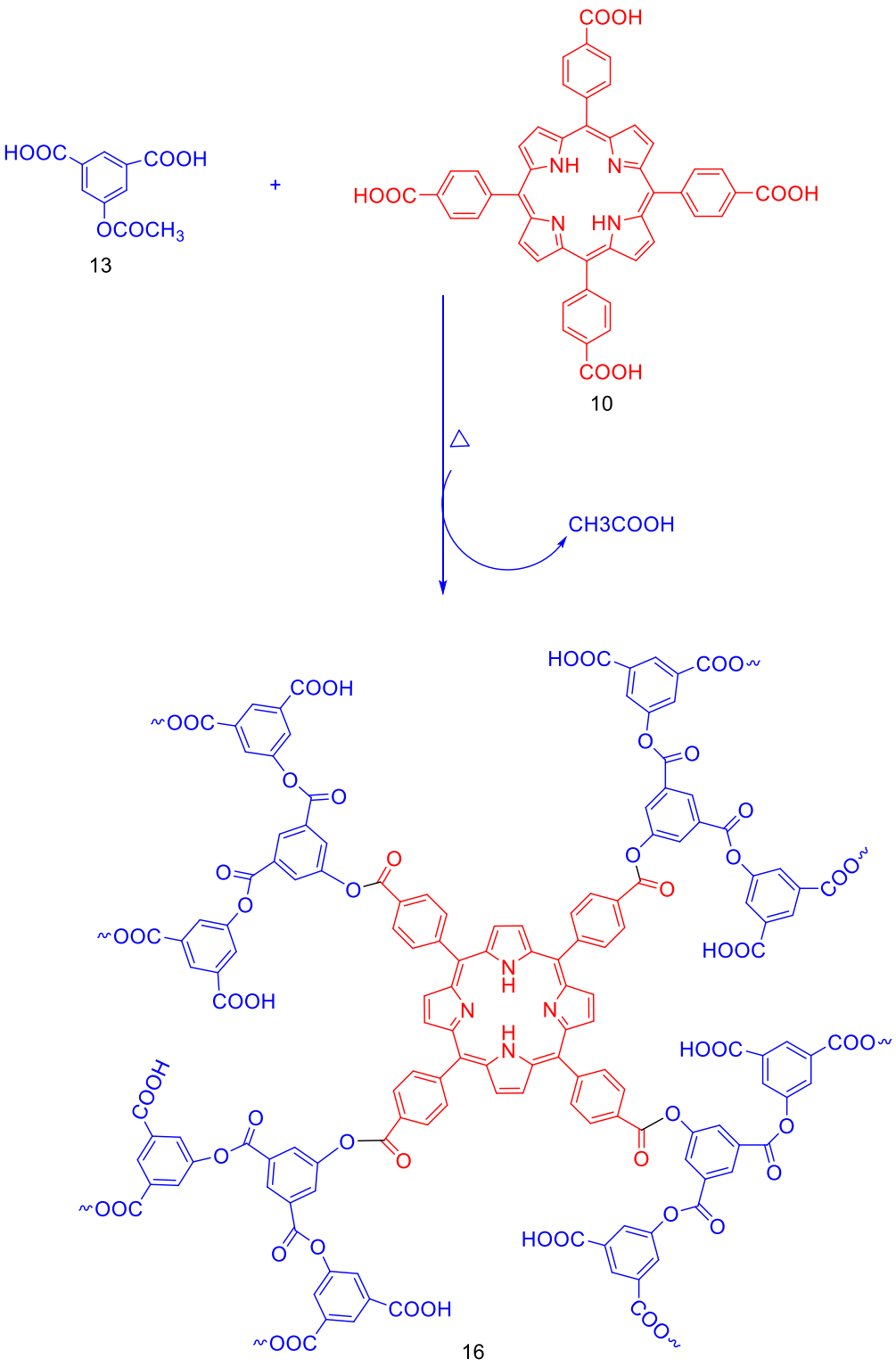

Scheme 3.11. The synthesis of a porphyrin core hyperbranched polymer bearing carboxylic acid terminal groups (PH-HB-COOH).

The ^{1}H NMR spectrum of PH-HB-COOH (**16**) showed a broad singlet peak at δ = 8.9ppm, which was not present in the spectrum of HB-COOH (**14**) (**Figure 3.12**). This peak was assigned to the pyrrolic protons of TCPP. The presence of a broad peak in the shielded region of the spectrum (δ = -2.93ppm) is also consistent with the presence of TCPP. The UV/Vis spectrum of PH-HB (**16**) in methanol showed the characteristic Soret band at 418nm for TCPP. This band was shifted by 3nm compared to the spectrum of TCPP in methanol. This indicates that TCPP was in a different environment, and confirmed likely incorporation of TCPP within the hyperbranched polymer.

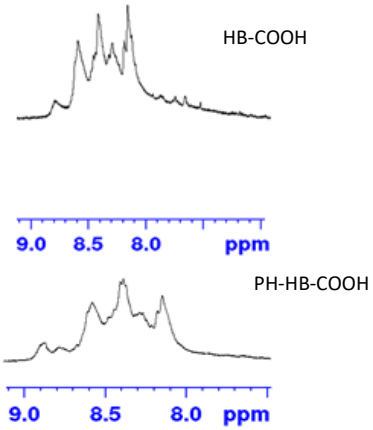

Figure 3.12. The ^{1}H NMR spectra (aromatic region) of HB-COOH and PH-HB-COOH.

3.13. Synthesis of porphyrin cored hyperbranched polymer bearing ethyl ester terminal groups (PH-HB-COOEt) (17)

As before, the product could not be analysed by GPC. Therefore, in order that GPC could be carried out and a molecular weight be determined for PH-HB-COOH (**16**), the carboxylic groups were esterified using the same procedure used for conversion of HB-COOH to HB-COOEt (**Scheme 3.12**). Converting the carboxylic groups in the hyperbranched polymer (PH-HB-COOH) into ester group was conducted over two steps.

Firstly, the carboxylic groups were converted into their corresponding acid chloride using thionyl chloride. The crude product was then used directly for the next step (assuming a 100% yield) and converted into their corresponding ethyl ester groups by stirring in ethanol with triethylamine.

The triethylamine chloride by-product was removed by filtration and the target product was precipitated in water. The obtained PH-HB-COOEt (**17**) product was isolated as was solid brown solid (**Scheme 3.12**).

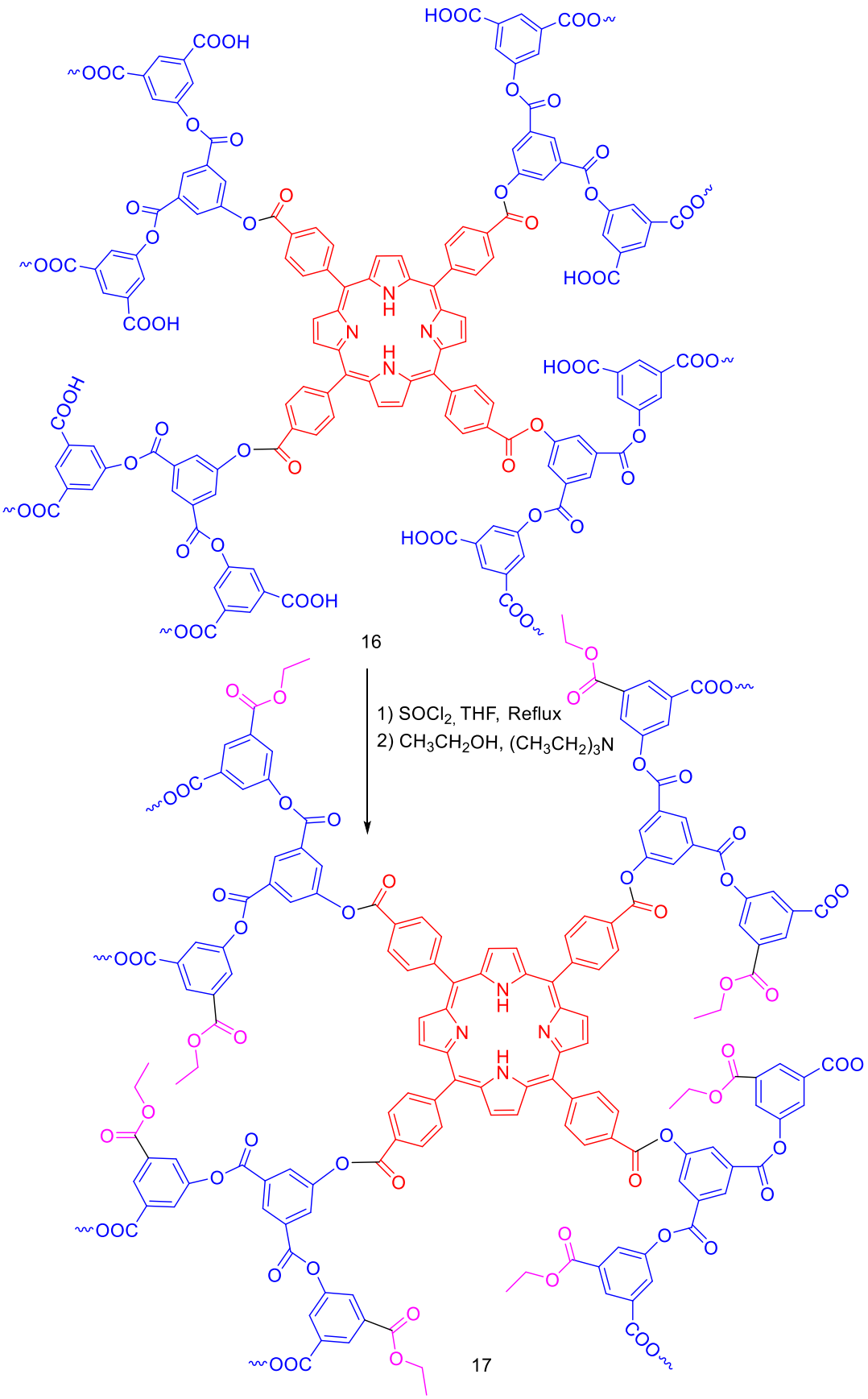

Scheme 3.12. The synthesis of porphyrin cored hyperbranched polymer bearing ethyl ester terminal groups (PH-HB-COOEt).

^{1}H NMR confirmed that PH-HB-COOH had been converted to PH-HB-COOEt. The loss of the broad peak at δ = 13.5ppm, which was assigned to the carboxylic acid groups proton and the presence of a new triplet peak at δ = 1.41 and quartet at δ = 4.46ppm were attributed to the newly formed ethyl ester groups. In addition, the broad aromatic peaks between δ = 7.5 – 8.33ppm were slightly shifted to (δ = 7.94 – 9.15ppm). Moreover, the IR spectrum exhibits a stretching band at 1715 cm^{-1}which indicated the presence of the ester carbonyl group. GPC measurements estimated a M_n of 2200 g/mol. A refractive index (RI) and UV detector (set at 415nm) were used and both gave quite similar traces confirms incorporation of TCPP in all molecular weight polymer. Furthermore, a M_n of 10,600 was calculated using ^{1}H NMR integration. Since the M_n calculated by ^{1}H NMR is higher than that obtained by GPC, we are certain that some of HBPs do not have a porphyrin core. Since molecular weight calculated by ^{1}HNMR over estimated and under estimated by GPC, we assumed that PH-HB-COOH had a molecular weight of 3000 g/mol.

3.14. Formation of porphyrin cored hyperbranched polymer (PH-HB-COOH) polyion complex

As incorporation of TCPP and HB-COOH into polyion was determined, the next step was to examine the capability of porphyrin cored hyperbranched polymer (PH-HB-COOH) (**16**) to incorporate into /and form polyion complex. To confirm the formation and stability of the DB/PH-HB polyion complex, and to prove that PH-HB-COOH (**16**) was incorporated into the polyion complex and not into individual micelles of mPEG-PDMA (**5C**) (DB), it was very important to run UV measurements were carried out at concentrations above and below the polymer CMC (0.1mg/mL). It was found that the solubility of PH-HB-COOH in phosphate buffer solution at pH 7.4 was very low

(**Figure 3.13**). The absorption should be high at a concentration of 0.3mg/mL, which is above the CMC. When this concentration was diluted 3 times to become 0.1mg/mL, the absorption should be a third of that observed at of 0.3 mg/mL. When 0.1mg/mL was diluted to 0.05 mg/mL, (less than the CMC) the concentration should be reduced by half. At this concentration no micelles were detected, which indicates that the PH-HB-COOH is inside the polyion complex. When the absorption is small or no absorption is observed, the absorptions observed at of 0.3 mg/ml and 0.1mg/mL originates from to the individual free porphyrin micelles.

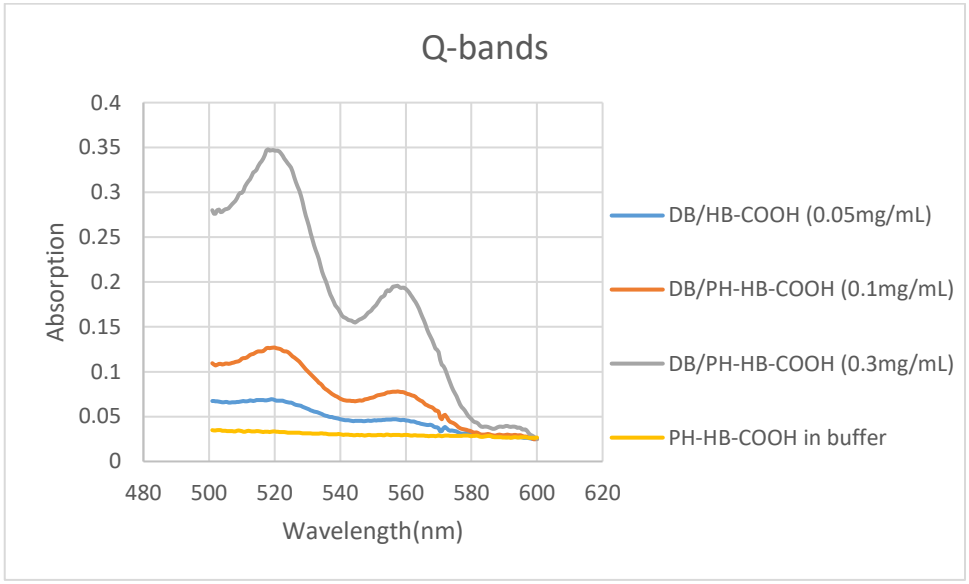

Figurer 3.13. The UV spectra of PH-HB and DB/PH-HB-COOH in PB (pH 7.4) at a concentration of 0.05, 0.1 and 0.3 mg/mL, respectively.

The figure showed a considerable base line drift, therefore, the absorptions was calculated using the difference in absorption between 520nm and 530nm (Δ Abs). The Δ Absorption of hyperbranched polymer in buffer (0.01M) at pH 7.4 was 0.002, which subtracted from those values, and the absorption intensities are summarised in (**Table 3.3).**

Table 3.3. The different in absorption of Q bands(Δ Abs) of DB/PH-HB-COOH at concentrations of 0.3, 0.1 and 0.05 mg/mL.

DB/PB-HB concentration (mg/mL)	Dilution	Predictable change in the absorption	Δ Abs	Decrease in absorption	% decrease in absorption
0.3	0	0	0.076	0	0
0.1	3	0.025	0.023	0.302	30.2
0.05	6	0.012	0.015	0.197	19.7

The data in the table 3.2 shows a Δ Absorption intensity of 0.076 for DB/PH-HB-COOH polyion complex at 0.3mg/mL. When this solution was diluted 3 times, the Δ absorption also decreased by 3 times to 0.023. If we dilute the solution from 0.1 to 0.05mg/mL, which is below the CAC, the Δ absorption intensity also decreased by 50%. AS The PH-HB-COOH almost insoluble, then these results confirms we are dealing with a stable polyion complex and not individual polymer micelles.

3.14.1. Preparation of the PH-HB-COOH polyion complex

The polyion complex of this system was prepared following the same procedure used for the mPEG-PDMA/TCPP system as follows. A solution of mPEG-PDMA in MeOH (stock solution1) was prepared. A solution of PH-HB-COOH in MeOH (stock solution 2) was prepared. From stock1 solution, a diluted solution was prepared in MeOH. Likewise, a dilute solution was prepared from stock solution 2. The solutions were mixed and the resulting solution was stirred for 5 minutes. After removal of the solvent using rotary evaporator, a certain volume of buffer solution or water was added and the solution stirred at room temperature for 5 minutes. To eliminate any insoluble PH-HB-

COOH, the coloured solution was then filtered through disposable syringe filter (0.45µM).

To discover the appropriate stoichiometry for this polyion complex system, the optimal ratio of DB:PH-HB-COOH needed was subsequently determined. This ratio decides the electrostatic interactions between the polycation and the polyanion, and subsequently, the behaviour and features of the formed polyion complex. DB:PH-HB-COOH ratios of 1:1, 1:2 and 2:1 w/w were studied. It was desirable to have a ratio which produces polyion complexes containing the most PH-HB-COOH, as the concentration of porphyrin is very small in the hyperbranched polymer and as an important requirement for PDT. Unlike TCPP, the number of carboxylic acid groups of PH-HB-COOH is not recognised because the precise polymer molecular weight was not determined. Therefore, we tried to find the best ratio that gives a neutral solution by the measuring of the pH of the polyion complex solution. On this basis, we prepared the polyion complex in water instead of buffer and then carried out the pH measurements for each ratio studied (**Table 3.4**).

Table 3.4. pH, colour intensity and precipitate formation of DB:PH-HB-COOH in water.

DB:HBP ratio	pH	Intensity	Precipitate	Solubility
1:2	6.7	Pale	Yes	Very poor
1:1	7.2	strong	No	high
2:1	7.7	pale	No	high

When the DB:PH-HB-COOH ratio was 1:2, the pH was 6.7. For the DB:PH-HB-COOH ratio of 2:1, the pH was 7.7. This indicates that stoichiometry is not perfect, as some of free acid or base is still present. The pH was 7.2 for DB:PH-HB-COOH ratio of 1:1, which results suggest that the DB:PH-HB-COOH ratio of 1:1 was optimal because the solution of DB/PH-HB-COOH polyion complex was close to neutral indicating that there were no acidic or basic groups left . This means that at this ratio, the negative charges (polyanion) was equal to the positive charges (polycation). In addition, this will help keep a neutral environment close to a physiological system. At the DB:PH-HB-COOH ratio of 1:2, some a free PH-HB-COOH still remained as a precipitate, and the solubility of the complex solubility in an aqueous solution was very low, which is confirmed by the low intensity of the colour. Therefore, this ratio was not suitable for further analysis. When the DB:PH-HB-COOH ratio was 2:1, the intensity of the colour was light and the sample was soluble, but the solution appeared to be dense, which indicated that there was a very little porphyrin in the polyion. When the DB:PH-HB-COOH ratio was 1:1, the obtained polyion complex solution was homogeneous, with high solubility in the aqueous medium, and strong colour. In addition, DLS measurements showed no clear aggregates at ta DB:PH-HB-COOH ratio of 1:2, but a at DB:PH-HB-COOH ratio of 2:1 and 1:1, aggregates with an average size of 90-140nm were observed (**Figure 3.14**).

DLS measurements, especially for the 1:1 polyion complex showed that the size of the aggregates formed was between 95-105nm with a narrow size distribution (**Figure 3.14**). These aggregates exhibited high stability in an aqueous solution over a pH range from 6 to 7.5. The stability was attributed to the interaction between the PDMA segment of mPEG-PDMA and the globular structure of the macroion. As before, we need to establish and test the stability under physiological conditions (at pH 7) and pH 5 (tumour

cell). Knowledge about stability could be very voluble in determining how the system could be used as a drug delivery system. Specially, whether or not these aggregates accumulate in a solid tumour before releasing the drug or immature release. TEM measurements shows small aggregates into large aggregates (**Figure 3.15).**

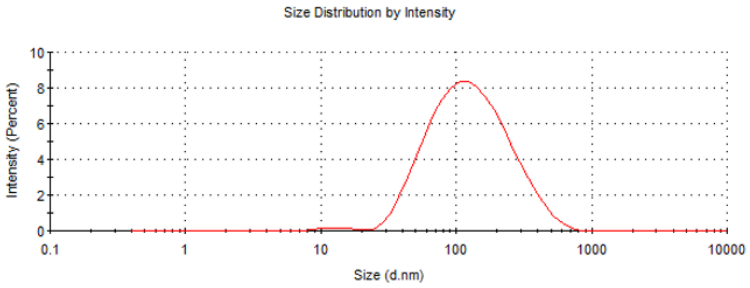

Figure 3.14. The DLS of the polyion complex particles comprised of mPEG-DMAEMA/ PH-HB at 25 ºC.

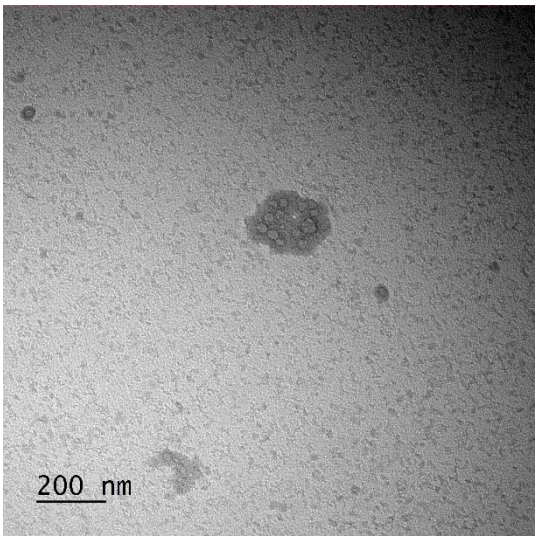

Figure 3.15. TEM image of DB/PH-HB-COOH, bar shows 200nm.

The aggregate size is promising with regards to a long blood circulation half-life, a characteristic is necessary for effective drug delivery systems (DDS). In DDS, the size of the aggregates is necessary for the EPR effect.

3.14.2. In vitro drug release studies

PH-HB-COOH release from the mPEG-PDMA/PH-HB-COOH polyion complex was studied at pH 7.4 phosphate buffer solution (PB) for 10 days. The procedure used to study the release of TCPP from the mPEG-DMAEMA/TCPP polyion was follows. A certain amount of the mPEG-PDMA /PH-HB-COOH polyion complex in PB (pH 7.4) was charged into a dialysis bag. This bag placed in a flask containing PB (pH 7.4) equipped with a lid and a magnetic stirrer. The dialysis system was then placed into a water bath at temperature at 37 ^{o}C with stirring speed of 100 rpm. An aliquots were withdrawn from the bulk solution and replaced with aliquots of fresh buffer solution. The aliquot was studied using UV/Vis spectroscopy to measure the amount of PH-HB-COOH released by monitoring the Soret band absorption of the porphyrin within PH-HB-COOH at 421nm. From the UV absorbance spectrum, the molar concentration (C_0) of the polyion solution in the bag was calculated before placing the bag into the dialysis solution. Then, the concentration of the released PH-HB-COOH in the flask (C_f) was calculated from the UV absorption after 1 day from the placing the bag into the dialysis solution. C_F was subtracted from C_0 to calculate the molar concentration of PH-HB-COOH remaining in the bag (C_t). The percentage of released polymer was calculated using C_t/C_0 x100. This process was repeated for several days and the obtained data was plotted as a function of time (days).

It was expected that that the amount and rate of PH-HB-COOH released would be similar or lower to that of the TCPP polyion system. This is due to the higher number of negative charges compared to TCPP and as such, the electrostatic interaction should be larger. The data from the UV measurements is shown in **Figure 3.16**.

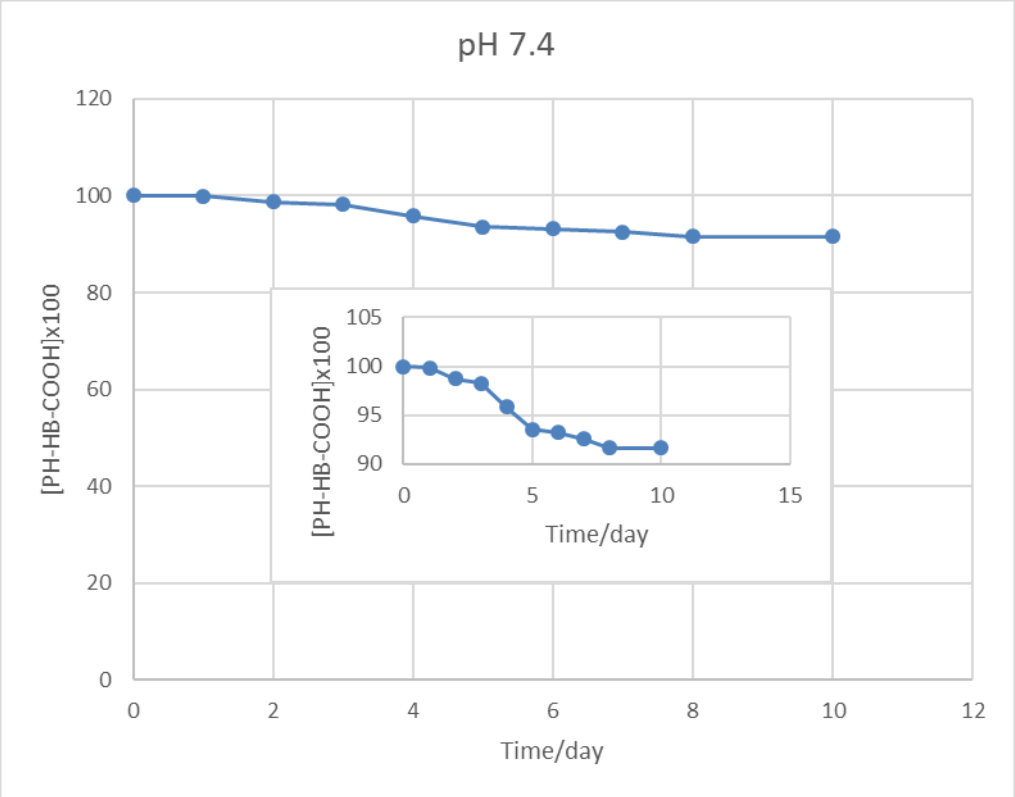

Figure 3.16. The in vitro released of PH-HB from the DB/PH-HB-COOH polyion complex in pH7.4 PB solution versus time. Insert shows a close up of the initial release.

Figure 3.15 shows that the amount of released PH-HB-COOH was 9-10% over 10 days. This percentage release was 5 times higher than that observed in the TCPP polyion system. This was more than expected and attributed to the large globular conformation of the hyperbranched polymer, which may prevents all of the carboxylic groups from connecting to the positive polymer (polycation) due to their location within the hyperbranched polymer. Specifically, some of the carboxylates could be buried and therefore unable for binding. If this was the core, then water would not get in and the pH would unaffected by these buried carboxylic acid groups (within the hydrophobic core). This result in a slightly weaker polyion complex compared to the TCPP polyion system.

Again, for the purpose of comparison, the same dialysis technique was repeated using PH-HB-COOH on its own. The UV experiment showed that about 90% of PH-HB-COOH passed through the dialysis bag over 6 days (**Figure 3.17).**

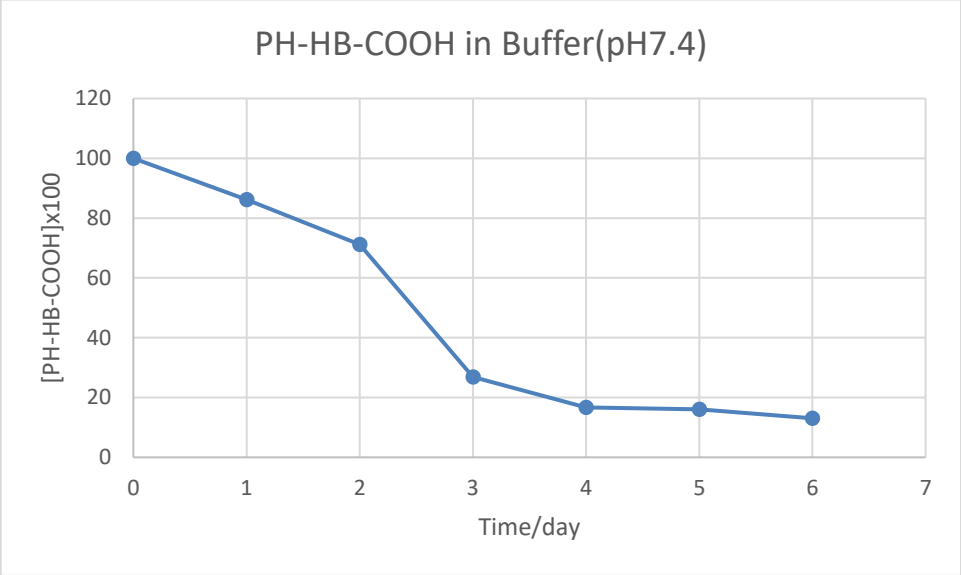

Figure 3.17. The in vitro PH-HB-COOH transfer from the dialysis bag to the dialysis solvent in pH 7.4 PBS versus time.

PH-HB-COOH release from the DB/PH-HB-COOH polyion complex was also investigated at pH 5. The experimental results were the same of those recorded of pH 7.4 (**Figure 3.18**).

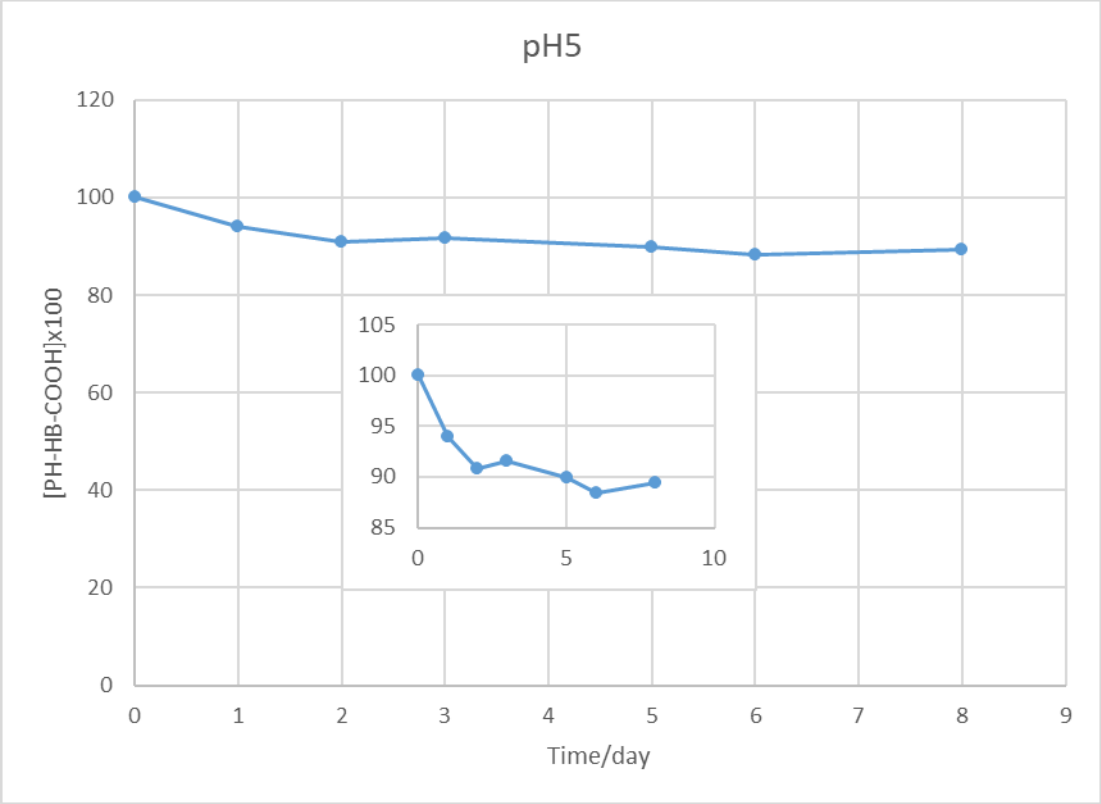

Figure 3.18. In vitro released of PH-HB from DB/HB-COOH polyion complex in pH5 PB solution versus time. Insert shows a close up of the initial release.

Figure 3.17 shows that 10-11% of PH-HB-COOH was released from the polyion complex in phosphate buffer solutions at pH5. This percentage is 3 times higher than that observed for the of TCPP polyion system. The reason for this is the same of that proposed for the system at pH 7.4. That is, some of carboxylic acid groups buried in the hydrophobic interior, and not bound to an amine from mPEG-PDMA polymer. Also, the hydrophobic interior is not accessible to the aqueous acid. These results indicate that the stability of the polyion complexes at pH 7.4 is very high.

This characteristic is valuable for in drug delivery system, as the particles can circulate and eventually accumulate into the targeted tissues via the EPR effect, which has a great potential for photodynamic therapy process.

Chapter 4
Polyion complex as a catalyst system

Chapter 4

4.1. Polyion as catalyst for epoxidation of alkenes

Most of studies in the field of catalysis are focused on biocatalysts (enzymes). Therefore, artificial catalysts and mimicking enzymes and their application in aqueous media is the main target of this research.

The use of metal functionalised porphyrins as the catalyst for an assortment of catalytic reactions have previously been performed by Twyman group[129-132].

An iron functionalised porphyrin and an iron functionalised porphyrin cored hyperbranched polymer have applications in different fields, such as an artificial blood and catalytic system. The iron inserted inside the porphyrin can bind to oxygen or a substrate. For the catalytic system, it is well known that porphyrins are an excellent catalyst because they are soluble in a range of organic solvents. This is a required property as the catalytic system would be homogeneous. However, porphyrins are difficult to recover from the catalytic reaction to be re-used. On the other hand, heterogeneous catalysts are very easy to recover from the catalytic reaction and can be re-used. However, they are poor catalysts as their solubility is very low or insoluble. Therefore, a homogeneous catalyst that can be recovered is highly desirable. Hyperbranched polymer and colloidsomes have been used as a macro-catalyst within the Twyman group[133]. These catalysts can be recovered by filtration and/or precipitation, but were poor or had limited solubility in water. Hence, and for environmental reasons, it is important to find and use water-soluble catalysts. On this basis, using a polyion complex as a catalytic system will resolve these problems, as it is a large, water soluble, and homogeneous catalyst. Hence, it is worth investigating a Fe(III) cored porphyrin-polyion complex as a catalytic system. In this study, cyclohexene will be the substrate and iodosylbenzene is the oxygen source. It is

expected that this system could provide an optimal environment for the catalysis reaction.

AS the iron porphyrin is responsible for the catalysis, it is worth discussing the use of porphyrins as catalytic systems.

4.2. Porphyrin as a catalyst for the alkenes

Porphyrins have been widely used in catalytic reactions within our group[130,131,134-137], and others. Porphyrin can bind to a variety of metals due to the central cavity. This characteristic allows of porphyrins to be used in a range of reactions as a catalyst[138-142]. For example, an iron functionalised porphyrin catalyst was used by Evans and Smith to catalyse the oxidation of ethylbenzene. They showed that this reaction produces a variety of oxidation products, including the water soluble, benzoic acid[143] (**Scheme 4.1**).

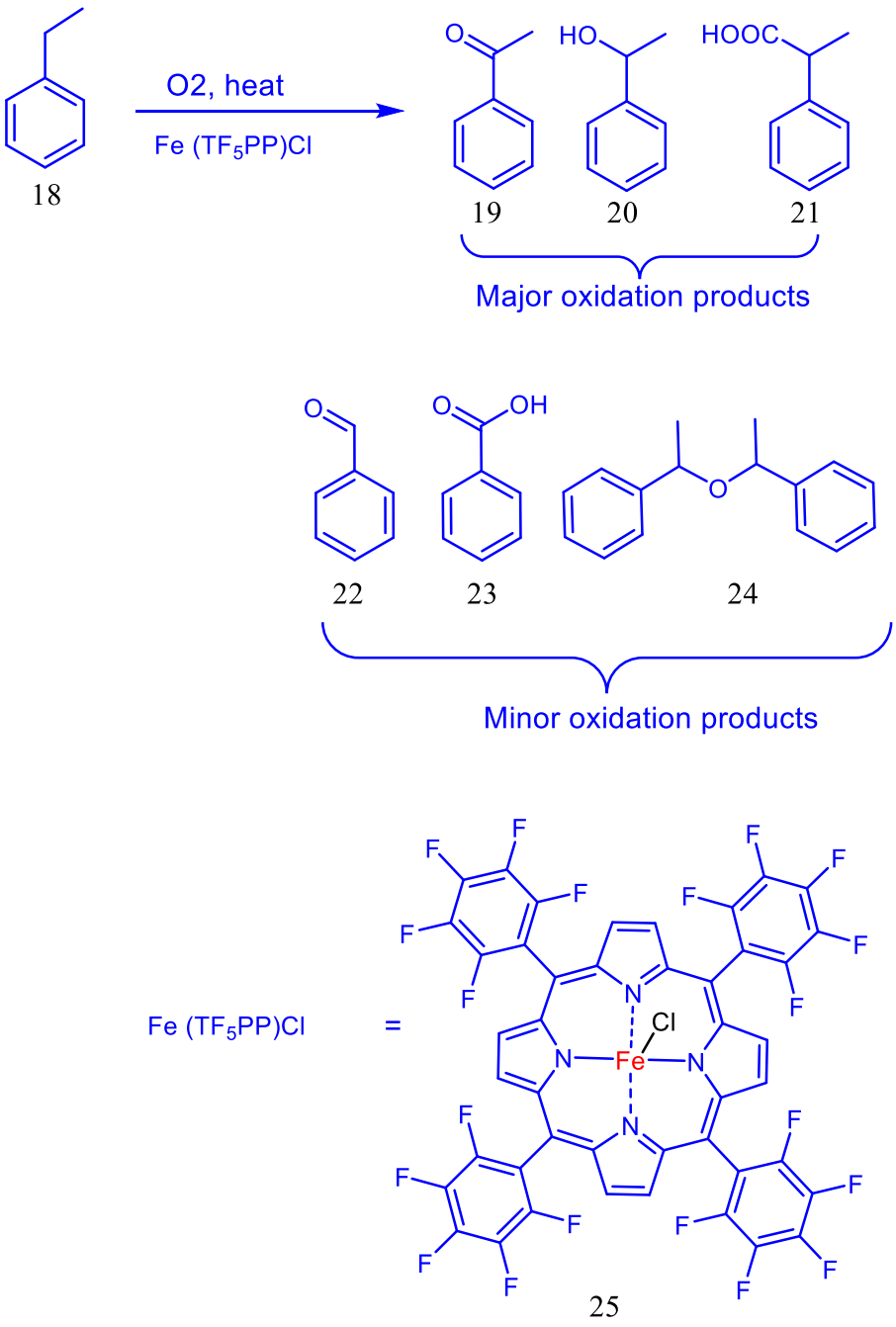

Scheme 4.1. Oxidation of ethylbenzene by oxygen using metallated porphyrin as a catalyst.

In our group we have used various porphyrin systems to catalyse the breaction between alkenes and iodosylbenzene (a source of oxygene) in organic solvents. We will attempt to use polyion complex to catalyse the same reaction in water instead of orgainc solvent.. In order to form iron containing polyion, it was nesessary to synthesise iron cored tetraphenyl porphyrin (Fe-TCPP).

4.3. Synthesis of iron(III)-functionalised tetracarboxyphenyl porphyrin (Fe-TCPP)

Iron(III) functionalised tetrcarboxyphenyl porphyrin (Fe-TCPP) and iron-porphyrin core hyperbranched polymer (Fe-PH-HB-COOH), were used to form the polyion complex or as control with mPEG-PDMA (**5C**). The result for the polyion complex will be compared with those of the control system. A comparison will determine whether or not the structure of the polyion complex provides any advantage in the oxidation of cycloalkene. We initially tried to syntheses of iron(III) functionalised tetraphenyl porphyrin (Fe-TCPP) through the refluxing a mixture of TCPP (**10**), iron(II) chloride and 2,6-lutidine in THF (**Scheme 4.2**).

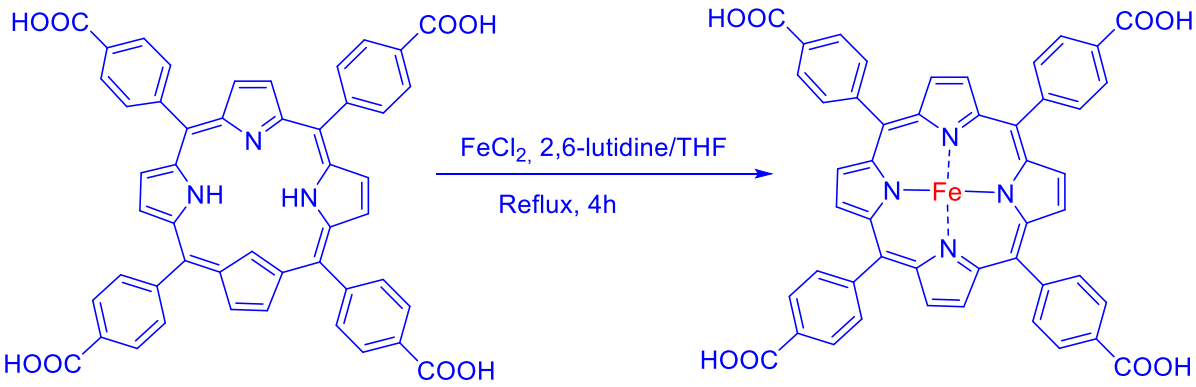

Scheme 4.2. The synthesis of iron(III) functionalised tetraphenyl porphyrin(Fe-TCPP)

Tetracarboxyphenyl porphyrin (TCPP) (**10**) was added to a round-bottomed flask equipped with and condenser. Prior to the addition anhydrous THF, the flask mixture was evacuated and flushed with nitrogen. 2,6-lutidine was added and the mixture heated at reflux for 20 minutes. $FeCl_2$ was then added and the reaction mixture heated at reflux for further 4 hours under a nitrogen atmosphere. Upon cooling to room temperature, the unreacted $FeCl_2$ and solids were removed via filtration. The solvent was removed from

the filtrate, but it didn't contain any product. The dark purple solid that was filtered remained insoluble in any solvent and could not be analysed further. The reaction was repeated a number of times, but the same results occurred each time. We suspect that the product forms an insoluble complex between the anionic carboxy groups and iron. This could occur between inserted and free iron as shown in (**Scheme 4.3)**.

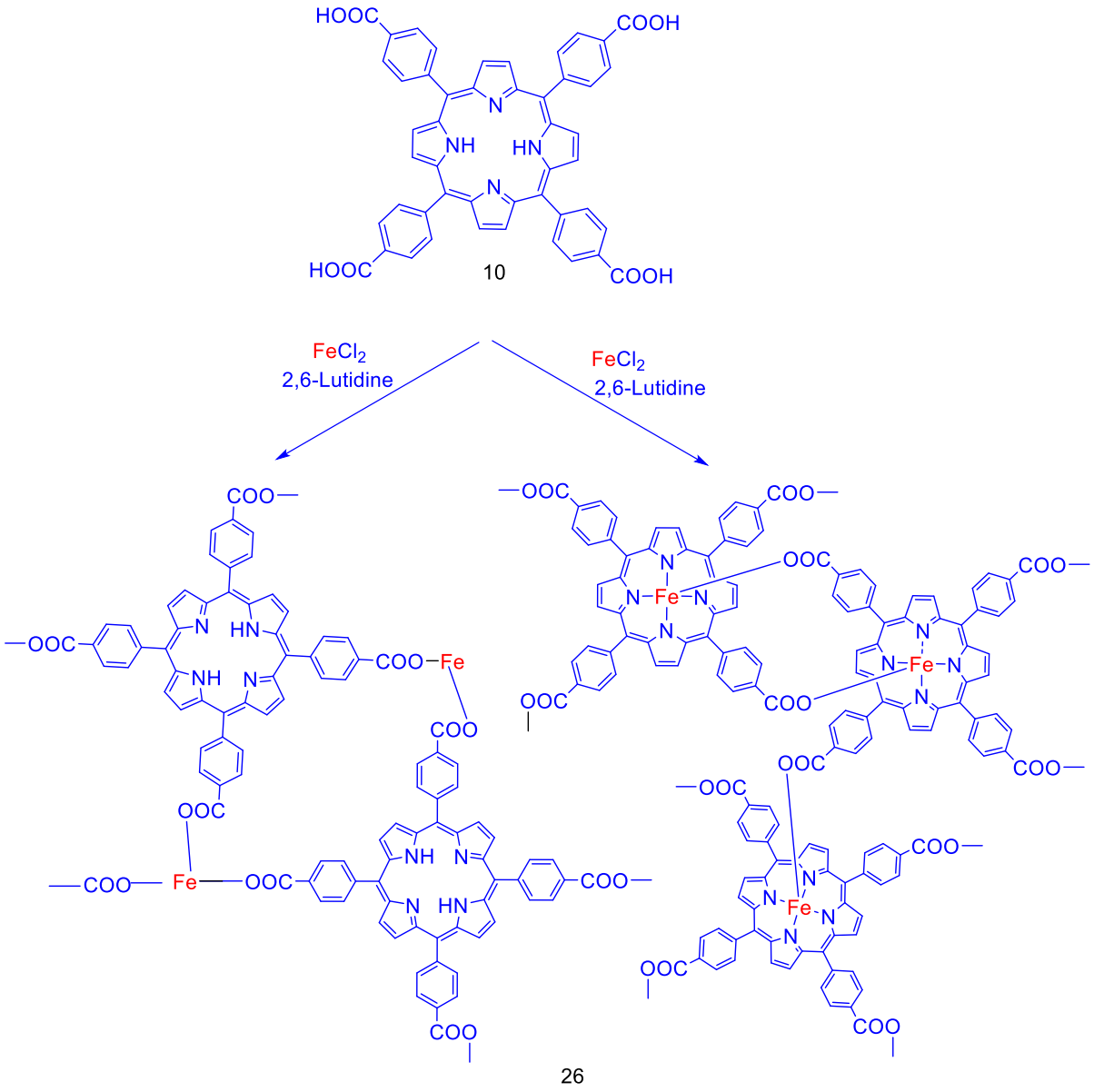

Scheme 4.3. Formation of the iron-porphyrin complex.

In addition, a portion of iron may be inserted inside of the TCPP and this may react with the carboxylic groups or forming coordination bonds with other Fe-TCPP molecules. As we have not found any literature precedent on a direct method to insert iron inside TCPP, we needed another route to form Fe-TCPP. We therefore decided to prepare a protected porphyrin and then insert the iron. Finally, the Fe-porphyrin could be converted into Fe-TCPP after a de-protection step.

4.4. Synthesis of tetracarboxymethylphenyl porphyrin (TCMPP) (28)

To prepare the iron-functionalised tetraphenyl porphyrin (Fe-TCPP), it was neceesasry to synthesis a porphyrine with groups that cannot react with iron, but can be converted to TCPP after insertion step. Therefore, tetracarboxymethylphenyl porphyrin (TCMPP) was chosen and prepared. TCMPP contains ester groups, which will not react with the iron. Also, these groups will udergo a hydrolysis reaction resuling in the formation of carboxylic acid groups. Tetracarboxy methyl porphyrin (TCMPP) was prepared by refluxing molar quantities of 4-carboxymethyl benzaldehyde (**27**) and freshly distilled pyrrole (**7**) in propionic acid (**Scheme 4.4**). The resulting product was then isolated via filtration and washed with cold methanol followed by warm water, then again with cold methanol, to give purple shiny crystals.

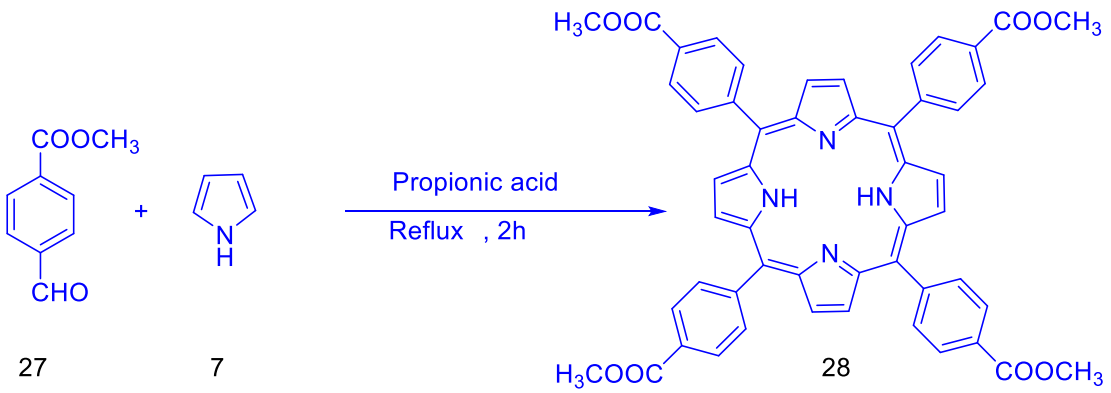

Scheme 4.4. The synthesis of tetracarboxymethylphenyl porphyrin (TCMPP).

The synthesis of TCMPP (**28**) was confirmed by ^{1}H NMR spectroscopy as it revealed a singlet peak at δ = 8.85ppm corresponding to the pyrrolic hydrogens. A doublet peak at δ = 8.47ppm and δ = 8.32ppm was visible and is consistent with the hydrogens on the phenyl ring. A singlet at δ = 4.14ppm corresponding to the methyl protons on the carboxymethyl group and the characteristic peak from the highly shielded inner protons at δ = -2.8ppm were also present. This result was in good agreement with literature data. There was a strong Soret band at 418nm in the UV spectrum and the IR showed a carbonyl peak at1720 cm^{-1}. The MS has a molecular ion peak at m/z = 847. Overall, the data confirmed the structure of the protected porphyrin (**28**).

4.5. Synthesis of iron(III) functionalised tetracarboxymethylphenyl porphyrin (Fe-TCMPP) (29)

Inserting of iron into TCMPP (**28**) was the next step prior to synthesising Fe-TCPP. Specifically, Fe-TCMPP was synthesised by refluxing TCMPP (**28**) in the prescence of excess iron(II) chloride and 2,6-lutidine in THF (**Scheme 4.5**).

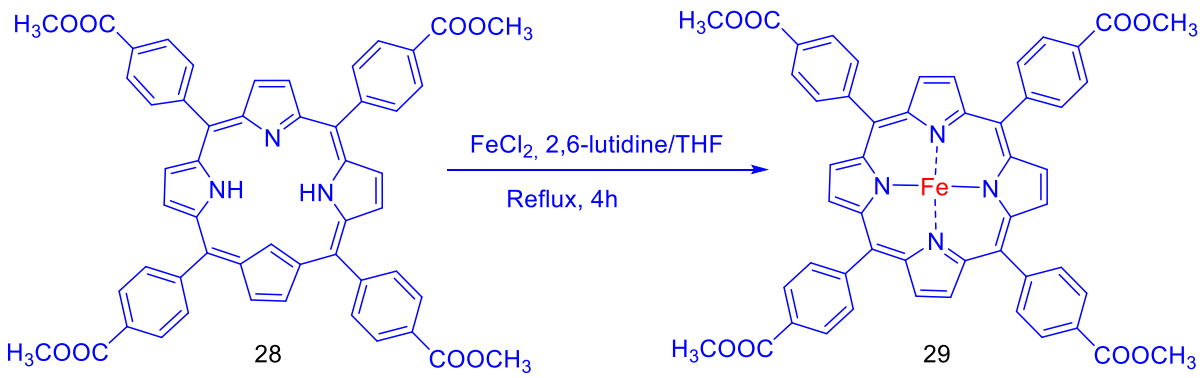

Scheme 4.5. The synthesis of iron(III) functionalised tetracarboxymethylphenyl porphyrin (Fe-TCMPP).

TCMPP (**28**) was placed in flask equipped with a condenser. The system was evacuated and flushed with nitrogen. A solution of 2,6-lutidine in anhydrous tetrahydrofuran was then added and the solution hated at reflux for 15 minutes before the addition of iron(II) chloride. The mixture was then heated to reflux for a further 5 hours to give the Fe(II) porphyrin. To convert Fe(II) to Fe(III), the system was left opened to the atmosphere and allowed to cool to room temperature. The unreacted iron(II) chloride was removed via vacuum filtration. The product solution was washed 1M HCl and water, where the aqueous layer was observed to become lighter in colour after each wash. Insoluble impurities were also observed at the solvent interface. The organic layer was then collected and dried over magnesium sulphate. After removing the solvent, the product purified using column chromatography via CH_2Cl_2 containing 25% MeOH (v/v) as the eluent to give Fe-TCMPP (**29**) in good yield. We were not able to obtain a ^1H NMR spectrum due to the paramagnetic nature of the metal centre. However, UV/Vis analysis showed a broad Soret band at 417.5nm which is characteristic of porphyrin functionalised compound. In addition, the UV/Vis spectrum exhibited only two Q-bands instead of four for the free base porphyrin (**Figure 4.1**).

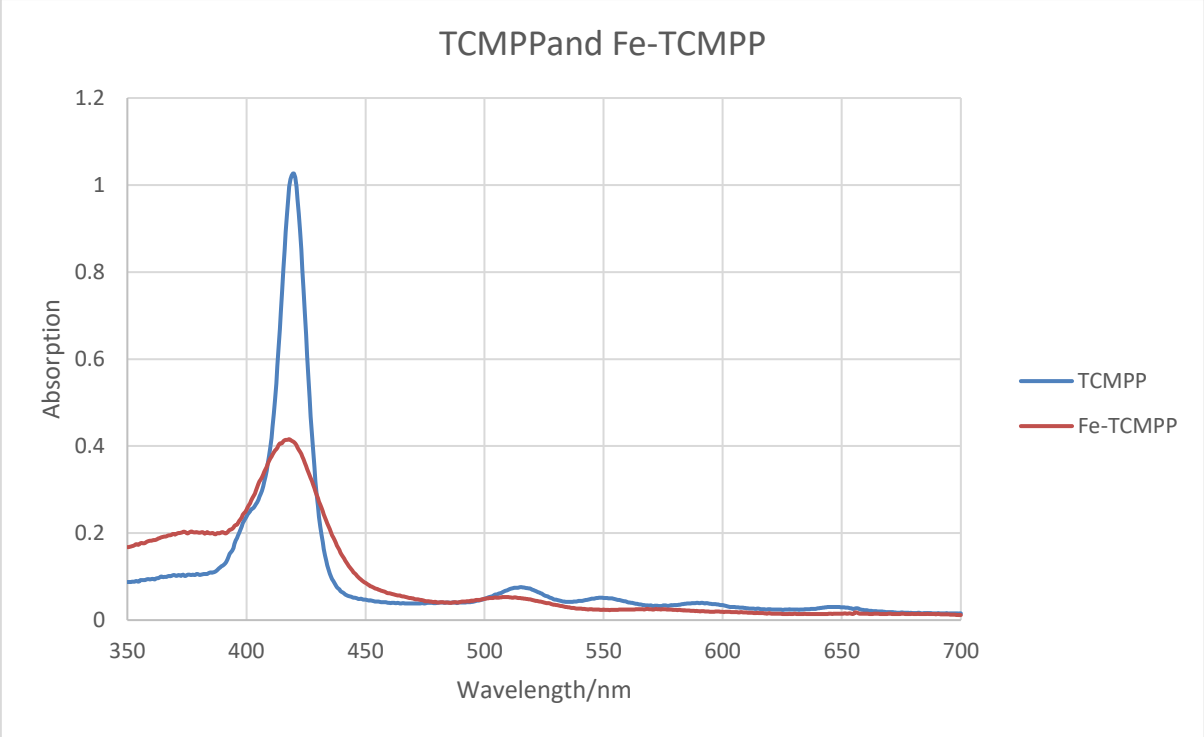

Figure 4.1. The UV spectra of TCMPP (blue) and Fe -TCMPP (red).

Mass spectroscopy showed a molecular ion peak at m/z = 900 MH^+ (ESI-MS) which is the precise molecular formula of Fe-TCMPP, which confirms that the insertion was accomplished.

4.6. Synthesis of iron inserted tetracarboxyphenyl porphyrin (Fe-TCPP)

The final step in the synthesis of Fe-TCPP involved removal and conversion of the ester groups into carboxylic acid groups. Fe-TCPP was prepared by refluxing of Fe-TCMPP in a solution of THF, methanol and KOH[144] (**Scheme 4.6**).

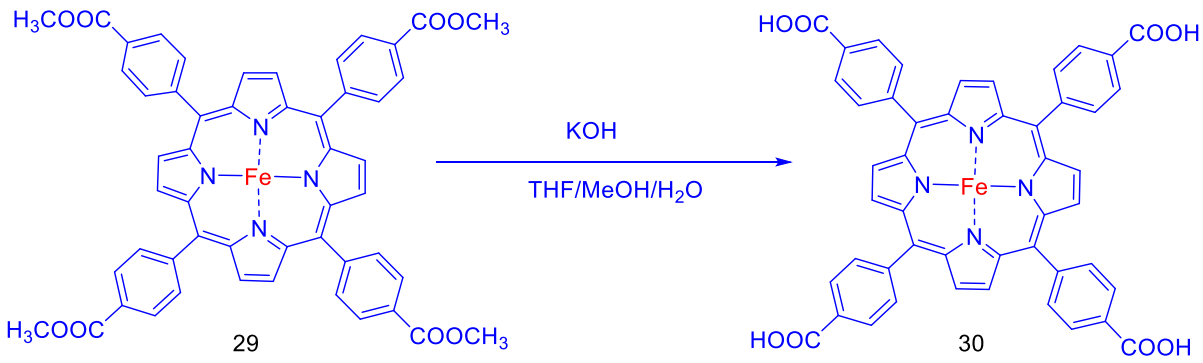

Scheme 4.6. The synthesis of Fe-TCPP from Fe-TCMPP.

The porphyrin was first dissolved in a 1:1 mixture of THF and methanol, and a solution of KOH was added. The resulting mixture was then heated at reflux overnight and the solvent (THF and MeOH) removed using a rotary evaporation. Water was then added and the mixture heated until homogeneous solution was observed. A few drops of 1M of hydrochloric acid was added, which caused the product precipitate from the solution. The obtained product was filtered, washed with water and dried under vacuum to give the desired porphyrin (Fe-TCPP) (**30**).

Due to the paramagnetic properties of Fe-TCPP, we could not use NMR analysis for characterisation. The UV/Vis spectrum showed a broad Soret band at 416nm. Mass spectroscopy (MH^+ (ESI-MS)) showed a molecular ion peak at m/z = 843, which is identical to the mass of Fe-TCP, confirming that Fe-TCMPP was converted into Fe-TCPP.

4.7. Synthesis of iron(III) cored hyperbranched polymer (Fe-PH-HB-COOH)

As synthesis of Fe-TCPP (**30**) was confirmed, the last step was synthesising the iron(III) functionalised porphyrin core hyperbranched polymer (Fe-PH-HB-COOH). Iron (III) functionalised porphyrin cored hyperbranched polymer has applications as a catalytic system[130]. The iron inserted inside the porphyrin can help oxygen to react with the substrate. In addition, Fe-PH-HB-COOH and mPEG-PDMA will be used to form polyion complex of (DB/Fe-PH-HB-COOH), which would be used as catalyst for the epoxidation reaction. We tried to insert iron inside porphyrin of hyperbranched polymer via direct reaction between PH-HB-COOH (**16**) and iron(II)chloride in presence of 2,6-lutidine (**Scheme 4.7**).

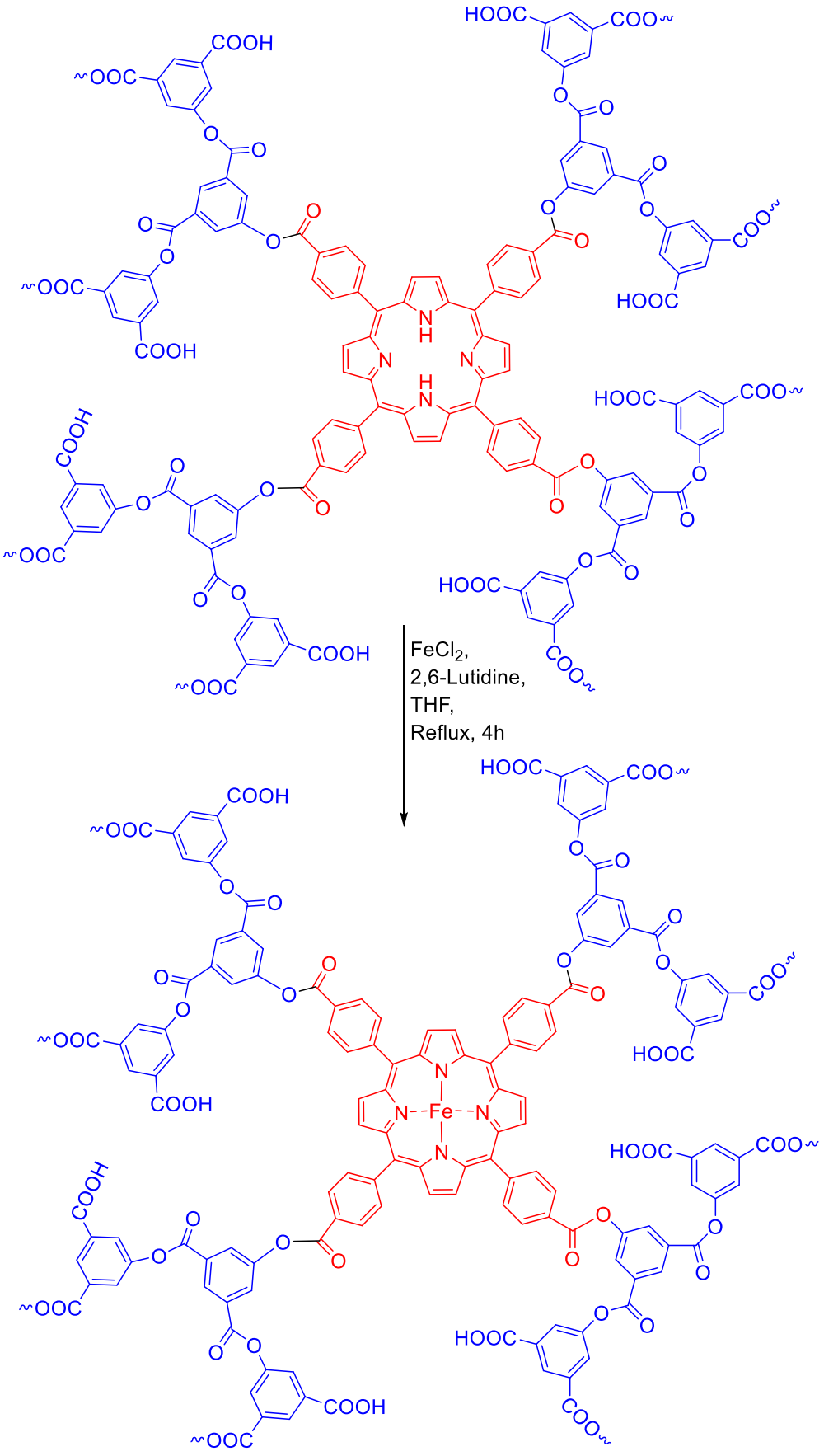

Scheme 4.7. The direct insertion of iron inside PH-HB-COOH.

The reaction was accomplished by refluxing the hyperbranched polymer (**16**) with an excess of iron chloride and 2,6-lutidine in THF for 5 hours. Upon cooling, the mixture was exposed to air and then it was filtered and the precipitate isolated. However, the purple precipitate wasn't soluble in any solvent, which prevented characterisation. Nevertheless, we were certain that the obtained precipitate was not our product, and we would expect this to be soluble. The reaction was repeated a further two times, but the same result was obtained. We suggest that the obtained product was cross linked aggregate where the carboxy group had coordinated with free iron to give the observed insoluble aggregates. This is similar to the result observed for the Fe-TCPP. Therefore, non-directed route was selected.

Fe-PH-HB-COOH (**31**) was prepared via the melt condensation polymerisation of the mixture of 5-actoxyisophthalic acid (**13**) and of Fe-TCPP (as a core unit) (**30**) with a ratio 10:1 (mol:mol). A reaction flask equipped with a distillation kit was charged with a mixture of 5-actoxyisophthalic acid (**13**) and iron (III)-TCPP (**30**). The system was evacuated and flushed with nitrogen. The mixture was then heated under Nitrogen to 250 ^{0}C and an isotropic melt was observed. The system was then exposed to a strong vacuum for one hour and where by-products were isolated. As before, a foam formed which collapsed when the vacuum was turned off. The system was then cooled to room temperature, and a mixture of THF/water was added in order to break down the anhydride linkage which form during the condensation. The mixture was then heated to reflux for 5 hours, and the product was precipitated from water. The product was re-dissolved in THF and then precipitated from diethyl ether. Fe-PH-HB (**31**) obtained, was collected and dried under vacuum to give dark brown solid.

(**Scheme 4.8).**

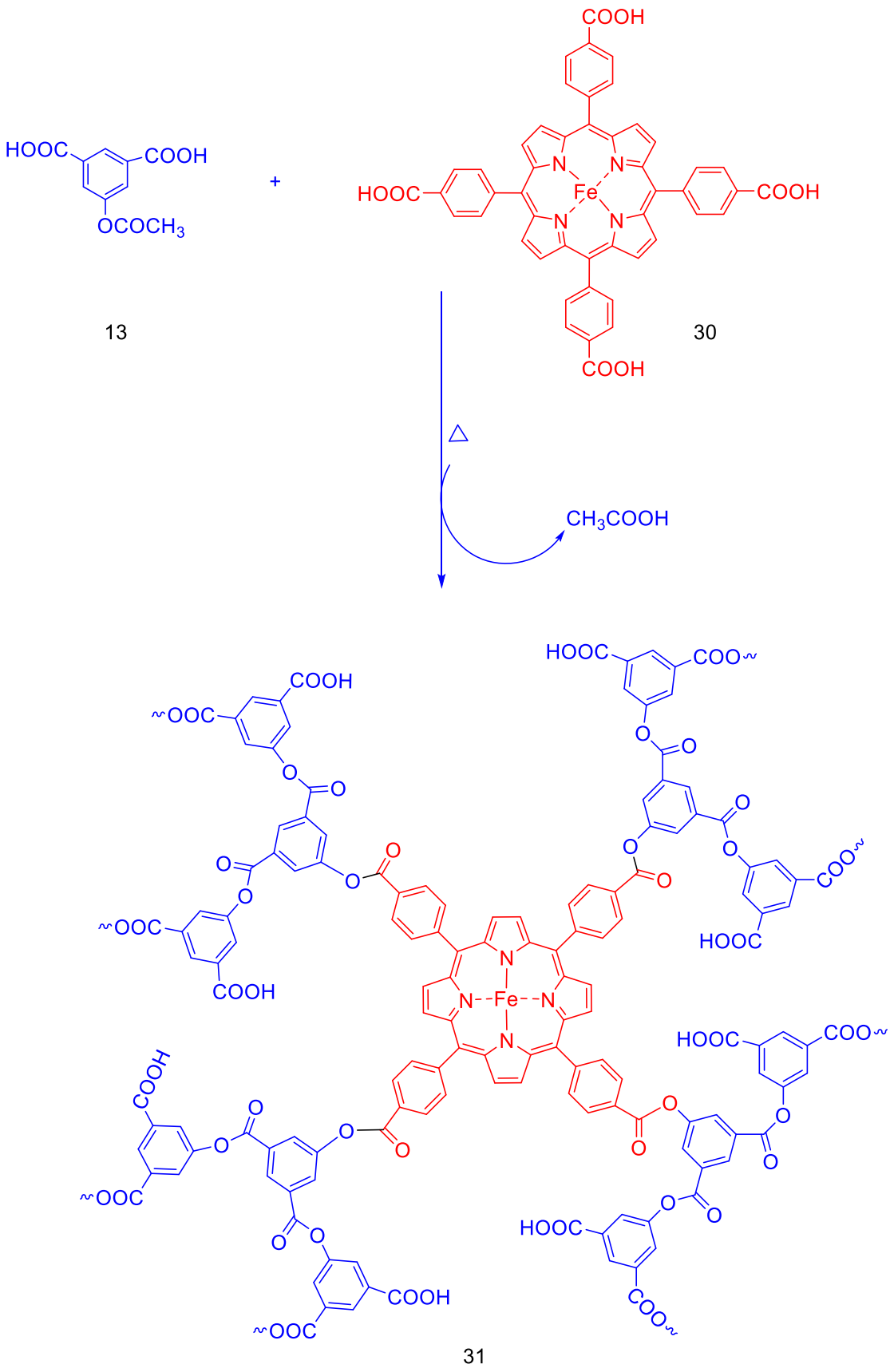

Scheme 4.8. Synthesis of iron(III) cored hyperbranched polymer (Fe-PH-HB-COOH).

Again we couldn't use NMR for characterisation because of the paramagnetic nature of the metal centre. The UV/Vis spectrum showed a broad Soret band at 411nm, which was 416 for Fe-TCPP on its own in the same solvent (methanol). This band is shifted by 5nm, which indicated that the porphyrin is in a different environment. Again we couldn't run the GPC analysis unless the carboxy groups convert to ester groups.

To measure the Mn of Fe-PH-HB-COOH (**31**) using GPC technique, it was necessary to the convert the terminal carboxy groups into ester groups, specifically, we prepared iron(III) core PH-HB-COOET hyperbranched polymer(Fe-PH-HB-COOEt) (**32**), which would be soluble in THF and could be analysed. Fe-PH-HB-COOEt (**32**) was prepared in two steps. Firstly, the carboxylic groups were converted into acid chloride groups, by addition of thionyl chloride to Fe-PH-HB-COOH (**31**) in THF. Upon refluxing for 6 hours, THF and excess thionyl chloride were removed. The product obtained was used directly for the next step (assuming 100% yield). The acid chloride groups were subsequently converted into ethyl ester groups by stirring in ethanol with (triethylamine) for 12 hours at room temperature. The triethylamine chloride by product was filtered off and the product was precipitated in water to give Fe-PH-HB-COOEt (**32**) as a brown solid (**Scheme 4.9**).

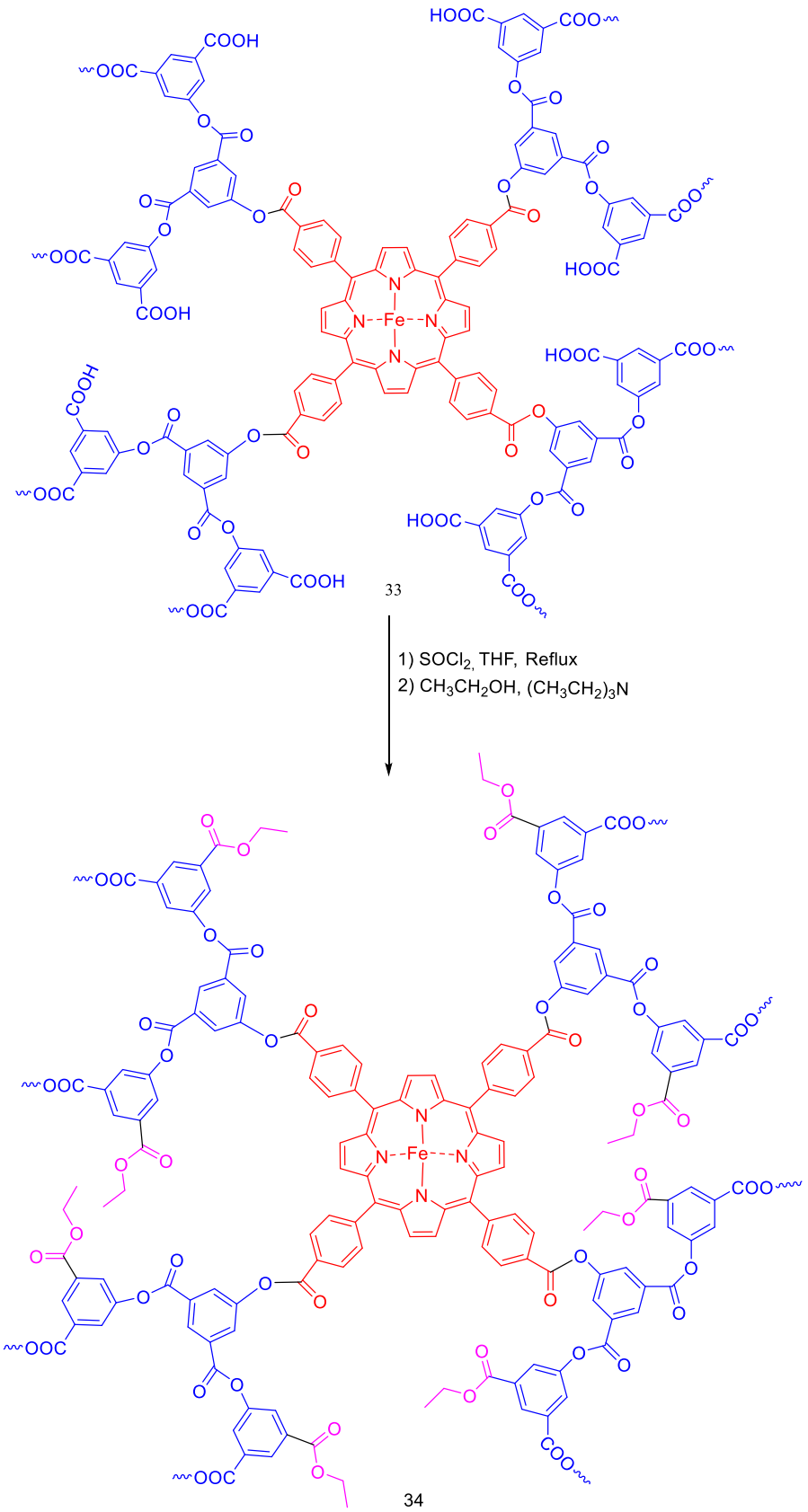

Scheme 4.9. Synthesis of iron(III) cored PH-HB-COOEt hyperbranched polymer (Fe-PH-HB-COOEt).

Again, NMR analysis was not suitable for this polymer (due to the paramagnetic nature of the iron centre). A Soret band was observed at 416nm, and two Q bands were seen at 514and at 578 nm, which is consistent with a metallated porphyrin and confirms that the porphyrin survives the esterification reaction. GPC analysis was carried out and revealed a molecular weight of 3000 g/mol. Therefore, we assume that Fe-PH-HB-COOH (**31**) had the same molecular weight.

4.8. Synthesis of iodosylbenzene (34)

For the catalytic epoxidation, it was first necessary to synthesise iodosylbenzene, the oxygen source. Iodosylbenzene was synthesised by the direct reaction of iodobenzene diacetate with a concentrated solution of sodium hydroxide (**Scheme 4.10**). The reaction was stirred for 45 minutes and the precipitate collected and washed with excess water and excess chloroform. The faint yellow powder obtained was dried and kept in a dark place to prevent degradation when exposed to light. Due to its sensitivity, iodosylbenzene was prepared prior to each catalytic experiment.

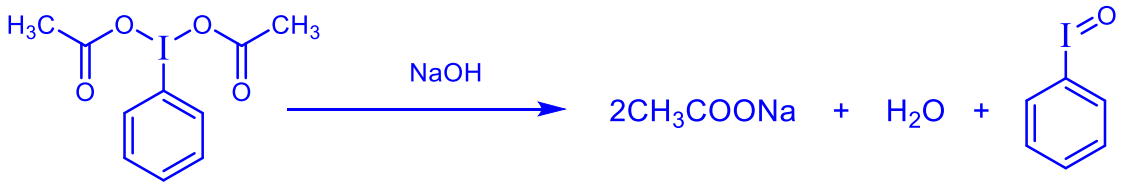

33 34

Scheme 4.10. The synthesis of iodosylbenzene.

^{1}H NMR confirmed the synthesis of iodosylbenzene as it showed a multiplet at δ = 8.06ppm corresponding to the *ortho*-protons and a multiplet at δ = 7.59ppm belonging to the *meta* and *para* protons. Mass spectroscopy showed a molecular ion peak at 220,

which is identical to the mass of iodosylbenzene. The mass spectrum also displayed a fragment at 204 and 205, due to loss of the oxygen (M+ and MH+). The melting point of the product was 210 °C, which then decomposed above 211°C. The data is in agreement with the literature[145] and therefore confirms the successful preparation of the product.

4.9. Cyclohexene epoxidation

To test that an iron porphyrin could catalyse the oxidation of cyclohexene in the presence of iodosylbenzene and to establish catalysis and analysis conditions, the reaction was carried out using chloroform and Fe-TPP. When the conditions were confirmed, we would then repeat the experiments using the Fe-TCPP polyion and the Fe-PH-HB-COOH polyion in water. The reaction and products are well known[130,146] and are shown in **Scheme 4.11**. The reaction occurs as the oxygen moved from the oxygen source (iodosylbenzene) to the centre of Fe-porphyrin, resulting in an iron porphyrin *oxo* intermediate. The alkene substrate can then react with this intermediate complex to generate the epoxide (**36**) as the main product, as well as a number of minor by-products (**37**), (**38**) and (**39**). In addition, iodobenzene (**40**) is also generated (and can be used to monitor the reaction).

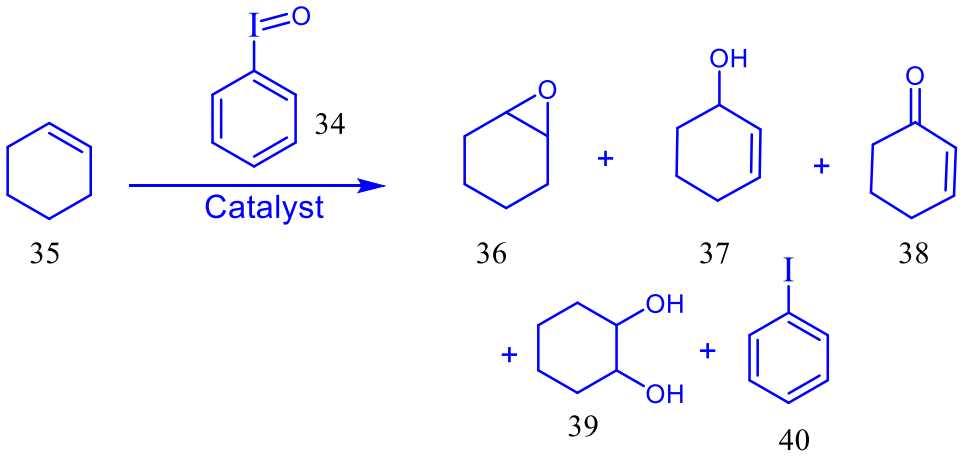

Scheme 4.11. Oxidation of cyclohexene by iodosylbenzene in presence of a catalyst.

4.9.1 Catalysis quantification

In order to determine the extent of the epoxidation reaction, gas chromatography was utilised. As such, it was very necessary to establish the position/retention time of the main products and starting materials. Neat samples of cyclohexene, cyclohexene oxide and iodobenzene, were run through the instrument at various concentrations. Pyrene was also run as an internal standard, which would enable us to calculate the yield of each oxidation product and remaining staring materials. Furthermore, a blank reaction was carried out in order to test whether or not the oxidation of cyclohexene could proceed without the iron porphyrin catalyst. The GC data from this experiment revealed a negligible total yield of the oxidation products (< 1%)

4.9.2 Control reaction 1 - Establishing the reaction conditions and the purity of iodosylbenzene

In order to examine the validity and the analytical purity of the source of oxygen (iodosylbenzene) and the reaction conditions, a known reaction was carried out using iron functionalised tetraphenyl porphyrin (Fe-TPP) and chloroform as solvent. The reaction flask was charged with iodosylbenzene (0.1 mmol), the internal standard

(pyrene-0.04g, 0.198 mmol), cyclohexene (0.5 mL, 0.49 mmol) the Fe-TPP catalyst (1μmol) and Chloroform. The mixture was evacuated and flushed with nitrogen. The suspension was stirred in a dark place for half an hour before adding 5 mL of chloroform. The solution was filtered through a Whatman® GD/X syringe filter (0.45μm) and filtrate transferred into a GC vessel for analysis. After reaction, the GC showed strong peaks and a high yield for the oxidation products. This results confirms the reaction conditions and that iodosylbenzene can be used oxidise by the alkene substrate.

4.9.3 Control reaction 2 – confirming that iron is required for catalysis

In order to confirm that the iron is required for the catalytic oxidation reaction, a control reaction using a non-metallated (unfunctionalised) porphyrin was carried out. The reaction was carried out using the same procedure described above **– 4.9.2**. The GC results did not show any oxidation products. The same result was obtained when the reaction was repeated using DCM as the solvent. This confirms that that the iron cored porphyrin and iodosylbenzene are required for catalysis. This results encouraged us to go forward and to test the capability of iron cored TCPP and iron cored hyperbranched polymer (Fe-PH-HB-COOH) as the catalyst.

4.9.4. Oxidation of cyclohexene in water using the polyion complexes

Having confirmed the reactivity of iodosylbenzene and established the GC conditions, the reaction was repeated using the polyion complexes. Only some of the reaction components were soluble in all solvent. For example, the polyion complexes were not soluble in chloroform, but were the only things soluble in water. As such, the reactions would be carried out in heterogeneous conditions. The first experiments were carried out using water as the solvent. In a typical reaction the flask (flask 1) was charged with a mixture of iodosylbenzene and cyclohexene substrate (0.5mL, 0.49 mmol). The flask was evacuated and flushed with nitrogen and the system kept under nitrogen

atmosphere. In another flask (flask 2), the polyion complexes (DB/Fe-TCPP or DB/Fe-PH-HB-COOH) were prepared in water. This flask was evacuated and flushed with nitrogen and the system kept under nitrogen atmosphere. The polyion complex solution in flask 2 was then added to flask 1 with stirring. The mixture was then left to stir vigorously in a dark place for 24 h. The internal standard (pyrene) and 5mL of chloroform added. The organic layer was filtered through Whatman® GD/X syringe (pore size of 0.4μm) and the filtrate analysed by GC. Unfortunately, GC did not show any trace of oxidation products for both polyion systems. The failure of the reaction was attributed to the substrates poor solubility in water. We had anticipated that the organic substrates would enter the polyion and form an encapsulation complex, which could then react with the internal iron porphyrins, but clearly this did not happen. We repeated the reactions using DCM as the solvent. However, the reaction failed and no oxidation products were observed using GC. Therefore, we decided to repeat the reaction using a tow phase mixture of solvents that could dissolve all species.

4.9.5. Oxidation of cyclohexene using polyion complex DCM

Due to the orthogonal solubility properties of the substrates and catalysts, the reactions were carried out using a two-phase mixture of DCM/H_2O. The reactions were performed as previously described, except the cyclohexene substrate was added (to the aqueous solution of polyion complex), as a solution in DCM. Once again, the results were disappointing, as we did not observe any speaks for the reaction products in the GC chromatogram. Although everything was soluble, the failure was attributed the lack of "mixing" between the two phases. This indicates that we need to use a solvent or solvent mixture that could dissolve all species involved in the reaction (substrates and catalysts). We therefore proposed to use a mixture of methanol/chloroform as a solvent.

4.9.6. Control to establish the feasibility of using a mixed solvent system for the oxidation of the alkene

As a compromise, we decided to test whether or not the reaction would occur using a small amount of a second solvent that could ensure dissolution of all reaction species (alkene, iodosylbenzene and catalyst). Specifically, we added enough methanol to the dissolve the iron porphyrin Fe-TCPP (**30**) or the iron cored hyperbranched polymer Fe-PH-HB-COOH (**31**) in addition to the main solvent, chloroform. The GC results showed the oxidation products in around 50%. The success was attributed to the presence of methanol, which improved the environment conditions of the reaction by allowing all species to be solubilised. However, we did not have time to explore this further and this aspect of the project will be continued in the future.

5. Conclusion and further work

This study focuses on the preparation of various polyion complexes that could be applied to a number of practices, such as drug delivery systems for photodynamic therapy and potential catalytic systems. The formation of polyion complexes were achieved using mPEG-PDMA amphiphilic diblockcopolymers as the cationic block and TCPP and hyperbranched polymers bearing terminal carboxy groups as the anionic component. Iron-functionalised tetraphenyl porphyrin and iron cored hyperbranched polymer bearing terminal carboxy groups were also prepared. Polyion formation was confirmed via UV, DLS and TEM. In vitro drug release studies at pH 7.4 and 5.0 showed 2% release of TCPP at pH 7.4 and 4% at pH 5.0. DB/ porphyrin cored HBP polyion system showed 9% and 11% release at pH 7.4 and pH 5.0. The outcome of this were unexpected as they indicated that the TCPP system, with only four anion sites, was more stable than the hyperbranched polymer system, which had many anion sites. The reason behind this difference is attributed to the globular structure of hyperbranched polymer. In this case, some of the anionic/ carboxylic sites may be buried inside the polymer and are unable to interact with the amines on the amphiphilic diblockcopolymer. In addition, the large size of the hyperbranched polymer may be geometrically unfavourable with respect to maximising any interactions with the amphiphilic diblockcopolymer.

The application of polyion complex as catalysts did not match expectations and did not catalyse the epoxidation of cyclohexene in water (heterogeneous medium) using iodosylbenzene as a source of the oxygen. The same experiment was carried out, using DCM, which could dissolve cyclohexene substrate. However, as before no catalytic reactions were observed. The results also showed a lack of the epoxidation reaction.

As DB/TCPP and DB/ HBP polyion complex particles were 150-200nm in size, future studies will examine the application of polyion complexes in photodynamic therapy (PDT). The application of polyion complex formed from amphiphilic diblockcopolymer and iron cored hyperbranched polymer bearing terminal carboxy groups will also be studied for use as an artificial blood product. Future work on catalysing the epoxidation of alkene in a mixture of methanol and water will be undertaken as this mixture could be the optimal solvent for the reaction.

Chapter 6

Experimental

6. Experimental

6.1 Instrumentation

6.1.1. Chemicals & Apparatus

All chemicals and solvents used in the study were mainly purchased from Sigma-Aldrich and used without further purification. Dry solvents were purchased from Grubbs solvent dispensing system in the department of Chemistry-the University of Sheffield.

6.1.2. NMR spectroscopy

^{1}H NMR and ^{13}C NMR analyses were recorded using a Bruker AV1400-HD machine at 400 MHz and 100 MHz, respectively. Analyses of the spectra were carried out using Bruker NMR software TopSpin^{TM} 3.2. All the chemical shifts were quoted in ppm and referenced internal solvent signal calibrations. Residual solvent peaks were assigned according to Gottlieb *et al., J. Org. Chem.*, 1997, *62*, 7512.

6.1.3. Infrared (IR) spectroscopy

All infra-red absorption spectra were recorded using Perkin-Elmer Paragon 100 FT-IR machine with the universal ATR Accessory. All absorption peaks were recorded to the nearest wavenumber in cm^{-1}. All data were analysed using Perkin-Elmer spectrum application.

6.1.4. Melting point measurements

Melting point ranges for all solid samples were measured using a Galenkamp MFB-

595 melting point instrument. Any samples which remained as solids at 300 ^{o}C were simply quoted to have a melting point value of 'above 300 ºC' as their determination was not possible.

6.1.5. UV/Vis spectroscopy

UV/Vis spectra were recorded using solutions in quartz cuvettes, recorded using Perkin-Elmer Lambda 35 dual-beam equipment. Upon a reference reading, absorbance measurements was carried out for each solution. WinASPECT software were used for analysis the spectra.

6.1.6. Gel permeation chromatography (GPC) measurements

GPC measurements were carried out using a low molecular weight column, (2 x 600 PL gel, 500 Å). Samples were prepared at a concentration of 5 mg/mL. All samples were filtered using Whatman® GD/X syringe filters with 0.45µm pores before analysis. Fischer Scientific GPC grade THF was used as a solvent and toluene was used as the flow marker. The solvent stream had a flow rate of 1mL min^{-1} supplied by a Waters 515 HPLC pump. The samples were introduced through a 200 µL injection loop and subsequent molecular weight determinations were carried out using a Cirrus software (GPC Offline).

6.1.7. Mass spectroscopy

Mass measurements were carried out using Bruker Reflex III mass spectrometer. Mass-to-charge ratio of the samples with low molecular weight was determined by Electrospray Ionisation (ES) using Waters LCT Premier XE spectrometer. Matrix

Assisted Laser Desorption Ionisation Time of Flight (MALDI-TOF) was employed for samples with high molecular weight,

6.1.8. Dynamic light scattering (DLS) measurements

A Malvern Zetasizer NanoZS model ZEN 3600 instrument was utilised to measure intensity–average hydrodynamic diameters. The instrument operating system was fixed at a scattering angle of 173° and samples were analysed using disposable cuvettes. All data were averaged over three consecutive runs and Z-average hydrodynamic diameters were calculated using the Stokes–Einstein equation.

Hydrodynamic diameters of nanoparticles determination was carried out also using the Brookhaven instrument 90Plus Particle Size Analyzer (Holtsville, NY, USA) 35mW solid state standard laser. Particle Sizing Software 9kpsdw32.exe.ver.3.80 was used for characterisation. Light was scattered at an angle of 90° and samples were analysed using 5 runs, each lasting 2 minutes at 25 °C. Whatman® GD/X syringe filters (Kent, UK) with a pore size of 0.45µm was used for filtration of samples prior to analysis. Results reported are based upon volume distribution.

6.1.9. pH measurements

Jenway 210 pH Meter instrument was used for pH measurements. Calibration was carried out using pH 7 and pH 10 standard solutions (Sigma-Aldrich).

6.1.10. Fluorescence spectroscopy

Perkin Elmer Fluoromax-4 Spectrofluorometer was utilised to carry out the fluorescence measurements using a quartz cuvette. All the measurements carried out at 25 ^{o}C. Emission and excitation wavelength selection was dependent on the sample under run. Both excitation emission slit was 5nm for all measurements. The instrument was attached to software (FluorEssence V3).

6.1.11. Gas Chromatography

Gas chromatography measurements was carried out utilising PerkinElmer Clarus 400 Gas Chromatograph. A hydrogen gas flow and nonpolar Altech AT1 column (length 30 metres, Film Thickness: 5.00 um) was used to run the samples at injection temperature of 250 ^{o}C. The ven temperature adjusted 50 ^{o}C and remained for 5minuites, before it then increased to 250 ^{o}C over a 20 minuets period. Total Chrome Nav softwarewas employed to process the obtained data.

6.1.12. Field Emission Scanning Electron Microscope (FESEM)

The microstructural characterizations were performed using a JEOL-7001F field emission scanning electron microscope (FESEM) operated at 15 KV. Dry powder was used for the FESEM analysis.

6.2. Analytical procedures:

6.2.1. Critical aggregation concentration (CAC) measurements using TPP as a fluorescent probe

Critical aggregation concentration (CAC) of mPEG-PDMA using TPP as a hydrophobic probe was determined as follows: A stock solution of mPEG-PDMA in a pH 7.4 buffered solution (5 mg/mL) was prepared. From this solution, a number of diluted solutions ranging from 0.001-1mg/mL were prepared. To these polymer solutions, 1 mL of TPP solution in dichloromethane ($1X10^{-6}$ M) was added dropwise with a robust stirring. The mixture left stirring overnight and the organic solvent evaporated from the open vessel. The resulting solutions were filtered using Whatman® GD/X syringe filter with 0.45µm pores to remove the non-encapsulated

TPP prior to recording the fluorescence spectra. The emission spectra of encapsulated TPP within mPEG-PDMA were recorded over the wavelength area of 540- to 800 nm. The excitation wavelength was 420nm with a slit width of 5nm for both excitation and emission. The emission peak seen at 650 nm for each sample was recorded as a function of the concentration of mPEG-PDMA solution.

6.2.2. Critical aggregation concentration (CAC) measurements using pyrene as a fluorescent probe

Critical aggregation concentration determination (CAC) using pyrene as a probe was carried out as follows: Firstly, the preparation of a stock solution of pyrene in acetone was carried out, and from this stock solution, a $1x\ 10^{-6}$ M solution of pyrene was prepared. A certain volume of this solution (3mL) was transferred into a number of vials. Upon evaporating the acetone solvent, a certain volume of mPEG-PDMA (**5**) solution (ranging from 0.001mg/mL to 1mg/mL) were added into each vial. The mixtures were left to equilibrate over night at room temperature before running the measurements. The solutions were filtered using Whatman® GD/X syringe filter with 0.4µm pores to remove any insoluble pyrene prior to recording the fluorescence spectra. The emission spectra of pyrene in the solution were recorded over the wavelength region of 350 to 470nm. The excitation wavelength was 340nm with a slit width of 5nm for both excitation and emission. The intensities of the peaks seen at 373 and 383nm which are characteristic for pyrene were fixed as I_1 and I_3, respectively. The peak intensity ratios at 373 and 383nm (I_3/I_1) of pyrene fluorescence spectra were recorded as a function of logarithm of mPEG-PDMA concentration (mg/mL).

6.2.3. General procedure for preparation of the polyion complex.

The polyion complex of this system was as follows: A 5mg/mL solution of mPEG-PDMA in MeOH at (stock solution1) was prepared. A 5mg/mL solution of porphyrin or porphyrin cored hyperbranched polymer (PH-HB-COOH) in MeOH (stock solution 2) was prepared. From stock1 solution, a diluted solution was prepared in MeOH. Likewise, a dilute solution was prepared from stock solution 2. The solutions were mixed and the resulting solution was stirred for 5 minutes. After removal of the solvent using rotary evaporator, 5mL of buffer solution or water was added and the solution stirred at room temperature for 5 minutes. To eliminate any insoluble porphyrin or PH-HB-COOH, the coloured solution was then filtered through Whatman® GD/X syringe filter with 0.45µm pores and the resulting solution was ready for analysis.

6.2.4. General procedure for drug release experiment

5mL of the mPEG-PDMA /PH-HB-COOH polyion complex in phosphate buffer (PB) with regards to the pH was charged into a dialysis bag. This bag placed in a flask containing 50mL of phosphate buffer at the same pH equipped with lid and magnetic stirrer. The dialysis system was then placed into a water bath at temperature at 37 ^{o}C with stirring speed of 100 rpm. 3mL aliquots were withdrawn from the bulk solution and replaced with 3mL aliquots of fresh buffer solution. The aliquot was studied using UV/Vis spectroscopy to measure the amount of PH-HB-COOH (regarded as a drug) released by monitoring the Soret band absorption of PH-HB-COOH at 42nm. From the UV absorbance spectrum, the molar concentration (C_0) of the polyion solution in the bag was calculated before placing the bag into the dialysis solution. Then, the concentration of the released PH-HB-COOH in the flask (C_f) was calculated from the UV absorption after 1 day from the placing the bag into the dialysis solution. C_F was

subtracted from C_0 to calculate the molar concentration of PH-HB-COOH remaining in the bag (C_t). The percentage of released polymer was calculated using C_t/C_0 X100. This process was repeated for several days and the obtained data was plotted as a function of time (days).

6.2.5. General procedure of catalytic reaction

As a typically procedure: A reaction flask was charged with of iodosylbenzene (0.1 mmol). The flask was evacuated and flushed with nitrogen. To this system, a mixture of the internal standard (pyrene, 0.198 mmol), cyclohexene substrate (0.49 mmol) and porphyrin containing catalyst (1μmol), and chloroform was then added using syringe. Under Nitrogen atmosphere, the suspension mixture was robustly stirred in a dark place for half an hour. Whatman® GD/X syringe filter, with a pore size of 0.45μm, was utilised to isolate the solid products upon the reaction being accomplished. The filtrate obtained was transferred into a GC vessel, which was then analysed by the GC instrument.

6.2.6. General catalytic procedure –Polyion complex in water

In a typical procedure: A reaction flask (flask 1) was charged with of iodosylbenzene (0.1 mmol), cyclohexene substrate (0.49 mmol) and the internal standard (pyrene). The flask was evacuated and flushed with nitrogen and the system kept under nitrogen atmosphere. In another flask (flask 2), a polyion complex in water was prepared using appropriate amount of mPEG-PDMA and iron functionalised porphyrin or iron cored hyperbranched polymer (using the same procedure for preparing the polyion complex mentioned before). This system was flushed, evacuated, and kept under nitrogen. The polyion complex was then added gradually to the suspension in flask1. The mixture was

then stirred vigorously in a dark place for 24 hour. The organic solvent was then removed and the suspension stirred for further half an hour under nitrogen atmosphere. The organic products were extracted by 5mL of chloroform. The organic layer was attained and filtered through Whatman® GD/X syringe filter with a pore size of 0.45µm. The obtained organic solution was added to GC vial, which was then analysed by the GC instrument.

6.2.7. General catalytic procedure –Polyion complex in DCM

The reactions were performed using the general procedure of water system, except the adding solution of cyclohexene substrate in DCM to the mixture reaction. The reaction was stirred in the dark for 24h. DCM was then evaporated, and the resultant solution was also left stirring in the dark for 24h. the organic materials were extracted buy DCM, filtered and added to GC vial.

6.3. Synthetic procedures

6.3.1. Methoxypoly(ethylene glycol) bromoisobutyrate macroinitiator (mPEG-Br) (3)

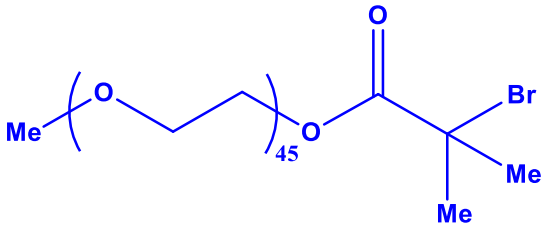

mPEG (10.00g, 5.00 mmol) was dissolved in dry toluene (200mL) and added to 500 mL two-neck round bottom flask. Azeotropic vacuum distillation was used to remove any traces of water from mixture solution The solution was cooled to 0 °C in an ice bath and triethylamine (1.1mL, 7.89 mmol) added followed by α-bromoisobutyryl

bromide (0.95mL, 7.7 mmol) to be dropwise added via 1.0mL syringe within one hour. The reaction mixture was stirred at room temperature for 24h. Vacuum filtration was used to remove by-product. The filtrate was concentrated using rotary evaporation, and then precipitated from excess of diethyl ether and filtered to give a cream coloured solid. The crude product was purified by recrystallization from absolute ethanol, filtered, then dried under vacuum to give methoxypoly(ethylene glycol) bromoisobutyrate (mPEG-Br) (6.5g, 60%) as a white solid. ^{1}H NMR (400MHz; $CDCl_3$; ppm) δ 1.95 (6H, s, -$CO_2Br(C\underline{H}_3)_2$), 3.4 (3H, s, $C\underline{H}_3O$-), 3.66 (178H, s, -$OC\underline{H}_2C\underline{H}_2O$-), 4.34 (2H, t, -$C\underline{H}_2OCOCMe_2Br$); ^{13}C NMR (100 MHz; $CDCl_3$; ppm) 30.6, 58.8, 70.57; IR (cm^{-1}) 1734, 1275, 1238, 1059, 643.

6.3.2. General procedure for the synthesis of mPEG-PDMA diblockcopolymer (5)

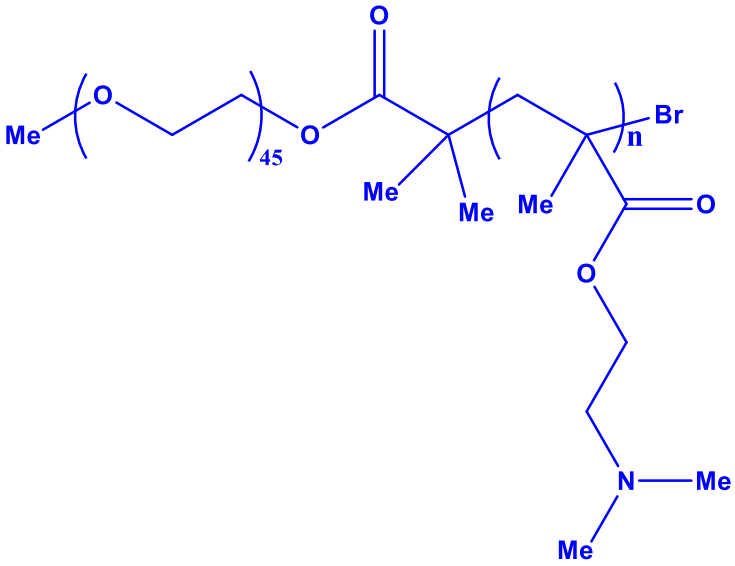

To a 50mL two-neck round-bottom vial equipped with stirrer bar and sealed with a rubber septum, copper(I) chloride (46.5mg, 0.47 mmol) and 2,2'-bipyridyl (145mg,

0.931 mmol) were added. The mixture vessel was then evacuated and refilled with nitrogen gas three times. In a discrete round-bottom vial, a mixture of mPEG-Br macroinitiator and dimetylaminoethyl methacrylate (DMA) monomer (was distilled under reduced pressure to remove the trace of inhibitor) and mPEG-Br (DMA ratio is varied to the PEG units of mPEG-Br) in 50% v/v deionized water was prepared and degassed by five freeze-pump-thaw cycles. The latter solution was transferred into the first vial which containing the catalyst using a two-tipped needle. A dark brown solution which became a dark green viscous liquid within 10 minutes of initiation was formed. The reaction mixture was stirred under positive nitrogen pressure overnight. The crude product was dissolved in THF and the resulting blue solid removed by vacuum filtration. The filtrate was reduced under vacuum yielding green oil. The catalyst was removed using a flushed basic alumina column (5×5cm) in chloroform. The solvent was removed by rotary evaporation and the product dried in a vacuum oven at 40 °C to yield methoxypoly(ethylene glycol)-*block*-poly[2-(dimethylamino) ethyl methacrylate] copolymer (mPEG-PDMA) as an elastic light colorless solid.

6.3.2.1. mPEG-PDMA 1:20 (5a)

mPEG-Br (1.018g, 0.4737 mmol) and DMA (1.72mL, 10.2 mmol) were reacted according the general procedure mentioned before to yield mPEG-PDM_{26} (1.75g, 67%); ^{1}H NMR (400MHz; $CDCl_3$; ppm) δ 0.91-1.07 (143 H, br, $(C\underline{H}_3)_2CH_2C(C\underline{H}_3)$(COO-)Br), 1.84-1.91 (84H, br, -$C\underline{H}_2$CMeCOO-Br), 2.31 (268H, s, $N(C\underline{H}_3)_2$), 2.58 (98H, d, *J*= 3.1, -$\underline{H}_2N(CH_3)_2$), 3.4 (3H, s, $C\underline{H}_3$O-), 3.65 (178H, m, -$OC\underline{H}_2C\underline{H}_2$O-), 4.07 (94H, d, *J* =4, -$C\underline{H}_2$OOC-); ^{13}C NMR (100 MHz; $CDCl_3$; ppm) δ 44.7, 45.7, 57.1, 62.9, 70.6, 176.4, 177.2; IR (cm^{-1}) 1726, 1277, 1237, 1146, 1103, 750; GPC (LMW; THF) M_n = 2920, PD= 1.07.

6.3.2.2. mPEG-PDMA 1:30 (5b)

mPEG-Br (1.002g, 0.4663 mmol) was reacted with DMA (2.5mL, 15.02 mmol) according the general procedure mentioned before to yield mPEG-$PDMA_{37}$ (2.3g, 69%); ^{1}H NMR (400MHz; $CDCl_3$; ppm) δ 0.9-1.1 (174H, b, -$(C\underline{H}_3)_2CH_2C(C\underline{H}_3)$(COO-)Br), 1.84-1.92 (105H, br, -$C\underline{H}_2CMe$(COO-)Br), 2.3 (336H, s, $N(C\underline{H}_3)_2$), 2.58 (119 H, d, *J*= 3.1, -$\underline{H}_2NMe_2$), 3.39 (3H, s, $C\underline{H}_3O$-), 3.66 (180H, m, - $OC\underline{H}_2C\underline{H}_2O$-), 4.07 (116H, d, *J*= 4.0, -$C\underline{H}_2OOC$-); ^{13}C NMR (100 MHz; $CDCl_3$; ppm) δ 45.6, 45.8, 57.1, 63.0, 70.6; IR (cm^{-1}) 1722, 1270, 1240, 1145, 1100, 747; GPC (LMW; THF) M_n = 2970, PD= 1.06.

6.3.2.3. mPEG-PDMA 1:40 (5C)

mPEG-Br (1.005g, 0.4676 mmol) was reacted with DMA (3.54mL, 20 mmol) according to the procedure mentioned before to yield mPEG-$PDMA_{47}$ (4.2g, 96%); ^{1}H NMR (400MHz; $CDCl_3$; ppm) δ 0.91-1.05 (174H, br,-$(C\underline{H}_3)_2CH_2C(\underline{CH}_3)$(COO)Br), 1.83-1.91 (105H, b, $C\underline{H}_2CMe$(COO-)Br), 2.30 (336H, s, $N(C\underline{H}_3)_2$), 2.6 (119 H, d, *J* 3.1, -$\underline{H}_2NMe_2$), 3.4 (3H, s, $C\underline{H}_3O$-), 3.65(180 H, m, -$OC\underline{H}_2C\underline{H}_2O$-), 4.08 (116H, d, *J* = 4.0, -$C\underline{H}_2OOC$-); ^{13}C NMR (100 MHz; $CDCl_3$; ppm) δ 44.7, 45.8, 57.1, 63.4, 70.6, 176.4, 177.2; IR(cm^{-1}) 1721, 1268, 1240, 1143, 1100, 747; GPC (LMW; THF) M_n = 4500, PD=1.03

6.3.3. Tetraphenyl porphyrin (TPP) (8)

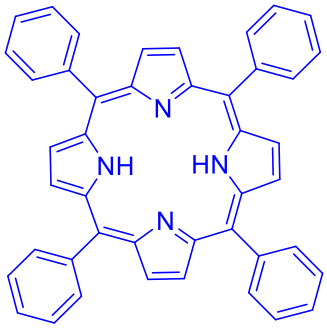

A freshly distilled pyrrole (7.00mL, 0.101 mol) was added via a syringe to a refluxing solution of benzaldehyde (10.0mL, 0.0985 mol) in 300mL propionic acid and stirred for one hour under reflux. The reaction mixture was allowed to cool to room temperature. Upon filtration under vacuum, the precipitant was first washed with cold methanol then warm water (60℃) and again with cold methanol. The product then was recrystallised from methanol/dichloromethane and dried under vacuum overnight to yield shiny purple crystals of meso- tetraphenyl porphyrin (2.9g, 20%).^{1}H NMR (400MHz; $CDCl_3$; ppm) δ 8.90 (8H, s, pyrrole-H), 8.26 (8H, m, o-H), 7.81 (12H, m, p/m-H), 2.73 (2H, s, NH); ^{13}C NMR (100 MHz; $CDCl_3$; ppm) δ 142.19, 134.58, 127.73, 126.7,120.17; IR(cm^{-1}) 3019, 1472, 1176, 696; m/z (ES) 615 (MH^+); UV/Vis (CH_2Cl_2) λ = 417nm.

6.3.4. Tetracarboxyphenyl porphyrin (TCPP) (10)

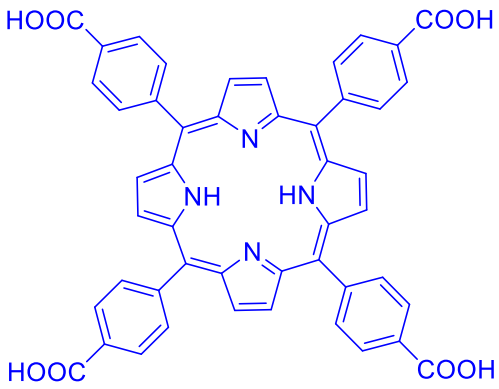

A freshly distilled pyrrole (3.7mL, 55.14 mmol) was added to a refluxing solution of 4-carboxybenzaldehyde (8.25g, 54.95 mmol) in 250mL of propionic acid. The mixture was refluxed for further two hours. A hot filtration was used to separate the resulting product. The filter cake was washed with dichloromethane, and then with cold methanol. The obtained product was collected and dried under vacuum to give TCPP as a purple solid. Yield: 2.5 g, 34%. ^{1}H NMR (DMSO, 400 MHz), δ 13.20 (s, 4H, COOH), 8.77 (s, 8H, pyrrolic-β-CH), 8.21 (q, 16H, phenylic CH), -2.96 (s, 2H, NH), ^{13}C NMR (DMSO, 100 MHz) δ 168.1, 146. 135.1, 131.1, 128.4, 120; IR (cm^{-1}): 2626, 2725, 1678, 1602, 1555, 1398, UV/Vis (MeOH): 415, 513, 549, 588, 648; MH^{+} (ESI-MS) = 790 (calculated 790 g/mol).

6.3.5. Tetrahydroxyphenyl porphyrin (THPP) (12)

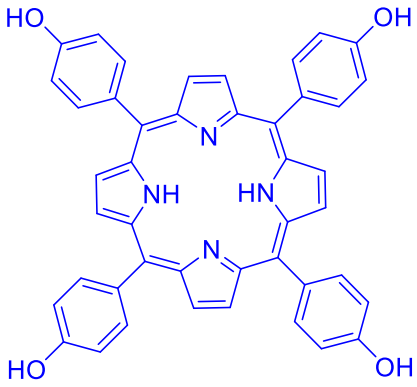

A freshly distilled pyrrole (6.2mL, 91.37 mmol) was added via a syringe to a refluxing solution of 4-hydroxy benzaldehyde (15g, 91.4 mmol) in 300 mL propionic acid and stirred for two hours under reflux. The reaction mixture was allowed to cool to room temperature. Then, it was kept overnight at -20 ℃ . Upon filtration under vacuum, the filter cake was first washed with a mixture of propionic acid and ethanol (1:1). Then, it was washed with chloroform and dried under vacuum to give shiny purple crystals of meso-5,10,15,20-tetrakis (4-hydroxyphenyl)-21H,23H-porphyrin (2g , 14%) .^{1}H NMR (400MHz; DMSO-d_6 ; ppm) δ 9.99 (s, 4H, phenylic p-OH), 8.87 (s, 8H, pyrrolic β-H), 7.99 (d, *J*=8.5, 8H, phenylic m-CH), 7.2 (d, *J*=8.28, 8H, phenylic o-CH), -2.89 (s, 2H, NH; ^{13}C NMR (100 MHz; DMSO-d_6; ppm) δ158, 136.1, 132.4, 120.5, 114.4, 60.2; IR (cm^{-1}) 2924 (NH), 3286 (OH); 1609(C=N); UV/Vis (MeOH) = 418 nm; MH^+ (ESI-MS) = 679 (calculated 679 g/mol).

6.3.6. 5-actoxyisophthalic acid (AIPA) (13)

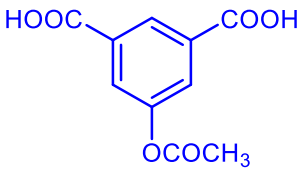

To a 500mL round-bottomed flask equipped with a rubber stopper and containing 5-hydroxyisophthalic acid (45.5g, 0.25 mol), was added acetic anhydride (102g, 95mL, 1mol). The mixture was brought up to reflux for half an hour, where the acid was completely dissolved. The mixture was left to reflux for additional 5 hours. Within one hour a white precipitate was observed. To get rid of the excess of acetic anhydride, the mixture flask was subjected to a vacuum. The crude white product was purified by recrystallisation from ethyl acetate/ petroleum ether (twice). The yield of resulting white powder was 52.5g, 93%. ^{1}H NMR (400 MHz; DMSO-d_6; ppm): δ 2.32 (s, 3H), 7.9 (d, *J*=1.5**,** 2H,), 8.36 (t, *J*=1.5, 1H), 13.5 (s, br, 2H, COOH); ^{13}C NMR (100 MHz, DMSO-d_6; ppm) δ 169.8, 166.5, 151.3, 127.5, 21.5; IR(cm^{-1}) 3100, 2824, 1769, 1693, 1598); MH+ (ESI-MS) = 224 (calculated 224 g mol^{-1}).

6.3.7. Hyperbranched polymer bearing carboxylic acid terminal groups (HB-COOH) (14)

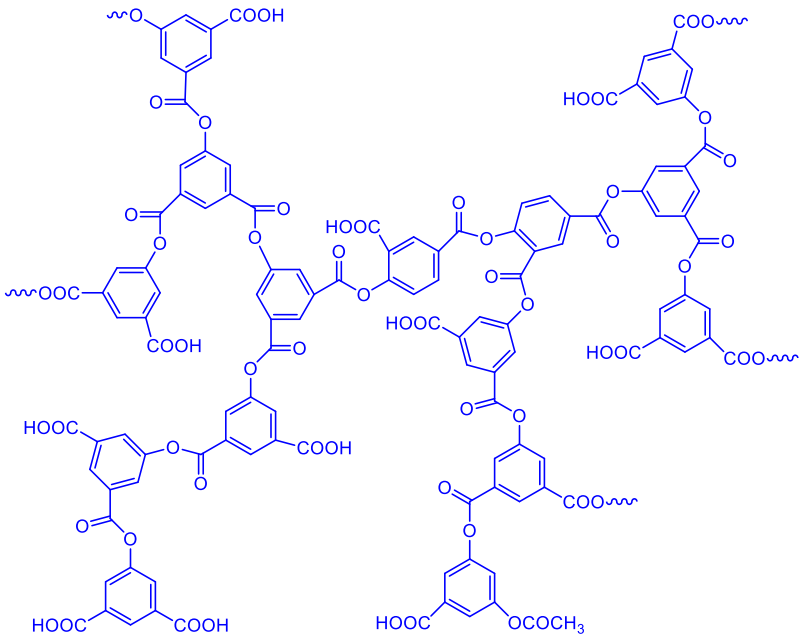

5-Acetoxyisophthalic acid (10g, 0.0446 mol) was added to 500mL round-bottomed flask. The reaction flask was flushed three times, then it was heated to 250 ºC. During the first 20 minutes, the reactor was subjected to a high flow of inert nitrogen gas. Then, a vacuum was applied for 30 min. A mixture of THF/H_2O (100:10) (V/V) was added in order to crush the brittle foam formed. The mixture then heated to reflux for several hours until a homogeneous solution can be seen. After precipitated from water, the resulting product was dried. Then, it was dissolved in hot THF and precipitated from diethyl ether to give (5.4g, 40%) colorless powder. ^{1}H NMR (400 MHz; DMSO-d_6; ppm): 7.51-8.84 (m, b, Ar-H), 13.5 (s, b, COOH); IR(cm^{-1}) 3086, 1696, 1594, 1435, 1192.

6.3.8. Hyperbranched polymer bearing ethyl ester terminal groups (HB-COOET) (15)

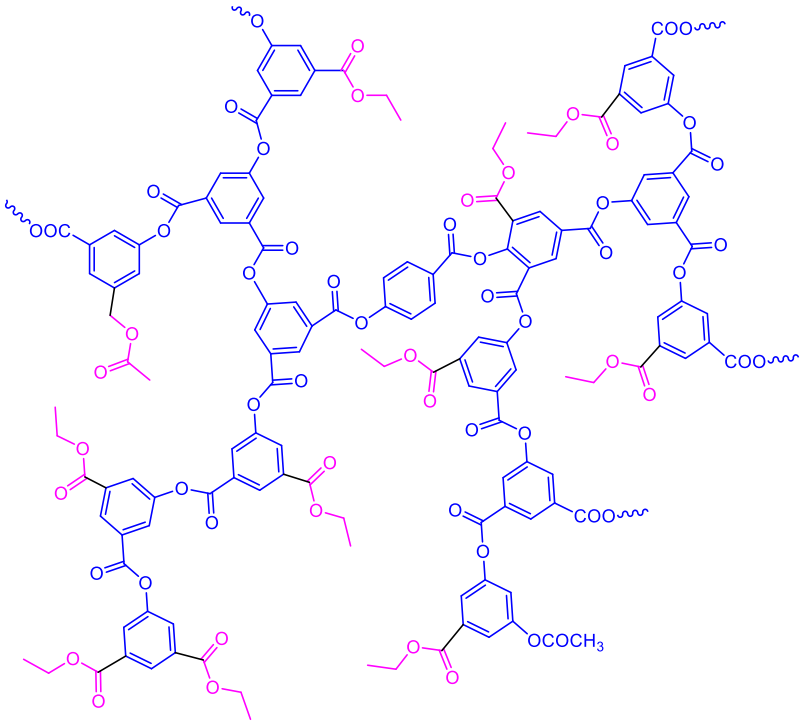

To a two neck round-bottomed flask equipped with a rubber septum and condenser, a solution of hyperbranched polymer with carboxylic acid terminal groups (HB-COOH) (0.5g, 0.166mm) in anhydrous THF was added. To this, Thionyl chloride (0.048mL, 0.025 mol) and three drops of dimethyl formide were added. The mixture was heated to reflux where a clear solution was observed. The mixture solution was refluxed for further six hours. The flask mixture was then placed in a rotary evaporator to eliminate of the excess of thionyl chloride and the solvent. To dissolve the resulting hyperbranched polymeric chloride, THF (20mL) was added. To this solution, a mixture of THF (20mL), ethanol (0.58mL, 0.01mol) and trimethylamine (1.3mL) was then added slowly. Then, the mixture solution was stirred for 24 hours

at room temperature. Et_3NHCl, was then filtered off under vacuum. The resulting product was then precipitated into H_2O (to improve the precipitation of the product, drops of hydrochloric acid were added), dried in a vacuum to afford hyperbranched polymer bearing ethyl ester terminal groups, colourless solid; yield (0.34, 68%). ^1H NMR (400 MHz; $CDCl_3$; ppm): δ 7.91-9.06 (m, b, Ar-H), 1.42 (t, CH_3, 4.43 (q, CH2); IR(cm^{-1}) 3082, 2983, 1718, 1593, 1439, 1191; GPC (LMW; THF) M_n = 3000 g/mol.

6.3.9. Porphyrin cored hyperanched poloymer bearing carboxylic acid terminal groups (PH-HB-COOH) (16)

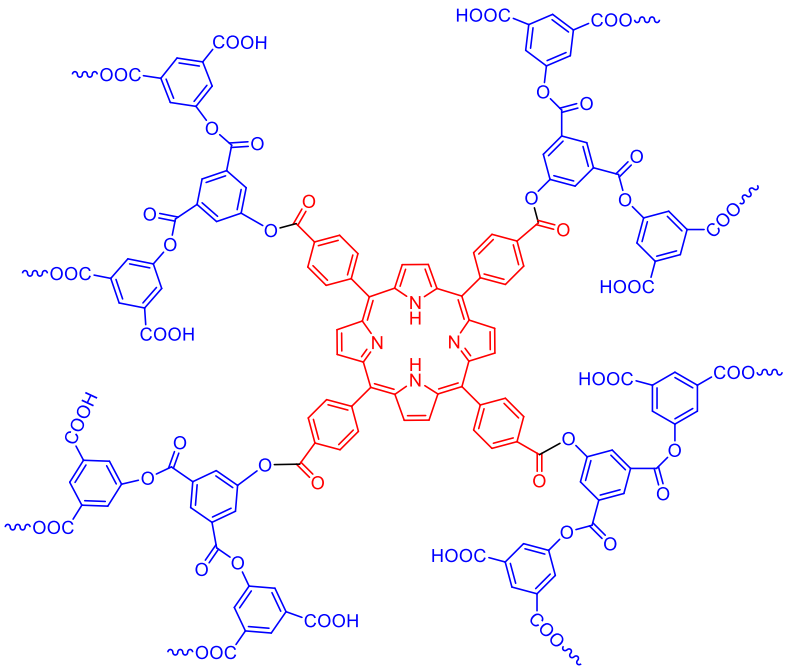

Tetracarboxyphenyl porphyrin (TCPP) (1.74g, 0.0022 mol) and 5- acetoxyisophthalic acid (5g, 0.022mol) were added to 250mL round-bottomed flask. The reaction flask was flushed three times, then it was heated to 250 ^oC. During the first 20 minutes, the reactor

was subjected to a high flow of inert nitrogen gas. Then, a vacuum was applied for 1 hour. A mixture of THF/H_2O (100:10) (V/V) was added in order to crush the brittle foam formed, which fill the entire flask. The mixture then heated to reflux for several hours until a homogeneous solution can be seen. After precipitated from water, the resulting product was dried. Then, it was dissolved in hot THF and precipitated from diethyl ether to give (2.4g, 36%) dark brown solid. ^{1}H NMR (400 MHz; DMSO-d_6; ppm): -2.93 (s, 2H, NH pyrrolic), 7.5-8.33 (m, b, Ar-H), 8.9 (s, b, pyrrolic porphyrin), 13.5 (s, b, COOH); UV/Vis (MeOH) = 418nm.

6.3.10. Porphyrin cored hyperbranched polymer bearing ethyl ester terminal groups (PH-HB-COOEt) (17)

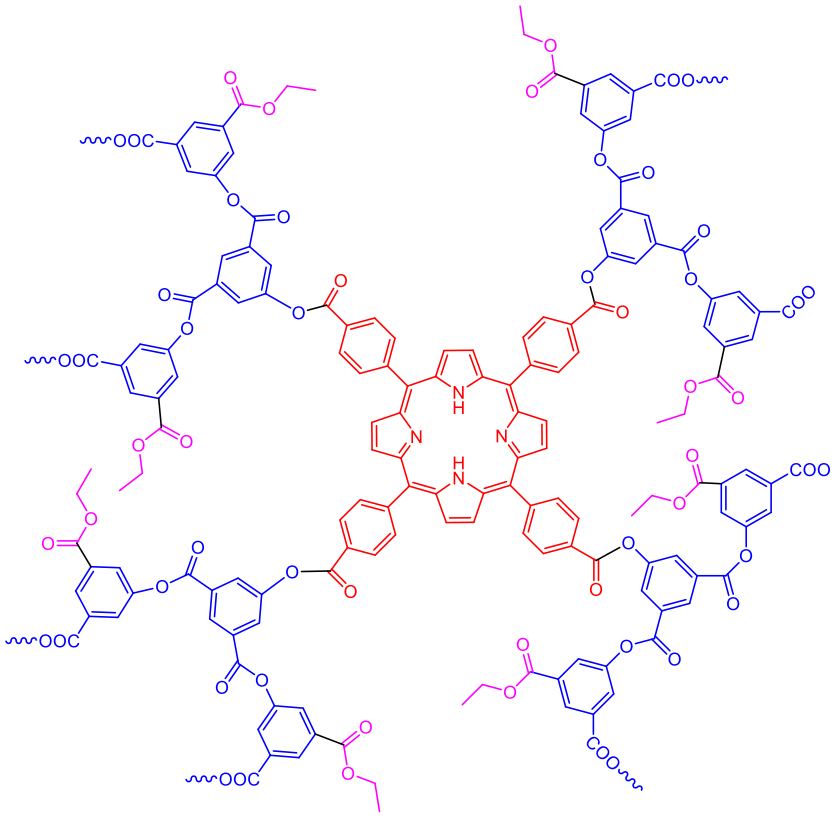

To a two neck round-bottomed flask equipped with a rubber septum and condenser, a solution of porphyrin cored hyperbranched polymer with carboxylic acid terminal groups (PH-HB-COOH) (0.5g, 0.166mm) in anhydrous THF was added. To this, thionyl chloride (0.048mL, 0.025 mol) and three drops of dimethyl formide were added. The mixture was heated to reflux where a clear solution was seen. The mixture solution was refluxed for further six hours. The flask mixture was then placed in a rotary evaporator to eliminate of the excess of thionyl chloride and the solvent. To dissolve the resulting hyperbranched polymeric chloride, THF (20mL) was added. To this solution, a mixture of THF (20mL), ethanol (0.58mL, 0.01mol) and trimethylamine (1.3mL) was then added slowly. Then, the mixture solution was stirred for 24 hours at room temperature. To remove Et_3NHCl, the mixture was filtered under vacuum. The resulting product was then precipitated into H_2O (to improve the precipitation of the product, drops of hydraulic acid were added), dried in a vacuum to afford porphyrin cored hyperbranched polymer with ethyl ester terminal groups (HB-PH-COOEt), colourless solid, yield (0.34g, 68%). ^1H NMR (400 MHz; $CDCl_3$; ppm): δ 7.94-9.15 (m, b, Ar-H), 1.41 (t, CH3), 4.46 (q, CH_2), -2.79 (s, 2H, NH-pyrrolic); IR(cm^{-1}) 3082, 2983,1718, 1593, 1439, 1191; GPC (LMW; THF) M_n = 3000 g/mol.

6.3.11. Tetracarboxymethylphenyl porphyrin (TCMPP) (28)

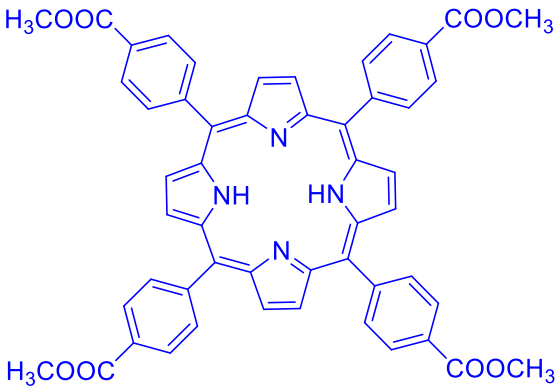

Freshly distilled pyrrole (6.2mL, 91.37 mmol) was added via a syringe to a refluxing solution of 4-carboxymethyl benzaldehyde (15g, 91.4 mmol) in 300mL propionic acid and stirred for 1hour under reflux. The reaction mixture was allowed to cool to room temperature. Upon filtration under vacuum, the precipitant was first washed with cold methanol then warm water (60 ℃) and again with cold methanol. The product then was recrystallised from methanol/dichloromethane and dried under vacuum overnight to yield shiny purple crystals of meso-5,10,15,20-tetrakis(4-carboxymethyphenyl)-21H,23H-porphyrin (2.7 g, 13.5%) .^{1}H NMR (400MHz; CDCl3; ppm) δ 8.84 (s, 8H, pyrrolic β-H) 8.45 (d, *J*=8.09, 8H, phenylic o-CH), 8.31 (d, *J*=8.09, 8H, phenylic m-CH), 4.14 (s, 12H, CH_3CO-), -2.80 (s, 2H, NH); ^{13}C NMR ($CDCl_3$) δ: 167.29, 146.6, 146.62, 134.48, 127.92, 119.30., 52.48; IR(cm^{-1}) 1719 (C=O), 1607, 1550, 1435 1400, 1271 ; UV/Vis (CH_2Cl_2) nm = 420, 515, 550, 593, 548; MH^+ (ESI-MS) = 847 (calculated 847 g/mol).

6.3.11. Iron functionalised tetracarboxymethylphenyl porphyrin (Fe-TCMPP) (29)

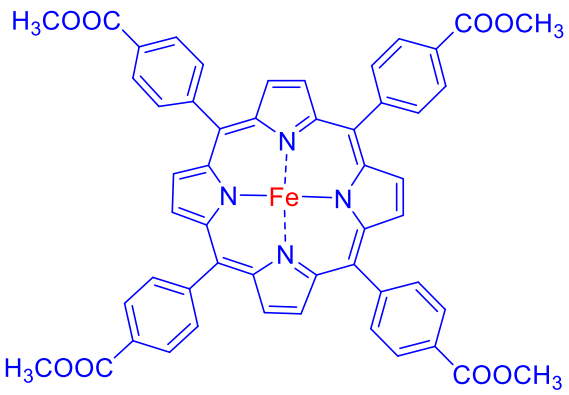

To a two neck round-bottomed flask equipped with a septum and condenser, tetracarboxymethylphenyl porphyrin (0.75g, 0.89 mmol) was added. The system was evacuated and flushed with inert nitrogen gas. The system kept under nitrogen pressure. Using a syringe, anhydrous THF (80mL) was added. To this solution, 2,6-lutidine (0.77 mL 6.54 mmol) was added. Upon mixture was refluxed for 20 minutes, $FeCl_2$ (1.12g, 13 mmol) was added. The reaction mixture was refluxed for further 5 hours. The resultant solution was then allowed to cool down to room temperature under atmosphere. Unreacted $FeCl_2$ was filtered off and rotary evaporator was utilised to remove THF from the filtrate. The resultant product was the dissolved in DCM. The solution washed twice with 1M HCl and three times with deionized water. Column chromatography with a solvent system of DCM containing with 25% MeOH (v/v) was used for the purification to give dark brown solid (0.535 g, 67 %). IR(cm^{-1}): 1710 (COOR), 1606, 1431, 1400, 1340; UV/Vis (CH_2Cl_2) nm = 417.5, 510, 573; MH+ (ESI-MS) = 900 (calculated 899 g/mol).

6.3.12. Iron functionalised tetracarboxyphenyl porphyrin (Fe-TCPP) (30)

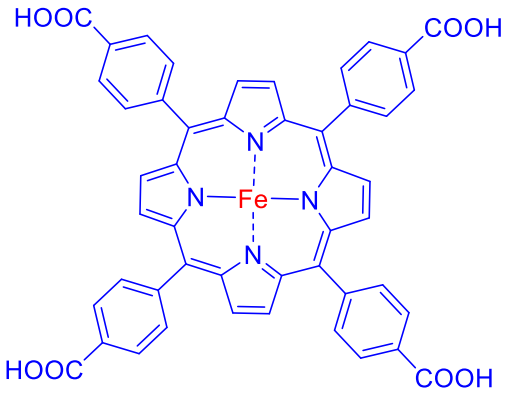

A mixture of THF (25mL) and methanol (25mL) was added to 250mL round –bottomed flask contains tetracarboxymethylphenyl porphyrin iron(III) complex (Fe-TCMPP) (0.75 g, 0.834 mmol) and equipped with stirrer bar and condenser. Upon the addition of a solution of KOH (2.63 g, 46.95 mmol) in deionised water, the mixture was then refluxed overnight. The flask mixture was cooled down to room temperature. After the remove of the solvent mixture (THF and methanol), deionised water was then added where a water phase can be seen. The flask mixture was heated until a homogeneous solution was observed. To this, a few drops of HCl (1M) were added in order to precipitate the product. Upon the filtration, the product was then washed with water (twice). The product was dried under vacuum to give dark brown solid (0.50 g, 71%). IR ($cm^{-1)}$: 1710 (COOR), 1606, 1431, 1400, 1340; UV/Vis (MeOH) λ(nm) = 416, 510, 576; MH^+ (ESI-MS) = 843 (calculated 843 g/mol).

6.3.12. Iron(III) cored hyperbranched polymer bearing carboxylic acid terminal groups (Fe-PH-HB-COOH) (31)

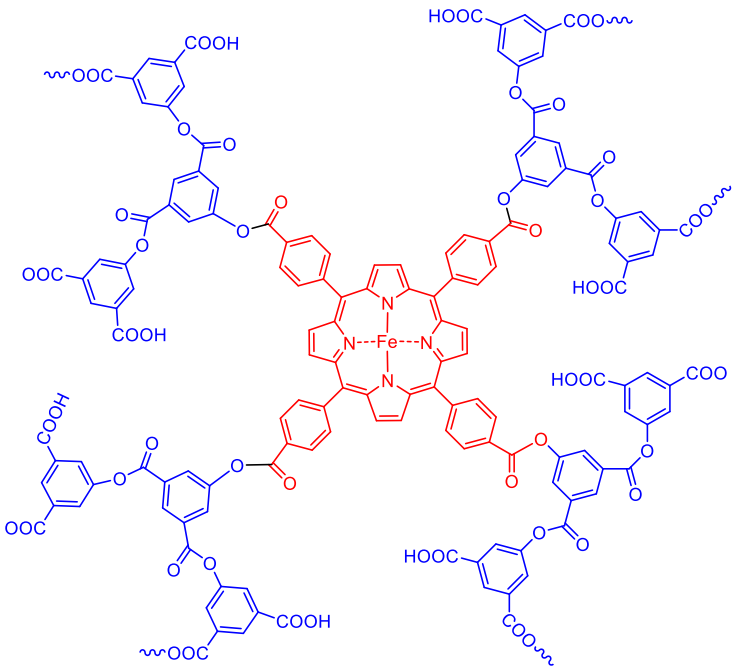

Tetracarboxyphenyl porphyrin iron(III) complex (Fe-TCPP) (1.7g, 0.002 mol) and 5-acetoxyisophthalic acid (5g, 0.022mol) were added to 250mL round-bottomed flask. The reaction flask was flushed three times, then it was heated to 250 ^{0}C. During the first 20 minutes, the reactor was subjected to a high flow of inert nitrogen gas. Then, a strong vacuum was applied for 1h. A mixture of THF/H_2O (100:10 V/V) was added in order to crush the brittle foam formed, which filled the entire flask. The mixture then heated to reflux for 5 hours until a homogeneous solution can be seen. After precipitated from water, the resulting product was dried. Then, it was dissolved in hot THF and precipitated from diethyl ether to give (4.4g, 66%) brown solid; UV/Vis (MeOH) λ (nm) = 411, 573, 617; Mn (GPC) ~3000 g/mol; IR(cm^{-1}) 3082, 2983, 1718, 1593, 1439, 1191.

6.3.13. Iron(III) cored hyperbranched polymer bearing ethyl ester terminal groups (Fe-PH-HB-COOEt (32)

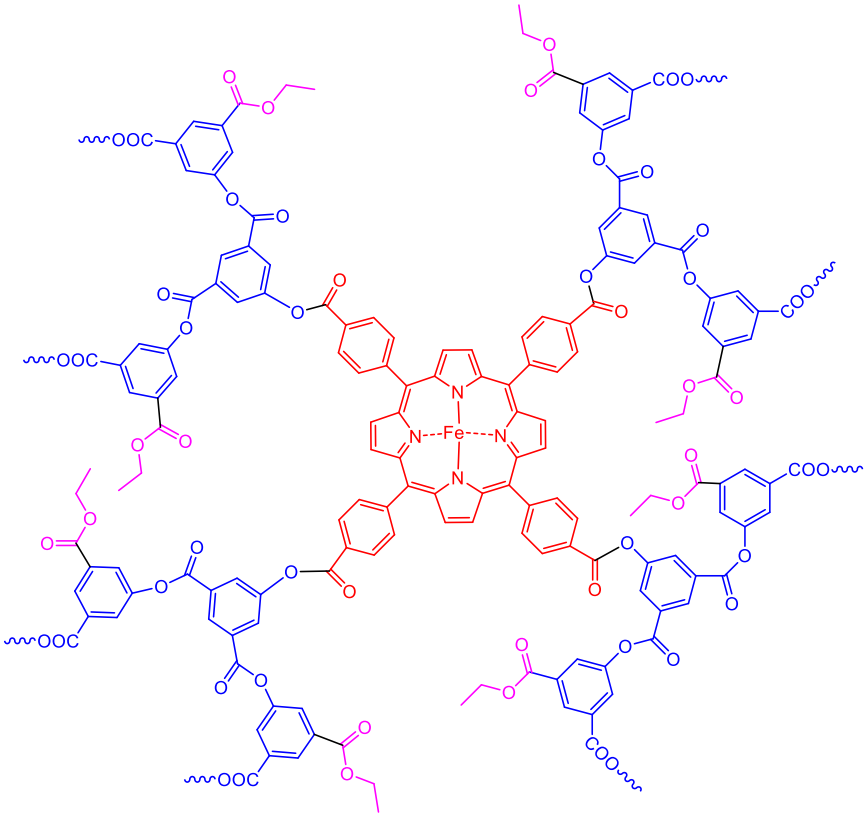

To a two neck round-bottomed flask equipped with a rubber septum and condenser, iron(III) cored hyperbranched polymer (Fe-PH-HB-COOH) (0.75g, 0.233 mmol) in anhydrous THF was added. To this, thionyl chloride (0.048mL, 0.025 mol) and three drops of dimethyl formide were added. The mixture was heated to reflux where a clear solution was seen. The mixture solution was refluxed for further six hours. The flask mixture was then placed in a rotary evaporator to eliminate of the excess of thionyl chloride and the solvent. To dissolve the resulting hyperbranched polymeric chloride, THF (20mL) was added. To this solution, a mixture of ethanol (0.58mL, 0.01mol) and trimethylamine (1.3mL) was then added slowly. Then, the mixture solution was stirred for 24 hours at room temperature. To remove Et_3NHCl, the mixture was filtered under

vacuum. The resulting product was then precipitated into H_2O (to improve the precipitation of the product, drops of hydraulic acid ere added), dried in a vacuum to afford iron(III) cored PH-HB-COOET hyperbranched polymer, colourless solid, light brown solid yield (0.4g, 57%); UV/Vis (CH_2Cl_2) λ , 415.5nm; IR(cm^{-1}) 3082, 2983, 1718, 1593, 1439, 1191; Mn (GPC) ~3000 g/mol.

6.3.14. Iodosylbenzene (34)

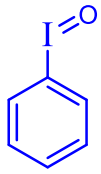

Diacetoxyiodobenzene (3.22g, 0.01 mol) was placed in a beaker equipped with a stirrer. To this, 15 mL of sodium hydroxide (3M) was added during 3 minutes with a robust stirring. Upon leaving the mixture stable for 45 minutes, the mixture was continuously stirred with the addition of 15 ml of water. Vacuum filtration was used to collect the product. Excess of water was then added with strong stirring for half an hour. The solid product was then stirred in $CHCl_3$ for half an hour, filtered, collected, and dried to give white-yellowish solid. Yield (1.4g, 63%). ^{1}H NMR (CD_3OD), 400 MH_Z) δ 8.06 (m, 2H, *Ar o*-C<u>H</u>) 7.6 (m, 3H, *Ar p*-C<u>H</u>, *Ar m*-C<u>H</u>); ^{13}C NMR (CD_3OD, 400 MH_Z) δ 131.91, 130.80, 130.63; IR(cm^{-1}) 3035 (aromatic C-H stretch) 1568, 1434, 735, 687; MH^+ (ESI-MS) = 220 (calculated 220 g/mol); mp 210°C.

Chapter 7

References

7. References

1. MinMin, Li; GuangYan, Q; MingXi, Z.; TaoLei, S., *Sci. China Chem.*, 2014, 57, 540.
2. Carothers, W. H., *Trans. Faraday Soc.*, 1936, 32, 39.
3. Staudinger, H., *Ber. Dtsch. Chem. Ges*., 1920, 53, 1073.
4. Rapoport, N., *Prog. Polym. Sci.*, 2007, 32, 962.
5. Vögtle, F.; Richardt, G.; Werner, N. *In Dendrimer Chemistry, Concept, Synthesis, Properties and Applications*; Wiley-VCH Verlag GmbH & Co. KGaA, 2009, pp 1.
6. Gao, C.; Yan, D., *Prog. Polym. Sci*., 2004, 29, 183.
7. Venturi, M.; Serroni, S.; Juris, A.; Campagna, S.; Balzani, V., *Spring. Berl. Heid*., 1998, 197, 193.
8. Kienle, R. H.; Hovey, A. G., *J. Am. Chem. Soc*. 1929, 51, 509.
9. Kim, Y. H., *J. Polym. Sci. Part A Polym. Chem*., 1998, 36, 1685.
10. Kim, Y. H.; Webster, O. W., *J. Am. Chem. Soc*., 1990, 112, 4592.
11. Kim, Y. H.; Webster, O. W., *Macromolecules*,1992, 25, 5561.
12. Voit, B., *J. Polym. Sci. Part A : Polym. Chem*., 2000, 38, 2505.
13. Carlmark, A.; Hawker, C.; Hult, A.; Malkoch, M., *Chem. Soc. Rev*., 2009, 38, 352.
14. Voit B. I., *C. R. Chimie*., 2003, 6, 821.
15. Jo, W. H. and. Lee, Y. U., *Macromolecules*, 2001, 10, 225.

16. Hawker, C. J.; Lee, R.; Fréchet, J. M. J., *J. Am. Chem. Soc*., 1991, 113, 4583.

17. Farrington, P. J.; Hawker, C. J.; Fréchet, J. M. J.; Mackay, M. E., *Macromolecules*, 1998, 31, 5043.

18. Jikei, M.; Kakimoto, M.-a. *Prog. Polym. Sci*., 2001, 26, 1233.

19. Wooley, K. L.; Fréchet, J. M. J.; Hawker, C., *J. Polym*., 1994, 35, 4489.

20. Wooley, K. L.; Hawker, C. J.; Lee, R.; Fréchet, J. M., *J. Polym*., 1994, 26, 187.

21. Matthews, O. A.; Shipway, A. N.; Stoddart, J. F., *Prog. Polym. Sci*., 1998, 23, 1.

22. Fréchet, J. M. J.; Hawker, C. J., *In Comprehensive Polymer Science*, 2nd Supplement, 1996, pp71.

23. Flory, P. J., *J. Am. Chem. Soc*., 1952, 74, 2718.

24. Cheng, L.; Peng, H.; Luo, J.; Tang, B. Z., *Polym. Prep.* (*Am. Chem. Soc., Div. of Polym. Chem.*), 2002, 43, 570.

25. Yamaguchi, N.; Wang, J.-S.; Hewitt, J. M.; Lenhart, W. C.; Mourey, T. H., *J. Polym. Sci., Part A: Polym. Chem*., 2002, 40, 2855.

26. Yates, C. R.; Hayes, W., *Europ. Polym. J*, 2004, 40, 1257.

27. Kim, Y. H.; Webster, O. W., *J. Am. Chem. Soc*., 1988, 196, 104.

28. Emrick, T.; Chang, H. T.; Fréchet, J. M., *J. Macromolecules*, 1999, 32, 6380.

29. Kim, Y. H.; Webster, O. W., *Polym. Prep.* (*Am. Chem. Soc., Div. Polym. Chem.*), 1988, 29, 310.

30. Uhrich, K. E.; Hawker, C. J.; Fréchet, J. M. J.; Turner, S. R., *Macromolecules*, 1992, 25, 4583.

31. Weimer, M. W.; Fréchet, J. M.; Gitsov, I., *J. Poly. Sci., Part A: Polym. Chem.*, 1998, 36, 955.

32. Chang, T. M., *Trends Biotech*., 2006, 24, 372.

33. Suzuki, M.; Ii, A.; Saegusa, T., *Macromolecules*, 1992, 25, 7071.

34. Jikei, M.; Kakimoto, M., *Prog. Polym. Sci.* 2001, *26*, 1233.

35. Cao, X.; Shi, Y.; Wang, X.; Graff, R. W.; Gao, H., *Macromolecules*, 2016, 49, 760.

36. Pastor-Perez, L.; Kemmer-Jonas, U.; Wurm, F.; Stiriba, S.-E.; Perez-Prieto, J.; Frey, H., *Macromolecules*, 2010, 43, 9583.

37. Liu, J.; Zhong, Y.; Lam, J. W. Y.; Lu, P.; Hong, Y.; Yu, Y.; Yue, Y.; Faisal, M.; Sung, H. H. Y.; Williams, I. D.; Wong, K. S.; Tang, B. Z., *Macromolecules*, 43, 4921.

38. Breslow, R., *Chem. Soc. Rev*. 1972, 1, 553.

39. Mallepally, R. R.; Smirnova, I.; Arlt, W.; Seiler, M.; Klee-Laquai, S. K.; Hills, G., *J. Appl. Polym. Sci.*, 2009, 112, 1873.

40. Ren, Q.-Z.; Yao, Y.; Ding, X.-J.; Hou, Z.-S.; Yan, D.-Y., *Chem. Comm.*, 2009, 4732.

41. Cowie, J. M.G. *Polymers: Chemistry & Physics of Modern Materials*, Blackie Academic & Professional, Glasgow, 1991, 2nd Ed., pp 4.

42. Picture taken from Huang, J.; Richard, S., *Polymer*, 2017, 116, 572.

43. Noshay, A.; McGrath, J. E., *Blockcopolymers: Overview and Critical Survey*; Elsevier: New York, 1977.

44. Hershkovits, E., Tannenbaum, A.; Tannenbaum, R., *Macromolecules*, 2008, 41, 3190.

45. Hillmyer, M., *Solid State Mater. Sci*., 1999, 4, 559.

46. Tuzar, Z.; Kratochvil, P., *Adv. Colloid. Interface Sci*., 1976, 6, 20.

47. Szwarc, M, *Nature*, 1956, 178, 1168.

48. Szwarc, M.; Levy, M.; Milkovich, R., *J. Am. Chem. Soc.*, 1956, 78, 2656.

49. Matyjaszewski, K.; Muller, A. H. E., *Polym. Prep.*, 1997, 38, 6.

50. Webster, O., *Science*, 1991, 251, 887.

51. Kato, M.; Kamigaito, M.; Sawamoto, M.; Higashimura, T., *Macromolecules*, 1995, 28, 172.

52. Wang, J. S.; Matyjaszewski, K., *J. Am. Chem. Soc.*, 1995, 117, 5614.

53. Fischer, H., *J. Polym. Sci. Part A-Polym. Chem.*, 1999, 37, 188.

54. Patten, T. E.; Matyjaszewski, K., *Acc. Chem. Res.*, 1999, 32, 895.

55. Patten, T. E.; Xia, J.; Abernathy, T.; Matyjaszewski, K., *Science*, 1996, 272, 868.

56. Fogg, D. E.; Radzilowski, L. H.; Dabbousi, B. O.; Schrock, R. R.,A Thomas, E. L.; Bawendi, M. G., *Macromolecules*, 1997, 30, 8433.

57. Royappa, A. T.; Saunders, R. S.; Rubner, M. F.; Cohen, R. E., *Langmuir*, 1998, 14, 6207.

58. Moad, G.; Chiefari, J.; Chong, B.Y. K.; Kristina, J.; Mayadunne, R. T.; Postma, A.; Rizzardo, E.; Thang; S. H., *Polym. Int.*, 2000, *49*, 993.

59. Erothu, H.; Kolomanska, J.; Johnston, P.; Schumann, S., Deribew, D., Toolan, D. T. W.; Gregori, A.; Dagron-Lartigau, C., Portale, G.; Bras, W.; Arnold, T., Distler,

A.; Hiorns, R. C.; Mokarian-Tabari, P.; Collins, T. W.; Howse, J. R.; Topham, P. D., *Macromolecules*, 2015, 78, 2107.

60. Stille, J. K., *J. Chem. Educ*., 1981, *58*, 862.

61. Zhang, C.; Zhu, Y.; Zhou, C., Yuan, W., Du, J., *Polym. Chem.*, 2013, 255.

62. Forster, S.; Antonietti, M., *Adv. Mater*, 1998,10, 195.

63. Blanza, A.; Armes, S. P.; Rayan, A. J., *Macro. Rapid Commun*., 2009, 30, 267.

64. An-chang S.; Baohui L., *Soft Matt.*, 2013, 9, 1398.

65. Adams, M. L.; Lavasanifar, A.; Kowon, G. S., *J. pharm. Sci.*, 2003, 92, 1343.

66. Myers D., *Association colloids: Micelles, vesicles, and membranes. In: Myers D, editor. Surfaces, interfaces, and colloids: Principles and applications*, 2nd Ed., New York: John Wiley & Sons, 1999, pp 383

67. Goon, P.; Manohar, C.; Kumar, V., *J. Coll. Interface Sci.*, 1997**,** 189, 177.

68. Kim, S.; Shin, I.; Lee, Y.; Cho, C.; Sung, Y., *J. Control Release,* 1998**,** 51,13.

69. Yokoyama, M.; Sugiyama, T.; Okano, T.; Sakurai, Y.; Naito, M.; Kataoka, K., *Pharm. Res*., 1993**,** 10, 895.

70. Halperin, A.; Alexander, S., *Macromolecules,* 1989**,** 22, 2403.

71. Merrett, F. M., *J. Polym. Sci.*, 1957, 24, 467; (b) Krause, S., *J. Phys. Chem*., 1964, 68, 1948.

72. Riess, G., *Prog. Polym. Sci*., 2003, 28, 1107.

73. Picture taken from Nishyama, N., *Nature Nanotech*., 2007, 2, 203.

74. Rapoport, N., *Prog. Polym. Sci.*, 2007, 32, 962.

75. Schacher, F. H.; Rupar, P. A.; Manners, I., *Angew. Chemie - Int. Ed.*, 2012, 51, 7898.

76. Li, Y.; Hindi, K.; Watts, K. M.; Taylor, J. B.; Zhang, K. Li, Z.; Hunstad, D. A.; Cannon, C. L.; Youngs, W. J.; Wooley, K. L., *Chem. Commun.*, 2010, 46, 121.

77. Na, H.; Dongjian, S.; Jihang, L.; Junfeng, L.; Mingqing, C., *J. Wuhan University of Technology-Mater. Sci.*, 2015, 30, 1092.

78. Takae, S.; Miyata, K.; Oba, M.; Ishii, T.; Nishiyama, N.; Itaka, K.; Yamasaki, Y.; Koyama, H.; Kataoka, K., *J. Am. Chem. Soc*., 2008, 130, 6001.

79. Shimizu, H.; Hori, Y.; Kaname, S.; Yamada, K.; Nishiyama, N.; Matsumoto, S.; Miyata, K.; Oba, M.; Yamada, A.; Kataoka, K.; Fujita, T., *J. Am. Chem. Soc. Nephrol*., 2010, 21, 622.

80. Kishimura, A.; Koide, A.; Osada, K.; Yamasaki, Y.; Kataoka, K., *Angew. Chem*., 2007, 119, 6197; *Angew. Chem. Int. Ed*., 2007, 46, 6085; (b) Lee, Y.; Ishii, T.; Cabral, H.; Kim, H. J.; Seo, J.-H.; Nishiyama, N.; Oshima, H.; Osada, K.; K. Kataoka K., *Angew. Chem*., 2009, 121, 5413; *Angew. Chem. Int. Ed*., 2009, 48, 5309; (c) ONeil, C.P. ; Suzuki, T.; Demurtas, D.; Finka, A.; Hubbell, J. A., *Langmuir*, 2009, 25, 9025.

81. Sutton, D.; Nasongkla, N.; Blanco, E.; Gao, J. M., *Pharm. Res.*, 2007, 24, 1029.

82. Halperin, A.; Alexander, S., *Macroml.*, 1989, 22, 2403.

83. Gref, R.; Minamitake, Y.; Peracchia, M. T.; Trubetskoy, V.; Torchilin; V.; Langer R., *Science*,1994, 263, 1600.

84. Matsumura, Y.; Maeda, H., *Canc. Res.*, 1986, 46, 6387.

85. Yang, C.; Liu, S. Q.; Venkataraman S.; Gao; S. J.; Ke; X. Y.; Chia, X. T.; Hedrick, J. L.; Yang, Y. Y., *J. Control. Release*, 2015, 208, 93.

86. Shuai, X. T.; Nasongkla, H. Ai, N.; Kim, S.; Gao, J. M., *J. Control. Release*, 2004, 98, 415.

87. Shuai, X. T.; Merdan, T.; Schaper, A. K.; Xi, F.; Kissel, T., *Bioconjugate Chem.*, 2004, 15, 441.

88. Nishiyama, N.; Okazaki, S.; Cabral, H.; Miyamoto, M.; Kato, Y.; Sugiyama, Y.; Nishio, Matsumura, K. Y.; Kataoka, K., *Cancer. Res.*, 2003, 63, 8977.

89. Danson, S.; Ferry, D.; Alakhov, V.; Margison, J.; Kerr, D.; Jowle, D.; Brampton, M.; Halbert, G.; Ranson, M., *Br. J. Cancer*, 2004, 90, 2085.

90. Matsumura, Y.; Hamaguchi, T.; Ura, T.; Muro, K.; Yamada, Y.; Shimada, Y.; Shirao, K.; Okusaka, T.; Ueno, H.; Ikeda, M.; Watanabe, N., *Br. J. Cancer*, 2004, 91, 1775.

91. Kim, T. Y.; Kim, D. W.; Chung, J. Y.; Shin, S. G.; Kim, S. C.; Heo, D. S.; Kim, N. K.; Bang, Y. J., *Clin. Cancer Res.*, 2004, 10, 3708.

92. Kataoka, K.; Harada, A; Nagasaki, Y., *Adv. Drug Delivery Rev*. 2001, 47, 113.

93. Jelonek, K.; Li, S.; Wu, X.; Kasperczyk, J.; Peg, P. L. A., *Int. J. Pharm*., 2015, 485, 357.

94. Pass, H. I., *J. Nat. Cancer. Inst.*, 1993, 85, 443.

95. Pushpan, S. K.; Venkatraman, S.; Anand, V. G.; Sankar, J.; Parmeswaran, D.; Ganesan, S.; Chandrashekar, T. K., *Cur. Med. Chem. - Anti-Cancer. Agents*, 2002, 2, 187.

96. Maeda, H.; Wu, J.; Sawa, T.; Matsumura, Y.; Hori, K., *J. Control. Release*, 2000, 65, 271.

97. Smallbone, K.; Gavaghan, D. J.; Gatenby, R. A; Maini, P. K., *J. Theo. Bio.*, 2005, 235, 476.

98. Du ,Y.; Wei,Y.; Lian, H.; Xiang, C.; Duan, L.; Xiao C., *J. Coll. and Inter. Sci.*, 2018, 522 74.

99. Lee, Y.; Kataoka, K., *Soft Matter*, 2009, 5, 3810.

100. Miyata, K.; Christie, R.J.; Kataoka, K., *React. Funct. Polym*., 2011, 71, 227.

101. Gaucher, G.; Dufresne, M. H.; Sant, V.P.; Kang, N. ; Maysinger, D.; Leroux, J. C., *J. Control. Release*, 2005,109 169.

102. Nostrum, C.F., *Adv. Drug Delivery Rev*., 2004, 56, 9.

103. Nishiyama, N.; Morimoto, Y.; Jang, W.-D.; Kataoka, K., *Adv. Drug Delivery Rev*., 2009, 61, 327.

104. Batrakova, E.V.; Li, S.; Reynolds, A.D.; Mosley, R.L.; Bronich, T.K.; Kabanov, A.V.; Gendelman, H.E., *Bioconjugate Chem*., 2007, 18 1498; (b) Bayó-Puxan, N.; Dufresne, M-A; Felber, A. E.; Castagner, B., Leroux, J-C., *J. Control. Release*, 2011,156, 118.

105. Heffernan, M.J.; Murthy, N., *Ann. Biomed. Eng*., 2009, 37 1993.

106. Kawamura, A.; Kojima, C.; Iijima, M.; Harada, A.; Kono, K., *J. Polym. Sci., Part A: Polym. Chem*., 2008, 46 384.

107. Dufresne, M. H.; Leroux, J. C., *Pharm. Res*., 2004, 21 160.

108. Kataoka, K.; Togawa, H.; Harada, A.; Yasugi, K.; Matsumoto, T.; Katayose, S., *Macromolecules*, 1996, 29 8556.

109. Nishiyama, N.; Kataoka, K., *Pharmacol. Ther*., 2006, 112, 630.

110. Zhang, G.-D.; Harada, A.; Nishiyama, N; Jiang, D.-L.; Koyama, H; Aida, T.; Kataoka, K., *J. Control. Release*, 2003, 93,141.

111. Jang, W.-D.; Nakagishi, Y.; Nishiyama, N.; Kawauchi, S.; Morimoto,Y.; Kikuchi, M; Kataoka, K., *J. Control. Release* 2006, 113, 73.

112. Nishiyama, N.; Nakagishi, Y.; Morimoto, Y.; Lai, P.-S.; Miyazaki, K.; Urano, K.; Horie, S.; Kumagai, M.; Fukushima, S.; Cheng ,Y.; Jang, W.-D.; Kikuchi, M,; Kataoka, K., *J. Control Release*, 2009, 133, 245.

113. Herlambang, S.; Kumagai, M.; Nomoto, T.; Horie, S.; Fukushima, S.; Oba, M.; Miyazaki, K.; Morimoto, Y.; Nishiyama, N.; Kataoka, K., *J. Control Release*, 2011, 155, 4940.

114. Kim, J. H.; Ramasamy, T.; Tran, T. H.; Choi, J. Y.; Cho, H. J.; Yong, C. S.; Kim, J. O., *Asian J. Pharmaceut. Sci.*, 2014, 9, 191.

115. Wolinsky, J. B.; Grinstaff, M. W., *Adv. Drug Delivery Rev.*, 2008, 60, 1037.

116. Qiu, L. Y.; Bae; Y. H., *Pharmaceut. Res.*, 2006, 23, 1.

117. Butun, V.; Billingham, N. C.; Armes, S. P., *Chem. Comm.*, 1997, 671.

118. Liu, S. Y.; Weaver, J. V. M.; Tang, Y. Q.; Billingham, N. C.; Armes, S. P.; Tribe, K., *Macromolecules*, 2002, 35, 6121.

119. Zhang, X.; Xia, J. H.; Matyjaszewski, K., *Macromolecules*, 1998, 31, 5167.

120. Fu, C.; Herbst, S.; Zhang, C.; Whittaker, A. K., *Polym. Chem*. 2017, 8, 4585.

121. Nurmi, L.; Peng, H.; Seppälä, J.; Haddleton, D. M.; Blakey, I.; Whittaker, A. K., *Polym. Chem*., 2010, 1, 1039.

122. Zhang, X.; Matyjaszewski, K., *Macromolecules*, 1999, 32, 1763.

123. Rapoport, N., *Prog. Polym. Sci*., 2007, 32, 962.

124. Yoo, H. S.; Park, T. G., *J. Control. Release*, 2001, 70, 63.

125. Kim, M. S.; Hyun, H.; Cho, Y. H.; Seo, K. S.; Jang, W. Y.; Kim, S. K.; Khang, G.; Lee, H. B., *Polym. Bulletin*, 2005, 55, 149.

126. Baines, F. L.; Armes, S. P. ; Billingham, N. C.; Tuzar, Z., *Macromolecules*, 1996, 29, 8151.

127. Kataoka, K.; Matsumoto, T.; Yokoyama, M.; Okano, T.; Sakurai, Y.; Fukushima, S.; Okamoto, K.; Kwon, G. S., *J. Control. Release*, 2000, 64, 143.

128. Turner, S. R.; Walter,F.; Voit, B. I.; Mourey, T. H., *Macromolecules*, 1994, 27, 1611.

129. Twyman, L. J.; King, A. S. H., *J. Chem. Res*., *Synop*., 2002, 43. 201.

130. Zheng, X.; Oviedo, I. R.; Twyman, L. J., *Macromolecules*, 2008, 41, 7776.

131. Twyman, L. J.; Ellis, A.; Gittins, P. J., *Macromolecules*, 2011, 44, 6365.

132. Kirkorian, K.; Ellis, A.; Twyman, L.J., *J. Chem. Soc. Rev*. 2012, 41, 6138.

133. Mann G, Ellis. Twyman L. J., *Macromolecules*, 2016, 49, 4031.

134. Twyman, L. J.; King, A. S. H., *Chem. Commun*., 2002, 910.

135. Ballester, P.; Gomila, R. M.; Hunter, C. A.; King, A. S. H.; Twyman, L. J., *Chem. Commun*., 2003, 38.

136. Twyman, L. J.; Ge, Y., *Chem. Commun*., 2006, 1658.

137. Twyman, L. J.; Ge, Y.; Gittins, P. J., *Supramol. Chem*., 2006, 18, 357.

138. Yamazaki, S.-i.; Ioroi, T.; Tanimoto, K.; Yasuda, K.; Asazawa, K.; Yamaguchi, S.; Tanaka, H., *J. Power Sources*, 2012, 204, 79.

139. Gao, B.; Chen, Y.; Lei, Q. J., *Incl. Phenom. Macrocy. Chem*., 2012, 74, 455.

140. Adilina, I. B.; Hara, T.; Ichikuni, N.; Shimazu, S. J., *Mol. Catal. A: Chem*., 2012, 72, 361.

141. Chatterjee, C.; Chisholm, M. H., *Inorg. Chem*., 2011, 50, 4481.

142. Chatterjee, C.; Chisholm, M. H., *Inorg. Chem*., 2012, 51, 12041.

143. Evans, S.; Lindsay, S. J. R., *Perkin*, 2000, 2, 1541.

144. Boitrel, B.; Hijazi, I.; Roisnel, T.; Oohora, K. and Hayashi, T., *Inorg. Chem*., 2017, 56, 7373.

145. Wei, J.-F.; Shi, X.-Y., *Indian J. Chem., Sect. A*: *Inorg., Bio-inorg., Phys., Theor. Anal. Chem*., 2005, 44, 2240.

146. Bhyrappa, P.; Young, J. K.; Moore, J. S.; Suslick, K. S. J., *Mol. Catal. A: Chem.* 1996, 113, 109.